AGE-RELATED MACULAR DEGENERATION
A LIGHT AND ELECTRON MICROSCOPICAL STUDY

(OUDERDOMS MACULA DEGENERATIE)
(EEN LICHT- EN ELECTRONENMICROSCOPISCH ONDERZOEK)

proefschrift

ter verkrijging van de graad van doctor
aan de Erasmus Universiteit Rotterdam
op gezag van de Rector Magnificus
Prof. dr. C.J. Rijnvos
en volgens besluit van het College van Dekanen.
De openbare verdediging zal plaatsvinden op
woensdag 21 April 1993 om 15.45 uur

door

Theodorus Laurentius van der Schaft

geboren te Rotterdam

PROMOTIECOMMISSIE:

PROMOTOR: Prof.Dr. P.T.V.M. de Jong

CO-PROMOTOR: Dr. W.C. de Bruijn

OVERIGE LEDEN: Prof.Dr. F.T. Bosman

                  Prof.Dr. G.F.J.M. Vrensen

                  Prof.Dr. J.F. Jongkind

"The aging process results in numerous changes in cells and tissues of the body, but few are as important to an elderly individual as those occurring in the 2 to 3 mm^2 area of macular retina, loss of which can profoundly affect the quality of life."

Lynette Feeney-Burns (Arch Ophthalmol 1990)

Aan Nicolette

Abbreviations

AMD/ARMD	Age-related Macular Degeneration
B	Basement membrane
BLD	Basal Laminar Deposit
BM/BrM	Bruch's Membrane
Bm	Banded material
BSA	Bovine Serum Albumin
Ch	Choroid
C	Calcification
CC	Choriocapillaris
C_3	Complement factor 3
C_1Q	Complement factor 1Q
D	Drusen
DAB	di-aminobenzidine
DS	Disciform Scar
E	Electron translucent spaces
EL	Elastic Layer
EM	Electron Microscopy
EPMA	Electron Probe Microanalysis
F	Fibrillar material
FITC	Fluorescein Isothiocyanate
FLSC	Fibrous Long-Spacing Collagen
GA	Geographic Atrophy
H	Homogeneous material
H&A	Hematoxylin-Azofloxin
HSPG	Heparan Sulfate Proteoglycans
Hy	Hyalin material
ICZ	Inner Collagenous Zone
Ig(A)	Immunoglobulin (A)
INL	Inner Nuclear Layer
IOL	Intra Ocular Lens
L	Lipofuscin granule
LDL	Low-Density Lipoproteins
LM	Light Microscopy
LSC	Long-Spacing Collagen
M	Melanocyte
ML	Melanolipofuscin granule

Mi	Mitochondrion
μm	micrometer (1x10^{-6} meter)
N	Number
nm	nanometer (1x10^{-9} meter)
NS	Not Significant
OCZ	Outer Collagenous Zone
ONL	Outer Nuclear Layer
OPL	Outer Plexiform Layer
P	Pigment granule
PAS	Periodic Acid-Schiff
PBS	Phosphate-Buffered Saline
pH	degree of acidity of an aqueous solution
POS	Photoreceptor Outer Segment
RPE	Retinal Pigment Epithelium
SD	Standard Deviation
SEM	Standard Error of the Mean
TEC	Trabecular Endothelial Cell
TEM	Transmission Electron Microscopy
XRMA	X-ray Microanalysis
UV	Ultraviolet
V	Villi
vol/vol	volume/volume
wt/vol	weight/volume
wt/wt	weight/weight
yr	year

CONTENTS

CHAPTER 1: General Introduction

1.1 Clinical definition

Age-related macular degeneration (ARMD) was first described by Haab in 1885[240] as an age-related abnormality of the macula lutea or "yellow spot", affecting central vision. It was almost exclusively seen after the age of 50 years.

Most studies define ARMD as a whole range of progressive aging or degenerative changes in the human macula starting with drusen, hyper- and hypopigmentation of the retinal pigment epithelium (RPE), areolar or geographic atrophy (which is called the "dry" endstage of ARMD), subretinal neovascularization, serous or hemorrhagic pigment epithelial detachment and a disciform scar (also known as "Junius-Kuhnt", which is also called the exudative or "wet" endstage of ARMD)[120]. In some studies a visual acuity of 2/3 or less, that cannot be attributed to any other eye disease, is included in the definition. An international consensus on this definition has not yet been achieved.

Geographic atrophy typically causes a gradual, mild to moderate impairment of vision, progressing over several months to years. The effects on vision of the exudative type of ARMD are frequently more devastating: patients may lose all central vision within a few days.

The majority of patients with ARMD suffer from the atrophic type (90%), whereas the exudative type accounts for 5%[120]. The remaining 5% have a mixed form of the atrophic and exudative type in the same macula[120]. In 2/3 of the patients the disease is bilateral, but often there is some time delay between the appearance of ARMD in the fellow eye[76,120,221].

Many investigators have tried to correlate ARMD with other eye diseases, systemic abnormalities or environmental conditions, in order to find risk factors for the development of ARMD.

A higher risk on ARMD was found to correlate with:

- age[71,120,249]
- myopia[71]
- hyperopia[36,50,71,139,235,249]
- choroidal sclerosis[209,235]
- light iris and hair color[224,235,249,250]
- hypertension[35,71,111,120,224,235]
- chronic pulmonary disease[120,235]
- cardiovascular diseases[92,249]
- cigarette smoking[92,249]
- decreased hand grip strength[120,249]
- family history[224]
- higher education [71]
- high body mass[224]
- high cholesterol[224]
- sunlight exposure[92,261]
- elastotic degeneration of the skin[249]
- nonspecific chemical exposure[92,249]
- low serum zinc levels[84,157,259].
- elevated serum zinc and copper levels[209,224]
- elevated serum glucose, lipids, gluthation peroxidase[261]
- elevated serum ceruloplasmin and leukocytosis[159,235,261]

In contrast to some of these findings, other investigators found no correlations between ARMD and myopia[36], high serum cholesterol or LDL[11,71,72], smoking[224], diabetes mellitus, vascular diseases, marital status[71] or the profession of the patient[139] as well as light iris color, light or grey hair[245]. The relationship between ARMD and senile cataract is also controversial: some authors reported a positive correlation[120]; others found no correlation[47,235] or even an inverse relationship[241]. The most precise conclusion is a positive correlation with cortical cataract and a negative correlation with nuclear cataract[129].

1.2 Prevalence

ARMD is the leading cause of social blindness (visual acuity ≤ 0.1) in the elderly in the western world[3,28,50,100,120,197,256]. For those under 60 years of age, diabetes mellitus is the main cause of blindness[120].

The prevalence of ARMD, mentioned in several studies, varies with the definition and the population described [47,50,139,168,177,241,246,247]. On the average the following prevalences are reported:

> 60-69 years: 4%
> 70-79 years: 12%
> above 80 years: 30%

Among Caucasians the prevalence has been found to be twice as high as in blacks [77,262]. No differences between left or right eye or sex have been found[247], but some authors reported a male/female ratio of 2:3 depending on the criteria for ARMD [50,120]. There are controversial findings on inheritance of ARMD: most investigators think ARMD is not hereditary [11], but in some families a much higher prevalence has been found[50].

1.3 Therapy

The possibilities for treatment of exudative ARMD are still disappointing. Drug treatment is of no avail and can even be hazardous, as it might give the extrafoveal newly formed vessels the opportunity to grow towards the subfoveal area, thus making a possibly treatable condition untreatable[163]. Some authors, however, have reported hopeful results with the systemic administration of interferon-alpha-2a, an angiogenesis inhibitor, to patients with recent, small subretinal neovascular membranes[163].

Laser photocoagulation is a destructive technique, which is meant to coagulate newly formed subretinal vessels, but it also destroys the photoreceptors in the treated area and creates a scotoma[163]. Argon green, krypton red and

yellow dye lasers are currently used[54,163]. In only 10-25% of the patients with subretinal neovascularization can laser coagulation of the newly formed vessels be temporarily helpful or at least prevent further deterioration of vision[100,163,201]. This applies especially in the case of extrafoveal subretinal neovascularization more than 200 μm from the foveal centre[31]. After laser photocoagulation severe visual loss is postponed for about two years[163]. Laser treatment of subfoveal neovascularization is controversial and has been recommended for restricted cases only, accepting an immediate drop in visual acuity after treatment, but it yields a better vision compared to untreated patients after two years[137,174,201]. After laser coagulation of occult neovascularization, vision may become worse compared to an untreated control group[214], because destruction of the new vessels is often incomplete and further outgrowth, preferentially towards the fovea, is stimulated by the laser treatment[163]. Moreover, laser coagulation itself can also induce neovascularization[214]. For patients with a small macular scar in one eye, laser treatment is not indicated when neovascularization occurs in the other eye, because they have only a 16% chance of developing a large scar in the second eye, with deterioration of visual acuity. In contrast, people with a large scar in one eye have a 50% chance of developing a large macular scar in the fellow eye[118]. Recurrent subretinal neovascular membranes were seen in 52% of the patients with extrafoveal neovascularization 24 months after laser treatment and in 66% of the patients with parafoveal new vessels[135,136,163]. Thus frequent inspection of the fundus for recurrence is needed in the first two years [135,136]. Subretinal vessels with only minimal leakage, seen on fluorescence angiograms, in patients over 80 years of age do not need laser photocoagulation, because in 57% of these patients there was a tendency toward involution of the new vessels and in 80% visual acuity improved without treatment[98].

Surgical treatment of a disciform macular scar with transplantation of homologous or autologous RPE and Bruch's membrane has been described, but as yet the results in most cases are disappointing[174]. Surgical removal of a recent subretinal hemorrhage has been tried, but the poor functional results justify this procedure only for monocular patients with a macular hemorrhage due to ARMD[243].

For geographic atrophy no adequate treatment is available, although some

advocate zinc supplementation[84,121,156]. This is based on the idea of providing enough zinc for the production of superoxide dismutase, a metallo enzyme which scavenges free radicals[105,156,209,235,249]. This would prevent phototoxic damage of the eye by radiant energy[262](see also Chapter 3.1). However, little is known about either the therapeutic or the toxic effect.
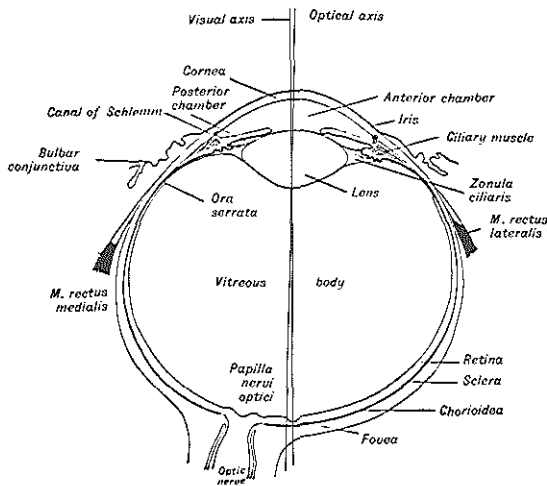

Fig 2.1.1 Schematic drawing of an eye, sectioned horizontally.

CHAPTER 2: Anatomy and Histology of the Human Macula

2.1 The macula

This section deals with the histology of the human macula as far as this is essential for a better understanding of this thesis. An extensive description of the histology of the macula can be found in the literature[90].

The macula lutea or yellow spot is located in the optic axis on the inner side of the posterior pole of the eye. The yellow colour is due to xantochrome granules in the inner layers of the retina and is best seen in the hemisectioned and formalin fixed globe.

It extends approximately 5.5 mm from the temporal edge of the optic disc and is vertically limited by the superior and inferior temporal retinal vessel arcades (Fig 2.1.2).
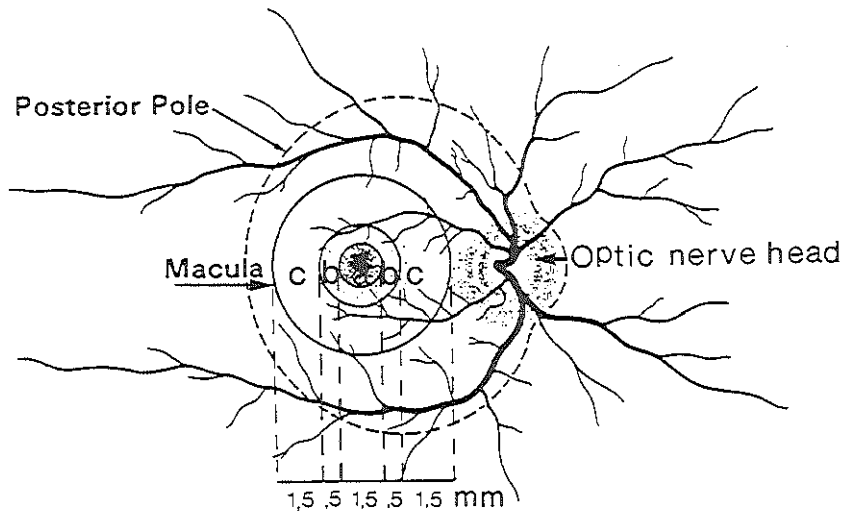
Figure 2.1.2 Schematic drawing of the posterior pole of the fundus of a human eye.

The center of the macula, the fovea (a), is a zone of slightly greater pigmentation and is approximately 1.5 mm in diameter (corresponding with 1 disc diameter). The center of the fovea is the foveola with a diameter of about 0.2 mm. Here the retina is maximally thin and only comprises the photoreceptors and their axons. In the foveola exclusively cone photoreceptors are found. Away from the foveola the cone/rod ratio decreases. The parafovea (b) surrounds the fovea and

has a width of 0.5 mm. The perifovea (c) surrounds the parafovea and measures 1.5 mm in width. The fovea is almost totally devoid of retinal bloodvessels. The parafoveal and perifoveal zones, however, are richly vascularized.

Histologically, the macula is defined as that part of the retina with two or more ganglion cell layers, including the foveola with only a photoreceptor cell layer. The fovea-foveola border is located at the site were the nuclei of the inner nuclear layer and ganglion cell layers appear. The parafovea is characterized by the thickest part of the retina with a ganglion cell layer of 6 to 8 rows thick. The perifovea commences at the point where the ganglion cell layer has four rows of nuclei and ends where the layer is reduced to a single layer, that is seen elsewhere in the retina.

The importance of the macular region for visual function is emphasized by the fact that one third of the nerve fibers of the optic nerve originates in this region.

2.2 The photoreceptors

The photoreceptor cells consist of a light sensitive outer segment, a metabolic inner segment and a cell body containing the nucleus. The outer segments are composed of a series of superimposed membranous discs, stacked on each other like a role of coins and surrounded by a membrane. These outer segments are in close contact with the apical microvilli of the retinal pigment epithelium (RPE, see chapter 2.3). The photoreceptor cells sequester each day packets of 30-100 discs from the distal part of their outer segments. These discarded discs are phagocytized by the RPE and digested by lysosomal enzymes. The photopigments are recycled and transported back to the photoreceptor inner segments.

The photoreceptor cell bodies with their nuclei form the outer nuclear layer of the retina. This layer is easily recognisable in light microscopical sections and is used as a marker for photoreceptor cell degeneration.

The photoreceptors in the macular region are mostly cones. However, in the macula they are long and slender and thus can light microscopically easily be confused with rods.

2.3 The retinal pigment epithelium

The retinal pigment epithelium (RPE) is a monolayer of pigmented hexagonal cells, which covers the innerside of Bruch's membrane. The cells are firmly attached to each other by junctional complexes, consisting of a desmosome, a gap junction and a tight junction. The latter is responsible for the outer blood-retina barrier. The RPE cells are more pigmented in the macular region than elsewhere in the retina. No racial differences are found in the rate of pigmentation of the RPE[37,251]. The average size of these cells is 14 μm wide and 10-14 μm tall. At the apical side, these cells have microvilli, which interdigitate with the photoreceptor outer segments. In the apical cytoplasm numerous melanin granules can be found. The nucleus is found in the basal part of the cytoplasm accompanied by many mitochondria. Within the cytoplasm phagolysosomes can be found, filled with the phagocytized photoreceptor outer segment discs. The basal part of the cell membrane does not run in a straight line, but has many basal infoldings and thus the basal cell membrane area is markedly extended. Normally, the RPE cells are in close contact with their basement membrane, which is produced by the RPE cells[22].

Lipofuscin granules, another pigment, can already be found in the RPE cytoplasm soon after birth[109] and the number of these granules increases with age. Lipofuscin granules are probably residual bodies, representing the end product of phagosomal activity[14,16]. More lipofuscin has been seen in whites than in blacks[250].

Under normal conditions, mitosis is not observed in the RPE cells [237,238]. It is generally believed that RPE cells are not replaced if they die, but that adjacent cells slide laterally to fill the space left by the dead cell. Although cell division is not seen, 1 out of 30 RPE cells has two nuclei[60,237]. Cell renewal is performed by autophagy and subsequent replacement of the sub-cellular structures[21].

The function of the RPE cells is: phagocytosis of the outer segment discs and recycling of the retinol, pumping fluid from the sub-retinal space to the choriocapillaris[9,168], regulating fluid flow from the choriocapillaris to the outer layers of the retina, absorbing the light which has passed the photoreceptors and scavenging the free radicals formed by the light energy[46,235], and the production of stimulating and inhibiting factors which act on the choriocapillaris.

The RPE cells are able to produce all substances which can be found in Bruch's membrane[23]. Probably the collagenous zones and the elastic layer of Bruch's membrane (for more detail see chapter 2.4) are also formed by the RPE cells although this has not been proven yet[23].

2.4 Bruch's membrane

Bruch's membrane is an a-cellular layer, between the retinal pigment epithelium and the choriocapillaris. It extends from the optic disc to the ora serrata.

It is composed of five layers[90]:(Fig.2.4.1)

1) The basement membrane of the RPE, which is produced by the RPE cells and consists of fine filaments that extend from the RPE cell membrane to the inner collagenous zone of Bruch's membrane. It measures about 300 nm and is separated from the RPE cell membrane by a space measuring 100 nm. This basement membrane does not follow the basal infoldings of the RPE cell membrane, but runs in a straight line parallel to the inner collagenous zone.

2) The inner collagenous zone (ICZ) consists of a loosely interwoven meshwork of collagen fibers. Ultrastructurally, these fibers have a banded pattern of 64 nm. Fine filaments, emanating from the RPE basement membrane, merge with the collagen fibers of the inner collagenous zone.

3) The elastic layer forms the "backbone" of Bruch's membrane. In the macula this layer consists of a thin, continuous, fenestrated meshwork of long elastic fibers. Outside the macula this elastic layer becomes thicker and relatively large gaps in the meshwork can be found.

4) The outer collagenous zone (OCZ) in first instance has the same structure as the inner collagenous zone, but with increasing age marked differences develop in the macular region, as will be discussed later (chapter 3.2, 5, 6, 10).

5) The basement membrane of the choriocapillaris forms the outer layer of Bruch's membrane. It measures about 140 nm and is thinner than the RPE basement membrane. It is produced by the endothelial cells of the choriocapillaris. Thus it is a discontinuous layer, because in the space between the capillaries - the intercapillary pillars - this basement membrane is absent.

Embriologically, the first layer of Bruch's membrane belongs to the retina and the fifth layer belongs to the choriocapillaris.
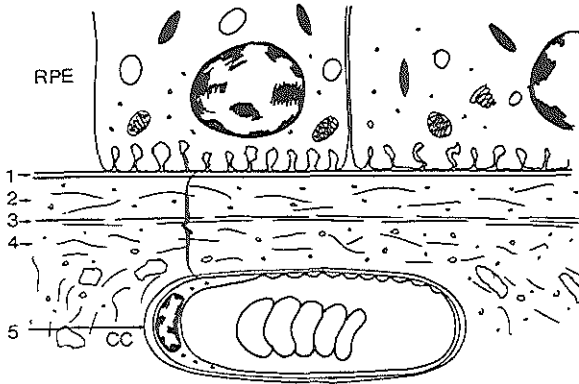

Figure 2.4.1. Schematic drawing of the five layers of Bruch's membrane.

2.5 The choriocapillaris

This is a thin network of capillaries at the choroidal side of Bruch's membrane. The vessels of the choriocapillaris differ from those in other organs, as well as those of the retina by the greater diameters of their lumina. This diameter is smallest in the macula and increases towards the peripheral choroid. The macular choriocapillaris forms a net with small meshes. These meshes become wider and longer towards the peripheral choroid[90].

The choriocapillaris forms the blood supply for the RPE and the outer part of the retina up to half way the outer plexiform layer. The fenestrated capillaries are readily permeable for O_2 and CO_2, water, electrolytes and small proteins, but impermeable for macromolecular substances. The most important barrier to free flow between choroidal vessels and the sensory retina are the tight junctions of the junctional complexes between the lateral borders of the RPE cells, that prevents fluid exchange through the intercellular spaces of the RPE. The normal flow is therefore regulated by intracellular processes.

The capillaries are surrounded by a basement membrane, formed by the endothelial cells. Pericytes are only rarely seen.

CHAPTER 3: Histology of the aging human macula

With increasing age the following histological changes can be found in the macula.

3.1 The retinal pigment epithelium

During life the RPE cells continuously phagocytize the discs, shedded by the photoreceptor outer segments. Each RPE cell is in contact with 20-30 photoreceptors and each photoreceptor discards 30-100 discs/day[78]. This results on average in an turn over rate of 2000 discs in the parafovea, 3500 in the perifovea and 4000 discs in the peripheral retina per day with a photoreceptor/RPE cell ratio of 24, 44 and 42 respectively[89]. Photoreceptors are highly susceptible for phototoxic effects of visible and ultraviolet light, due to the large amount of polyunsaturated fatty acids in the densely stacked phospholipid membranes. Lipid peroxidation in these membranes occurs by free radicals, which are formed by the absorbed radiant energy. These aberrant molecular lipids cannot be digested by the RPE cells' lysosomal enzymes[123,262]. When the digestion of the shedded discs is incomplete or stays behind with the ingestion of the material, vesicles with debris are formed, which are called lipofuscin granules[46,78]. These are considered to be residual bodies, which accumulate in the RPE cytoplasm. Lipofuscin is a heterogeneous aggregation of damaged molecules rather than a genetically programmed, native product[262]. Like melanin, it absorbs radiation from the infrared through the visible and far into the ultraviolet light, with an increasing efficiency as photon energy increases[262]. There is no evidence that these lipofuscin granules can be extruded from the cytoplasm[47]. The number of lipofuscin granules increases rapidly after birth during the first two decades of life[251] especially in the macula, although in the foveal center less lipofuscin has been found[46,100]. Between age 20 and 60 the amount of lipofuscin is relatively stable, but after age 60 the number of lipofuscin granules increases again[251]. There is an inverse relationship between the number of lipofuscin granules and the number of melanin granules in the RPE cells of the macula[46,47,250]. No correlation has been found between the amount of lipofuscin and the presence of

BLD (see chapter 3.4), drusen (see chapter 3.5) or the development of ARMD[131,250]. The increase in lipofuscin causes a detectable enlargement of the cells during normal aging[60,192,251]. As the cytoplasmic space available to the organelles is reduced, cell metabolism is gradually affected[192]. During life the number of RPE cells decreases because of cell death due to excessive accumulation of lipofuscin[37]. There is no feedback control and ingestion of discs of photoreceptor outer segments continues until cell death occurs[192]. The phagocytizing capacity of these cells has to be taken over by neighbouring RPE cells. Subsequently, these cells are engulfed by the photoreceptor discs, which have to be digested. This leads to a rapid accumulation of lipofuscin in the RPE cytoplasm. and hampers the cell metabolism resulting in RPE atrophy which might finally lead to ARMD[37]. Others investigators have reported that the photoreceptor/RPE cell ratio is constant during life, due to an equally diminishing of the number of photoreceptors[47].

3.2 Bruch's membrane

With advancing age, the thickness of Bruch's membrane increases in almost all eyes[192,199]. Thus the "normal" structure of Bruch's membrane in older individuals appears to be debris-filled[45]. In histological sections Bruch's membrane increases from a thin line in children to a thick membrane in the elderly[87,199]. In the macula this thickening is mainly seen in the OCZ, especially between the capillaries of the choriocapillaris, where the so-called intercapillary pillars are formed[107]. In the peripheral retina the age-related thickening is located predominantly in the ICZ[87].

With advancing age, an increasing amount of calciumphosphates is deposited, initially in the elastic lamina of Bruch's membrane[35,45,87]. With special lipid stains (Oil red O and Sudan Black), it was revealed that above age 30 the amount of neutral lipids and phospholipids increased[9,168], which makes the membrane hydrophobic and thus may form a barrier for the fluid transport from the retina to the choriocapillaris and vice versa[9]. The importance of PVC-plasticizer, found in these lipids in Bruch's membrane, is uncertain[9]. Glycosaminoglycans, such as heparan sulphate, dermatan sulphate and chondroitine sulphate can be found in Bruch's membrane and are responsible for the negative charge of the

membrane, which forms a chemical barrier for anionic electrolytes[1,87].

With electron microscopy this thickening of Bruch's membrane appears to be an accumulation of cellular debris, consisting of small vesicles, dense granules surrounded by a double membrane, curly membranes and membranous bags, filled with smaller vesicles, and banded material, which is called long-spacing collagen (LSC)[131,152,234]. These structures are probably derived from the RPE cells[16,45,107,108,168,199]. Because the RPE cells cannot divide under normal conditions, they must "renew" themselves by autophagy and the subsequent synthesis of new cell organelles[45]. Some subcellular structures, however, seem to be extruded from the basal side of the cells as membranous bags instead of being digested by the lysosomal enzymes of the RPE cells, although physical separation of bodies from the RPE has not been demonstrated until degeneration of these cells was in an advanced stage[192]. In the healthy situation this debris is probably cleared away by the choriocapillaris [167]. One hypothesis is that due to age-related atrophy of the choriocapillaris, this debris cannot be cleared away in due time and accumulates in Bruch's membrane[167,199]. However, this accumulation in Bruch's membrane appears to be the result rather than the cause of degeneration of the RPE.

Another hypothesis is that the accumulation of this debris in Bruch's membrane disturbs the interaction between the RPE and the choriocapillaris[167]. There is no indication that this cellular debris is a post mortem artifact[45]. This accumulation of abnormal material might be the cause of the cellular response which is seen in ARMD[108]. Leucocytes and macrophages can be found near breaks in Bruch's membrane on the choriocapillaris side. This is especially seen at places with BLD or drusen, which are sometimes presumed to be the initiating substances of this cellular reaction. This will be described in chapter 9.

3.3 The Choriocapillaris

In eyes with ARMD, changes in the structure of the capillary network [62] and atrophy of the choriocapillaris can be found[47,236]. These changes are often seen in the presence of degenerative RPE cells[162]. It is still uncertain whether these changes in the choriocapillaris are secondary to other changes in the macula

or whether this is rather one of the initiating factors of ARMD[36,236].

With advancing age a decrease in number and diameter of the capillaries of the choriocapillaris is reported[93,165], although quantitative information is still lacking. This situation could be correlated with the development of geographic atrophy[93]. Once the lumen of the choriocapillaris is obliterated the intercapillary pillars become eroded by cellular activity[192]. The relative ischemia might explain the development of chorioretinal anastomoses in ARMD[62]. In maculae with exudative degeneration or in the presence of BLD [131] the choriocapillaris appeared to be normal[89].

RPE cells are known to produce vascular stimulating as well as inhibiting factors, that can act on the choriocapillaris[24,115]. Experimental damage of the RPE induced atrophy of the choriocapillaris[115]. In other experiments, in which a slow degeneration of the RPE was induced, neovascularization was seen[265]. It is thought that in ARMD the interaction between the RPE and the choriocapillaris is disturbed[89].

After experimental laser coagulation of rat retinas, endothelial cells and pericytes of the choriocapillaris were seen to have dissolved their basement membranes and to have penetrated Bruch's membrane, 7 days after the laser treatment[108,179].

In maculae with a disciform scar, senile choroidal sclerosis can sometimes be seen with attenuation of the choroid and enlargement of the choroidal vessels, filling the entire thickness of the choroid[62,161]. This was not correlated with atherosclerosis or arteriolosclerosis[161].

3.4 Basal Laminar Deposit (BLD)

In the eyes of older people and in patients with ARMD, deposits have been found between the RPE and its basement membrane, that have been called basal laminar deposit(s) (BLD)[192], basal linear deposit(s)[131,199] or linear basal deposits[45]. BLD has been found predominantly in the posterior pole of the eye[125,198]. Although these deposits have only been described histologically in enucleated eyes, it has been proven that it is not a post mortem artifact[64,249]. The exact pathogenesis of BLD is unknown and the importance of BLD in the development of ARMD is uncertain[9,131], although some authors are convinced

of the fact that the presence of BLD is positively correlated with the development of ARMD[45,199].

The light microscopical (LM) and transmission electron microscopical (TEM) morphology of BLD will be described in more detail in Chapter 5 and 6.

The development of BLD beneath the RPE appears to be the most reliable histological criterion for the degree of degeneration of the overlying RPE cells[199]. The maculae were therefore classified according to the histological appearance of this deposit (see Chapter 5).

In Figure 3.4.1 a schematic drawing of the histology of the normal macula is shown (BLD class 0).
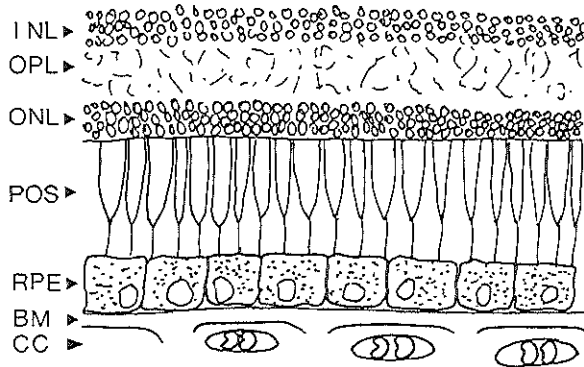

Figure 3.4.1 Schematic drawing of the histology of a normal macula. The innermost layers of the retina, i.e. the internal limiting membrane, the nerve fiber layer, the ganglion cell layer and the inner plexiform layer are not drawn in order to reduce the complexity.
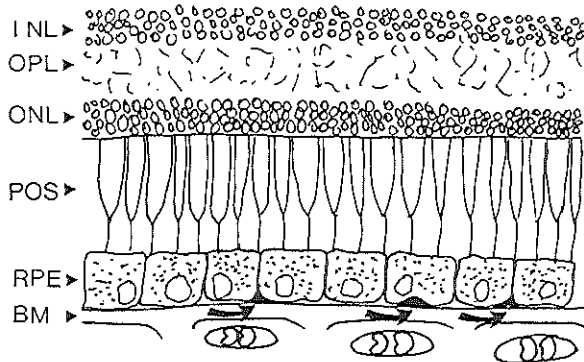

Figure 3.4.2 BLD class 1 (curved arrows)

Small patches of BLD (BLD class 1, Fig 3.4.2) under a few RPE cells will

probably not disturb fundus pigmentation nor do they influence visual acuity[199]. The photoreceptors are unaffected[192]. These changes are considered to be within the limits of normal aging. With increasing age, however, these deposits become larger and form a thin continuous layer (BLD class 2, Fig 3.4.3) and the most commonly visual acuity measured at that stage was
between 5/10 and 6/10 [192,199]. Loss of photoreceptors is mild[192] and on ophthalmoscopy hypo- or hyperpigmentation can be seen.
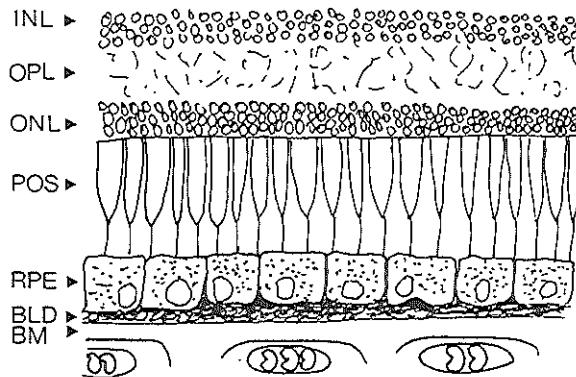
Figure 3.4.3 BLD class 2

In a more advanced stage (BLD class 3, Fig 3.4.4) a thick continuous layer of BLD is seen, which separates the RPE from the inner layer of Bruch's membrane. The overlying RPE becomes elevated and more irregular in shape. Migration of solitary, hypertrophied RPE cells between the photoreceptors can be seen. In this stage visual acuity is markedly decreased with a most commonly visual acuity of 3/10 [199]. Loss of photoreceptors becomes more apparent[192].

Figure 3.4.4 BLD class 3. A thick layer of BLD, of at least half the height of the RPE cells, is present. The RPE is partially degenerated and exhibits intraretinal migration (arrow).

At a later stage, in the eyes with a thick layer of BLD, the RPE cells become depigmented and atrophic finally resulting in the disappearance of the RPE cells and the accompanying photoreceptors. The BLD generally remains present after the RPE has disappeared[19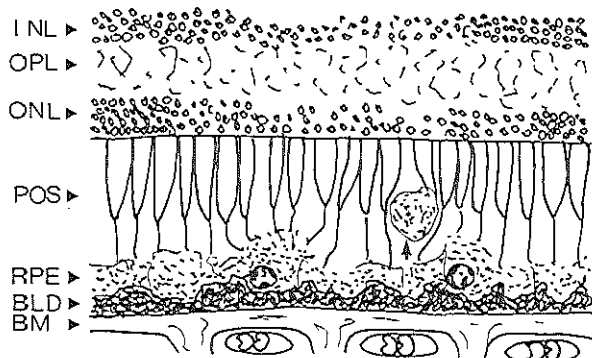9]. This is called the atrophic type of ARMD or geographic atrophy (Fig 3.4.5). Visual acuity is decreased to 1/10 - 3/60. The fall out of photoreceptors appears to be secondary to changes in and beneath the RPE. Alteration in the photoreceptors has not been observed independently of changes in the RPE[192].
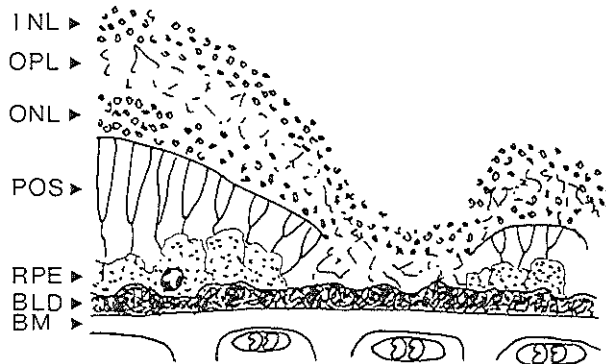
Figure 3.4.5 Geographic atrophy with RPE and photoreceptor cell degeneration. The outer plexiform layer is in direct contact with the persisting BLD.

In other eyes with advanced ARMD, capillaries were described coursing through the BLD, without a previous detachment of the RPE, with which neovascularization is commonly associated. This stage often leads to the formation of a fibrovascular scar in which the BLD is incorporated (Fig 3.4.6). Visual acuity is less than 1/10 when the fovea is involved[199].

24
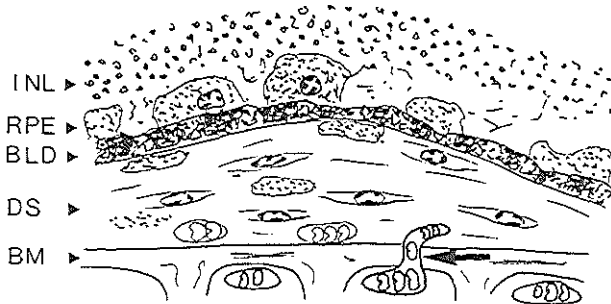
Figure 3.4.6 Disciform macular degeneration, with a fibrovascular scar between the RPE/BLD and Bruch's membrane. The RPE is atrophic or hypertrophic. The photoreceptor cells and the outer plexiform layer are disappeared. A capillary from the choriocapillaris penetrates Bruch's membrane (arrow). The thick layer of BLD persists.

With funduscopy the presence of BLD is still not recognizable as such, although in the past, case reports have been published describing patients with multiple confluent soft drusen, which histologically turned out to be BLD-like material[57]. Like drusen, BLD should be indirectly visible due to the atrophy and degeneration of the overlying RPE. Large amounts of BLD may be recognizable as a fine mottling of the RPE at an early stage of geographic atrophy. With fluorescein angiography BLD might appear as large confluent soft drusen, because BLD is located on the choroidal side of the junctional complex of the RPE and thus fluorescein will probably be accumulated in the BLD. Because of its extensive spread and indistinct borders BLD is probably recognized as soft drusen with fluorescein angiography. Clinico-pathological evaluation is necessary to found this hypothesis.

In other ocular abnormalities, such as Sorsby's fundus dystrophy [25,167], vitelliform macular degeneration [73] and dominant tapeto-retinal dystrophy [25,38,147] deposits can be found, which are histologically different from BLD. These deposits are not located between the RPE cell membrane and the basement membrane, but between the RPE basement membrane and the inner collagenous zone of Bruch's membrane and have a different ultrastructure.

3.5 Drusen

In the eyes of 26% to 85% of people above the age of 30 years another kind of deposit can be see, called drusen [17,29,120,226]. In some families autosomal dominant hereditary drusen are described, which can already be seen between 20 and 30 years of age and lead to a diminished visual acuity from the age of 50 years on. Commonly drusen are thought to be associated with ARMD, but only 0.5% - 2% of the population will finally develop an advanced stage of ARMD, despite the high prevalence of drusen[75]. Drusen have been described predominantly in the periphery of the eye[87], especially in the equatorial region[14,195], although others have described more drusen in the posterior pole[58,200,216]. There is no preference for the left or right eye[29,125] and there is no predilection for males or females[125], but drusen are seen more often in whites than in blacks. In the posterior pole, drusen are randomly scattered, but in some eyes drusen have been reported to be grouped above the collecting venules of the vortex system[58]. Some authors have mentioned that there is a preference for small hard drusen (for explanation see below) to develop above the intercapillary pillars of the choriocapillaris[58]. Clinically, drusen larger than 50 μm can be seen with normal funduscopy. With red-free light, drusen measuring from 25-50 μm can be observed and with fluorescein angiography drusen up to 25 μm are discernable[S.H.Sarks; personal communication, 29,192,211]. Small hard drusen are sometimes confused with lipid-laden RPE cells[21]. These RPE cells are smaller than 50 μm, but display autofluorescence due to a large number of lipofuscin granules and thus appear clinically larger. Drusen less than 100 μm wide are not associated with a decreased vision[120].

At present there is no satisfactory classification which takes into account all different clinical and histological features of drusen[75].

Several types of drusen are distinguished in literature[192]. These have been given several -often confusing- names for each type of drusen, due to separate development of knowledge about drusen by clinicians, pathologists and biochemists. A brief description of the histological terminology will be given here in order to clarify the terminology, used in the rest of this thesis.

The *"typical" or "hard" or "hyalin" drusen or "colloid bodies"* are the predominant type of drusen. These drusen can be found at a relatively young age and in the early types of macular degeneration[192]. Funduscopically such drusen appear as small yellow-white deposits surrounded by a slightly darker rim. By light microscopy these appear as smooth surfaced, globular or dome-shaped structures between the RPE and Bruch's membrane (Fig 3.5.1).
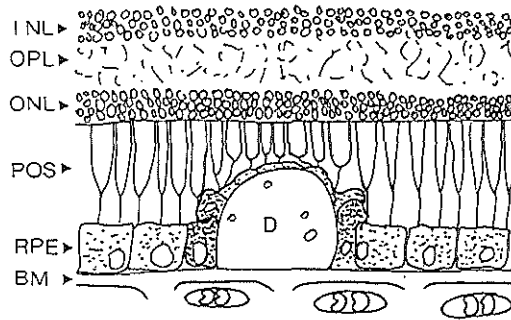

Figure 3.5.1 Schematic drawing of the histology of a human macula with a typical or hard druse (D) between the basement membrane of the RPE and the inner collagenous zone of Bruch's membrane. Notice the hypopigmented RPE cells overlying the druse and the hyperpigmented RPE cells adjacent to the druse.

Hard drusen consist of hyalin material and often contain multiple globular calcifications, lipids and mucopolysaccharides[57,239]. Ultrastructurally drusen are located between the RPE basement membrane and the ICZ of Bruch's membrane. Often the drusen seem to be extensions of the ICZ without a specific boundary. Most hard drusen mainly consist of amorphous, finely granular material with the same electron-density as the RPE basement membrane. Curly membranes and different kinds of vesicles and tubular structures can also be found within these drusen[75].

The RPE cells on top of the drusen are attenuated and hypopigmented, while the laterally located RPE cells are hypertrophic and hyperpigmented[21]. This arrangement of the RPE cells explains why these drusen appear with fundoscopy as small yellow dots surrounded by a slightly darker rim.

Small hard drusen are assumed to be low-risk drusen with respect to the development of advanced stages of ARMD[29,74,75,199,225] or with a decrease in visual acuity [87,120,226]. Small hard drusen did not appear to affect vision[65,199]. In the following chapters I will use the term "hard" drusen.

"Papillary" drusen are clusters of very small drusen-like deposits (Fig 3.5.2). Ultrastructurally these papillary drusen are local thickenings of the ICZ of Bruch's membrane[29,45]. Since these deposits do not exceed half the height of the RPE cells such drusen can not be clinically recognized[193]. Therefore these structures are generally not considered as drusen[4].
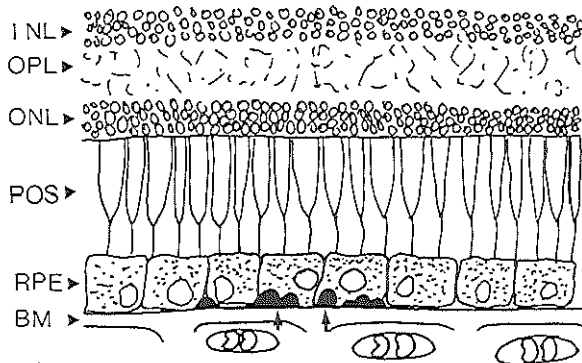
Figure 3.5.2 Papillary drusen (arrows)

"Degenerative", "mixed", "semi-solid", "serogranular" or "intermediate" drusen are drusen with degenerative features. These drusen are assumed to be "hard" drusen that have become "softer", due to the discharge of membranous debris from degenerating RPE, that has passed the RPE basement membrane[194,200]. By light microscopy such drusen are generally larger than the typical hard drusen and consist partly of hyalin material and partly of coarse granular material (Fig 3.5.3).
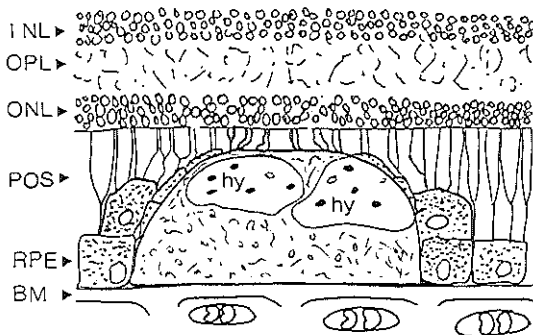
Figure 3.5.3 Degenerative druse. Hy = Hyalin material.

Often such drusen contain many calciumphosphate globules, that can easily be recognized with the von Kossa stain, although all types of drusen may show calcifications[75]. Because these drusen exhibit a variety of stages, from almost completely hyalinized to completely degenerative and because they probably comprise the same entity, I will classify these drusen as hard drusen too in order to avoid sub-classes of the same entity. Ultrastructurally these drusen are composed of small amounts of amorphous, finely granular material and relatively large amounts of membranous, tubular and vesicular material[106]. Different drusen in the same macula have different compositions, which clearly can be seen when these drusen are numerous and become confluent. In this situation the lateral borders of the drusen have disappeared, but the content still seems to be separated from each other by an invisible membrane. Fibrous long spacing collagen is only rarely found within drusen[106].

With increasing age these degenerative drusen are seen more often[29,199,216] and also secondary to trauma, inflammatory and other diseases of the eye[216].

Soft drusen can develop through the softening of hard drusen[75] or more commonly by the formation of soft drusen *de novo*. With funduscopy such drusen usually appear as large yellow-white spots with indistinct or "soft" borders. They are preferentially located within the fovea[192] so that RPE and photoreceptor atrophy developing in relation to soft drusen will commence closer to central fixation. Soft drusen evolve more rapidly than hard drusen. They tend to become confluent and separate the RPE from Bruch's membrane over relatively long distances[75]. Thus, with fundoscopy they often can not be distinguished from small RPE detachments[106,226]. In fact they might actually be serous RPE detachments[75].

By light microscopy (Fig 3.5.4.) soft drusen appear as large drusen with sloping edges and often seem to be empty or contain pale staining membranous or fibrillar material[193]. The overlying RPE is attenuated or atrophic. Similar to BLD, soft drusen are probably a reflection of diffuse RPE disfunction[75,199].

Ultrastructurally soft drusen are composed of double-layered coiled membranes, with some amorphous material and calcifications[108]. In most eyes with soft drusen, BLD is also found in the same area[75,125]. Eyes with large, confluent soft drusen and BLD are at high risk for subretinal neovascularization and

are thus called high-risk drusen[17,29,75,135].
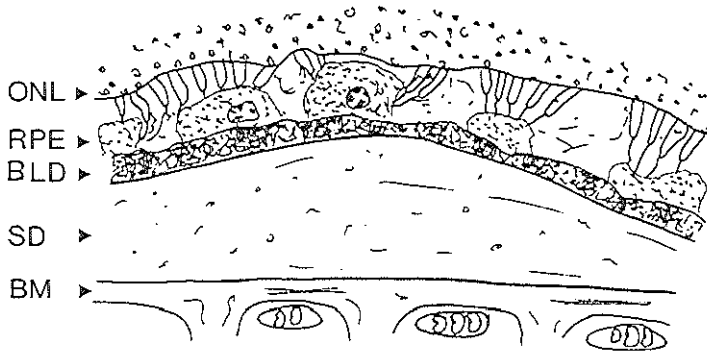
Figure 3.5.4 Soft druse between the BLD and Bruch's membrane. The photoreceptors and RPE are partially degenerated.

Diffuse drusen is a name for a diffuse thickening of the inner aspect of Bruch's membrane (Fig 3.5.5) and is commonly observed in eyes of older persons[106]. Ultrastructural studies disclosed the presence of vesicles, electron-dense particles, fibrils and clusters of long-spacing collagen. I have the impression that it is often used as an obsolete and erroneous name for BLD-like material, internal to the basement membrane of the RPE [29,31,74,75,216,234].
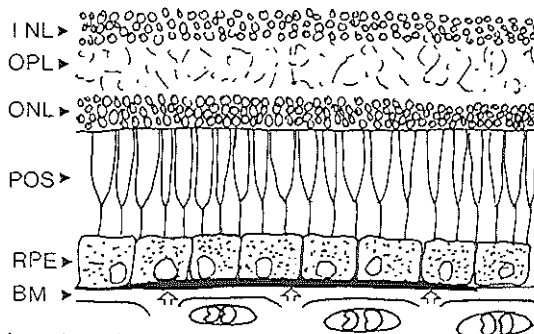
Figure 3.5.5 Diffuse druse (arrow).

Basal laminar drusen or cuticular drusen are nodular thickenings of the basement membrane of the RPE. This is often seen in pseudo-vitelliform degeneration[31]. This term is obsolete and should not be used anymore (ARMD

meeting sept. 1990, Williamstown, USA).

The term *miliary drusen* is an infrequently used name for numerous small hard drusen[31].

On a histochemical basis drusen have been differentiated into *lipid drusen and proteinaceous drusen*.

Drusen have also been divided into *hydrophylic drusen and lipophylic drusen* on the basis of staining intensity with fluorescein angiography[166].

Because there is a sliding scale between typical hard drusen, mixed-, serogranular-, intermediate-, semisolid- and degenerative drusen, which can only be distinguished on very subjective histological and, apart from the size, clinically irrelevant grounds, these drusen will all be classified as hard drusen in this thesis (and in most of the literature). Soft drusen are a different type of drusen, because they can clinically and histologically unequivocally be distinguished from hard drusen, they have a different composition and age of onset. Furthermore, soft drusen have a different clinical relevance from hard drusen. Terms as papillary drusen, diffuse drusen, basal laminar drusen and miliary drusen only mystify terminology and -in my opinion- should not be used. Terms like hydrophylic-, lipophylic-, lipid- and proteinaceous drusen are used in fluorescence angiograms and in biochemical studies and are beyond the scope of this thesis.

Clinically hard drusen are sometimes thought to regress[21,192], to be cleared away by macrophages[108,192,193] or to change into soft drusen prior to the development of geographic atrophy[75,125,194,216]. On funduscopy this process might be confused with the development of large amounts of BLD, which can mask the presence of hard drusen and might cause geographic atrophy. Histologically, in the maculae with geographic atrophy or a disciform scar, hard drusen have usually not been found, but large amounts of BLD are often present [125] and less frequently soft drusen can be found[125,200]. Occasionally neovascularization of regressing drusen is seen[192].

The origin of drusen has been a source of speculation. It has been postulated that drusen consist of exudative material from the choriocapillaris[193]. Others think that they comprise cellular debris from the RPE[43,75,94,108]. The cellular structures, which can be observed within the drusen, are sometimes believed to be derived from macrophages[78,193] or RPE-derived cells [21],

although others do not agree with this hypothesis[94]. Small hard drusen do not predispose to neovascularization[199]. Large drusen are considered to be at risk for neovascularization[78], especially when such drusen are hyperfluorescent on fluorescein angiography[166], due to the accumulation of the aqueous fluorescein. Hypofluorescent drusen are thought to contain more lipids and thus do not accumulate fluorescein. These hypofluorescent drusen might be a reflection of the amount of accumulated lipids in Bruch's membrane, which is sometimes considered to be the initiating factor in serous RPE detachment[166]. Others believe that the composition of drusen is not influenced by the underlying Bruch's membrane[158,199].

3.6 Geographic Atrophy

In geographic or areolar atrophy the RPE has disappeared or is shifted to the lateral borders of the atrophic area. Associated photoreceptor cell loss is seen, because they are metabolically dependent of the RPE[75]. This is histologically best indicated by a gradual loss of the outer nuclear layer of the retina. This results in a direct and firm contact between Bruch's membrane and the outer plexiform layer of the retina. This is one of the reasons why geographic atrophy prevents the development of a serous or hemorrhagic detachment of the retina in the same area[192]. It has also been postulated that new vessel formation is dependent of viable RPE and thus can only occur outside the area of atrophy[192]. The edge of the atrophic area is called the junctional zone. This zone is recognized by several layers of hypertrophic RPE cells and often the flocculent type BLD is present. The loss of the RPE and photoreceptors occurs in advance of the atrophy of the choriocapillaris, although vascular insufficiency might be involved in the pathogenesis of geographic atrophy[74,75]. Neovascularization, if present, tends to occur in this place accompanied by giant cells and macrophages[74,192,205].

In literature three patterns of geographic atrophy are distinguished[192]:
1) primary age-related atrophy. This process of atrophy is slow and leads to a slow deterioration of visual acuity[205]. Under the age of 70 years geographic atrophy is rarely seen, on age 70-80 years 3% of the people have geographic atrophy[17] and above 80 years this is seen in 15%[216]. The rate of progression of

geographic atrophy varies from 15 to 375 μm/year (mean 139 μm/year) and tends to progress faster under the age of 75 years[205]. Measurement of the visual acuity alone, is a poor guide in estimating the progression of geographic atrophy[192].

2) *Drusen-related atrophy.* These eyes typically display small, discrete, rounded patches of atrophy in relation to individual regressing drusen or drusen clusters[199]. Gradually this multifocal pattern becomes confluent and the drusen fade, but their earlier influence could be inferred from residual calcified particles and from surrounding patches of drusen-related atrophy. This pattern of geographic atrophy has been described at a younger age than the age-related atrophy, from the age of 51 years on[192].

3) *Other causes[154];* Geographic atrophy, following the resolution of a serous RPE detachment and those detachments formed by the confluence of soft drusen[10]. Also after trauma and after vascular occlusions of the retina or choroid.

The great majority of patients falls into the first two groups. The size of the affected area does not reflect visual acuity, but depends on the patient's ability to find a surviving island of retina within the atrophic area.

3.7 Subretinal Neovascularization and Disciform Macular Degeneration

In some aged eyes, subretinal new vessels have been found between the RPE and Bruch's membrane, preferentially in the presence of a thick-layer of BLD[11,195,197,199,200] and soft drusen[75]. These abnormal vessels originate from the choriocapillaris and penetrate Bruch's membrane by pre-existing or newly formed breaks. Most times, the serous detachment is the result of leakage of plasma from the new vessels[41]. These new vessels tend to exudate serous fluid, proteins, lipids or blood under the RPE, leading to a pigment epithelial detachment[75,216]. This fluid might even break through the RPE monolayer and cause a neurosensory detachment too. Therefore this type of ARMD is often called the exudative or "wet" type of ARMD. A subsequent fibrovascular, disciform scar is formed by fibroblasts that invade the hemorrhage[75]. This process is called the disciform reaction. The overlying RPE cells and photoreceptors are separated from their supply of nutrients from the choriocapillaris by the scar. The RPE cells are shifted laterally and start to clump, which often results in several layers of

pigmented cells, buried in a thick fibrotic scar. The overlying photoreceptors become atrophic and finally disappear. The result is a disciform scar in the macula and a seriously diminished visual acuity in 70% of these patients within 24 months[11]. Since the histological abnormalities, leading to neovascularization, extend over several disc diameters, the disciform response can be multifocal and particularly endanger the fovea, where the changes are generally most severe[199]. This exudative form of macular degeneration has been found in 0.5% of the population[17]. Disciform lesions account for 80%-90% of blindness due to ARMD[92,261]. Disciform macular degeneration is generally seen at a higher age than geographic atrophy[100]. New subretinal vessels often remain clinically occult[195,211].

In the peripheral retina near the ora serrata subretinal neovascularization, accompanied by flat fibrotic scars, are often histologically seen above the age of 60 years[58,86,196,211]. Clinically this is asymptomatic and remains unnoticed, because a fibrotic scar first becomes clinically visible when it histologically appears to be composed of at least 5-6 cell layers.[196].

ARMD is often bilateral, but a time interval of several years between fellow eyes in the development of ARMD is usually seen[118]. Patients with the exudative form of ARMD have a yearly risk of 12%-15% to develop an exudative lesion in the contralateral eye[50]. This risk has been calculated to be 17% to 29% within three years[221] or 23% within four years[191].

In patients with pseudoxanthoma elasticum and Paget's disease, ruptures in Bruch's membrane are often present, called angioid streaks. Most of these patients loose central vision, due to a disciform reaction[216], but sometimes no subretinal neovascularization is found in these eyes[196]. Probably, more stimuli are needed to induce angiogenesis. In ARMD this is suggested to be caused by the angiogenic stimulation of RPE cells[161] or macrophages[171]. These macrophages are seen at the choroidal side of Bruch's membrane in eyes with a disciform reaction. In these maculae, Bruch's membrane is thinner than normal for that age and is sometimes even discontinuous[195]. Subretinal neovascularization is often accompanied by a low-grade chronic inflammatory reaction as seen in histologic sections[192].

Chapter 4: Aim of the study

In the preceding chapters, current knowledge on the normal histology, age-related changes in the human macula and ARMD is summarized. However, this knowledge is frequently based on one single or only a few observations and it is often mainly descriptive without quantification and/or statistical analysis. Moreover, the results of different investigations are often controversial or even contradictory. Considerable research has been performed in the field of biochemistry, cell biology, histology, clinical evaluation and epidemiology, but several alternatives have remained unexplored or unquantified.

The primary aim of this study was to gain more information about the basal laminar deposit, a substance which until now was relatively unknown, but was thought to be associated with the development of age-related macular degeneration. Because experimental animal models in which ARMD can be induced are not known, we chose for a deductive method in which a large series of post-mortem human eyes of all ages were studied. Special attention was directed to the morphology, composition and age-distribution of BLD in the population (chapters 5,6,7,8,9).

In addition the histological and morphometrical age-related changes in the maculae (chapter 5), the peripheral retina (chapter 10) and the choriocapillaris (chapter 11) of these eyes were quantified and analyzed statistically.

We also investigated the histology of human pseudophakic eyes with and without an UV-filter in comparison to normal phakic eyes (chapter 12).

For this thesis various techniques have been used such as light microscopical histology, immunohistochemistry, immunofluorescence, transmission electron microscopy, immunoelectron microscopy, electron probe X-ray microanalysis and image analysis. In addition various computerized statistical procedures were applied.

CHAPTER 5

Histologic Features of the Early Stages of Age-related Macular Degeneration: a Statistical Analysis.

Theo L. van der Schaft,[1] MD; Cornelia M. Mooy,[1,2] MD;
Wim C. de Bruijn,[2] PhD; Frans G. Oron,[2] BSc;
Paul G.H. Mulder,[3] MSc; Paul T.V.M. de Jong,[1] MD, PhD, FCOphth.

From the Institutes of Ophthalmology (1), Pathology (2) and
Epidemiology and Biostatistics (3)
Erasmus University Rotterdam, the Netherlands

INTRODUCTION

For patients with clinical signs of age-related macular degeneration (ARMD), postmortem light microscopic (LM) examination has shown an accumulation of material between the retinal pigment epithelium (RPE) and Bruch's membrane in the macular area[199]. In the past, these basal deposits have been called *basal laminar deposit(s),[192] basal linear deposit(s)[131,199] and linear basal deposit(s)*[45], all indicating identical materials. We prefer the singular expression basal laminar deposit[202]. The presence of BLD has been found to increase with age [75,131,199,202] and large deposits have often been accompanied by visual loss[199]. Sarks[199] stated that the quantity of the histologically demonstrated BLD is the best indicator of the degree of RPE atrophy and photoreceptor degeneration[199]. This has led to the theory that the deposition of BLD might be associated with the development of ARMD.

BLD is extracellular material, located between the RPE and Bruch's membrane when seen by light microscopic examination[131,199]. Transmission electron microscopy (TEM) has shown that it consists mainly of long-spacing collagen, fibrillar and homogeneous material and a small number of vesicles and vesiculoid bodies[131,202] and that similar material is located in the outer collagenous zone (OCZ) of Bruch's membrane[202].

In the literature, extensive histologic data on changes in aging human maculae are available[15,45,75,107,131,192,193,199,202,216,234,260]. However to the best of our knowledge, this is the first report to include a statistical analysis of the histologic age distribution of BLD, drusen and changes in Bruch's membrane as well as the correlations between these changes in a large series of human maculae. Furthermore, we studied the presence of BLD-like material and drusen in the peripheral retina compared with BLD and drusen in the macula.

MATERIALS AND METHODS

We examined 227 human eyebank eyes from 182 subjects. Eyes from patients with a history of diabetes mellitus, an intraocular artificial lens, or panretinal photocoagulation were excluded from this study. There were 104 male

subjects (mean age: 64 years) and 65 female subjects (mean age: 72 years); in 13 cases, the sex of the subject was not available. We investigated 137 unpaired and 45 paired eyes, including 118 right eyes and 105 left eyes (4 eyes were unknown). The paired eyes were processed in an identical manner and examined independently from the fellow eye. The age at time of death ranged from 8 to 100 years (mean: 68 years, S.D. = 19 years).

The time interval between death and fixation was registered for 123 eyes; it ranged from 2 to 24 hours (mean: 9 hours, SD = 5 hours). Immediately after removing the cornea, 111 eyes were fixed with a mixture of glutaraldehyde (1% vol/vol) and a formaldehyde solution (4% vol/vol), and 85 eyes were fixed with only a formaldehyde solution (4% vol/vol) in a 0.1 M phosphate buffer (pH 7.2). For 31 eyes the kind of fixative was not registered.

After at least 24 hours of fixation, a horizontal tissue block, including the optic disc, the macula, and the ciliary body, was cut from the globe. The macula was cut from this block and dehydrated with graded alcohols followed by absolute chloroform. The macula and the remaining part of the block were embedded separately in paraffin according to routine procedures. Three levels in the maculae, with an in-between distance of 140 μm, 6 sections 7 μm thick were cut and stained with hematoxylin-azophloxin (H & A), periodic acid-Schiff (PAS), Mallory, Masson, Alcian blue, and von Kossa stains[30].

To check if these 3 examined levels were representative for a whole macula, serial sections of the entire macula were made of 4 eyes, aged 76, 90, 92 and 93 years. Each fifth section was stained and examined, which resulted in a mean number of 62 sections per macula. These 4 maculae were classified by studying similar combinations of 3 levels of sections with the same in-between distance of 140 μm as in the 227 maculae of the study.

The presence of BLD and drusen and the thickening and calcification of Bruch's membrane in the macula were assessed at 400X magnification using a modified version of Sarks' classification[199] (Table 5.1).

The drusen were divided into two groups: hard drusen, which were usually dome-shaped with a hyalinized appearance, and soft drusen, which were usually larger with sloping edges and a granular appearance. The presence of calcifications in both types of drusen was assessed with the Von Kossa stain.

Table 5.1 Classification of BLD and drusen and the calcification and thickening of Bruch's membrane in the maculae according to a modified version of Sarks[199]. In each triplet of sections the highest class was registered.

BLD   class 0   no BLD
            class 1   small, solitary patches on the basal
                              side of the RPE
            class 2   a thin, continuous layer
            class 3   a thick layer, at least half the height
                              of the retinal pigment epithelium cells

hard and soft drusen
            class 0   no drusen
            class 1   one to three drusen
            class 2   four to ten drusen
            class 3   many or confluent hard drusen

Bruch's membrane thickness
            class 0   not thickened, a thin line
            class 1   slightly thickened, $< 1/3$ of the capillary
                              diameter of the choriocapillaris
            class 2   thickened, between $1/3$ and $1/2$ of the
                              capillary diameter; with intercapillary
                              pillars reaching halfway through the
                              choriocapillaris
            class 3   marked thickening with intercapillary
                              pillars reaching the choroidal side of the
                              choriocapillaris

Bruch's membrane calcification
            class 0   no calcification
            class 1   less than 10 calcified patches
            class 2   10 or more calcified patches
            class 3   long stretches of continuous calcification

Thirty-five (35) maculae were examined independently by the first author and an ophthalmic pathologist (C.M.M.) to determine interobserver variation. The same maculae were examined a second time in a masked fashion by the first author 2 months later to determine intraobserver variation. Interobserver and intraobserver variations were calculated with the weighted kappa test.

To study changes in the peripheral retina, ranging from the nasal side of the optic disc to the ciliary body and from the temporal side of the macula to the ciliary body, 3 sections 7 μm thick were sliced from the remaining part of the

tissue block of 71 eyes from 50 subjects. Two sections from each tissue block were stained with the H & A and one with the Mallory stain.

The peripheral retina was examined for the presence of BLD-like material and drusen. Bruch's membrane was not classified, because of its different staining properties in the retinal periphery, which make it often difficult to distinguish Bruch's membrane from the choroid.

For statistical analysis, the Spearman rank correlation test was used to test the correlation between the ordinal variables BLD, hard and soft drusen and thickening and calcification of Bruch's membrane (class 0 to 3). The same tests were used to determine the correlation of these variables between the 45 paired maculae. The Mann-Whitney U test was used to determine the association between the above mentioned variables and left or right eye, geographic atrophy and subretinal neovascularization. Multiple linear regression was used to test the association between the variables and sex, adjusted for age. The dependency of the variables on age was estimated by fitting a polytomous logistic regression model. This analysis was chosen because our dataset has been sampled conditionally on age. This model is not dependent on the differences in sample size of the various age groups. P-values below 0.05 were considered statistically significant. For all statistical analyses and for the calculation of percentages, only one eye from each subject was used (except for correlations between paired eyes).

RESULTS

The age distribution of the 182 eyes is presented in Figure 5.1.

Histologic features

BLD was recognized in Mallory-stained sections as light blue granular material and in Masson stained sections as light green granular material, adherent to the basal side of the RPE. BLD did not stain with Alcian blue, but did not stain with P.A.S.

In eyes with class 1 BLD, the structure of the RPE in the macula was only slightly disturbed. In eyes with class 2 BLD, the RPE had been slightly lifted from Bruch's membrane and was more irregular in shape. Class 3 BLD consisted of a thick continuous layer with a granular appearance. The architecture of the RPE cells was more disturbed: the RPE cells were flattened or atrophic and contained fewer pigment granules than in classes 0 to 2 (Figs 5.2a-c).

40

Age distribution of 182 eyes
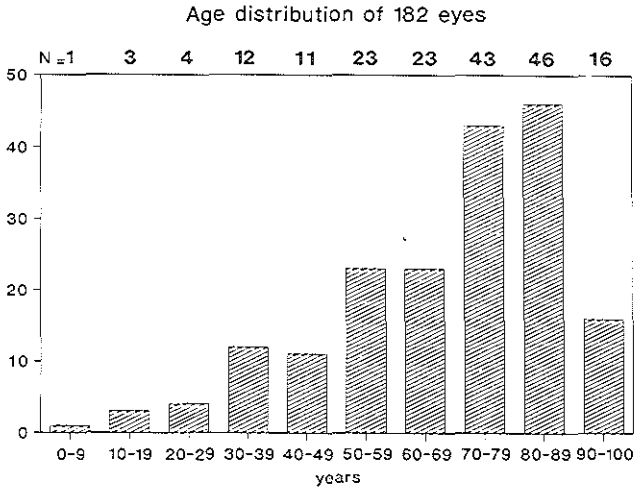
Figure 5.1) Age distribution of the 182 eyebank eyes used in this study.
The number of eyes (N) in each decade is given above each column. Only one eye from each person is represented.
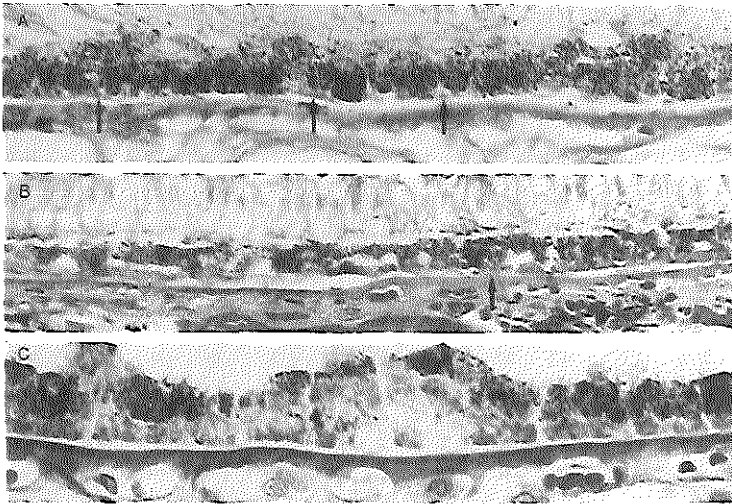
Fig 5.2) Sections of maculae stained with Mallory, which stains BLD blue (magnification x500).
a) BLD class 1: small patches of BLD (arrows) under a slightly distorted RPE layer.
b) BLD class 2: a continuous thin layer of BLD is present (arrow) with more distortion of the RPE.
c) BLD class 3: thick layer of BLD with atrophic RPE. Note the loose structure of the BLD.

Fig 5.3) Age distribution and classification of BLD in the maculae of 179 eyes. Each column represents 100% of the absolute number of eyes (N) given above the column. Note that BLD is seen after the fourth decade and occurs more frequently and in increasing amounts with increasing age.
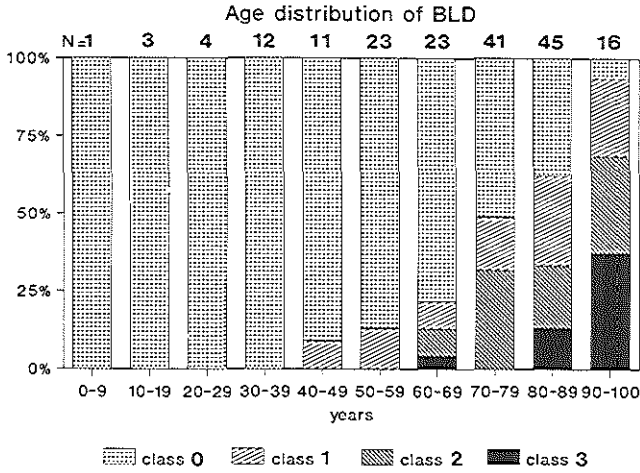
BLD was found in 39% of the 182 maculae; the youngest macula with BLD being 40 years old (Fig 5.3). The mean age plus standard deviation at which BLD, drusen and changes in Bruch's membrane were present are listed in Table 5.2 for each class.

	BLD			hard drusen			soft drusen			thickening BM			calcification BM		
		age			age			age			age			age	
	N	mean	(SD)	N	mean	(SD)	N	mean	(SD)	N	mean	(SD)	N	mean	(SD)
class 0	107	60	(19)	115	63	(20)	163	66	(19)	12	50	(26)	65	57	(22)
class 1	30	76	(13)	48	74	(16)	12	79	(11)	41	59	(20)	42	71	(13)
class 2	29	80	(10)	15	80	(10)	4	83	(12)	70	68	(16)	42	72	(15)
class 3	13	87	(9)	4	79	(9)	3	88	(5)	56	79	(12)	26	79	(12)
not available	3			0			0			3			7		
total	182			182			182			182			182		

Table 5.2 Classification of changes in the macula and mean age in years at which these changes were found. N indicates the absolute number of eyes. SD represents the standard deviation of the mean age (in years). Note the rise in mean age with increasing amount of BLD, number of drusen and extent of thickening and calcification of Bruch's membrane. Only one eye from each person was used for this table. Not available refers to unclassifiable or missing sections.
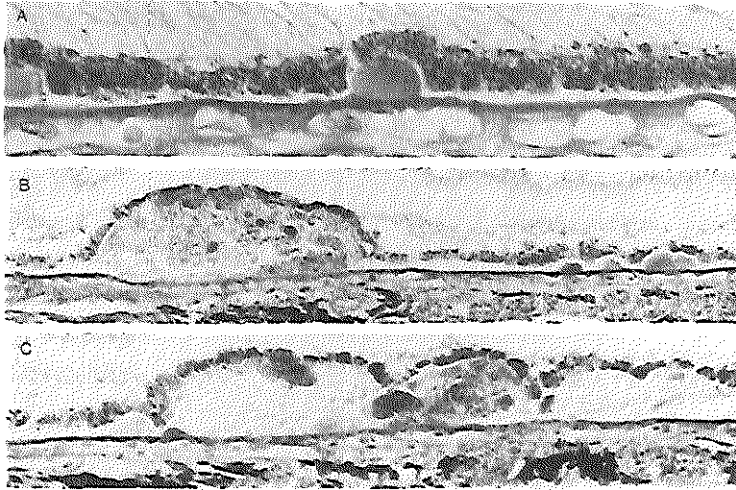
Fig 5.4) Sections of maculae stained with Mallory
a) druse class 1: small hard drusen with a hyaline structure (x500).
*b) drusen class 2: large druse and a few small drusen. Note the inhomogeneous composition of the
   large druse (x160).*
c) drusen class 3: large, confluent drusen (x200).

The hard drusen stained brownish-blue with the Mallory stain (Figs 5.4a-c), while the soft drusen had a pale blue granular appearance. Both hard and soft drusen were stained positive with P.A.S. stain and negative with Masson and Alcian blue stains. Most hard drusen extended under 3 or 4 RPE cells, lifting these cells up from Bruch's membrane. The RPE cells overlying drusen were flattened and often showed loss of pigmentation. The adjacent RPE cells were often hypertrophic. In class 3, hard drusen were often confluent with adjacent drusen, although the structure of the different hard drusen remained visible.

Age distribution of hard drusen
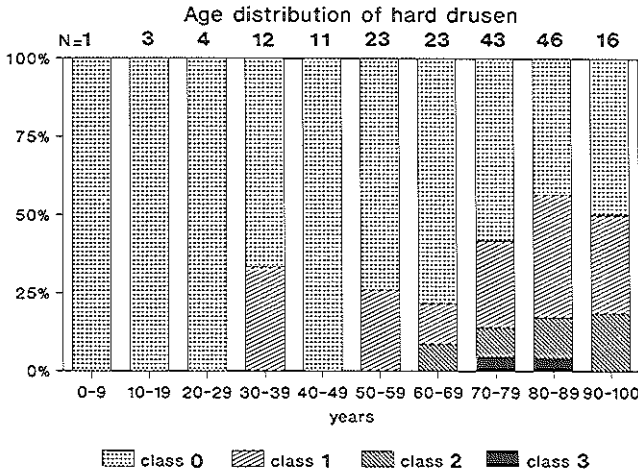
Fig 5.5) Age distribution and classification of hard drusen in the maculae of 182 eyes.

Hard drusen were found in 67 (37%) of the 182 maculae, the youngest being 34 years old (Fig 5.5, Table 5.2). Soft drusen were found in 19 (10%) of the 182 maculae, the youngest was 54 years old (Fig 5.6, Table 5.2). Numerous small globular calcifications were found within 42 (65%) of both hard and soft drusen (mean age: 77 years). Hard drusen without calcifications were seen at a mean age of 71 years.
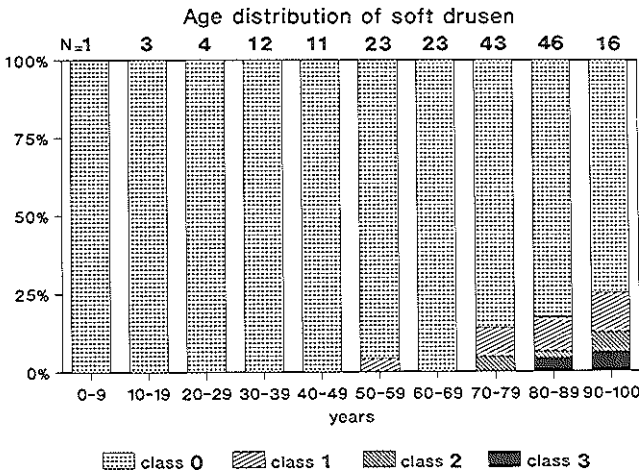
Age distribution of soft drusen

Fig 5.6) Age distribution and classification of soft drusen in the maculae of 182 eyes.

The staining properties of Bruch's membrane were pronounced in the P.A.S. and Mallory stains. In the first two decades Bruch's membrane consisted of a thin layer (Figs 5.7a-d). After age 19, however, thickening of Bruch's membrane was found in 92% of the 182 maculae (Fig 5.8, Table 5.2). This thickening was seen mainly on the choroidal side of Bruch's membrane and between the capillaries of the choriocapillaris where the intercapillary pillars are formed.
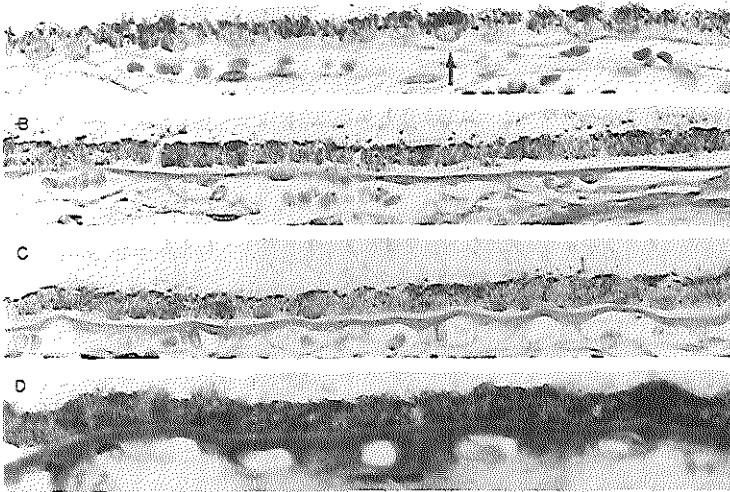
Fig 5.7) Sections of maculae stained with Mallory (a-c) and H&A (d).
a) Bruch's membrane class 0: a thin line (arrow, x500).
b) class 1, (x400).
c) class 2, (x400).
d) class 3 (freeze section, x500).

Age distribution of thickening of Bruch's membrane
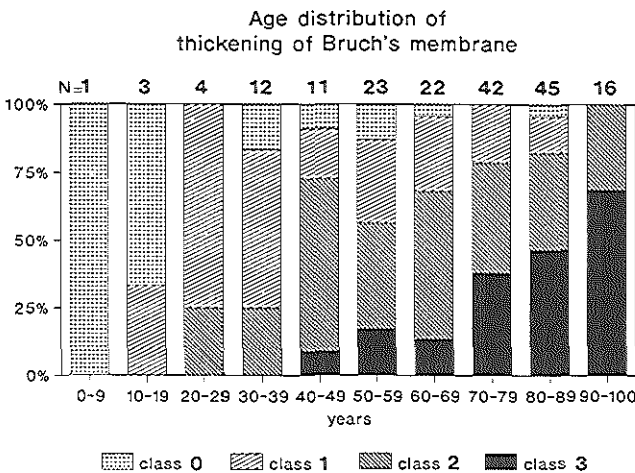
Fig 5.8) Age distribution and classification of the thickening of Bruch's membrane in the maculae of 179 eyes. Note that these changes start at a very young age and increase during life.

45

Calcification of Bruch's membrane, which stained black with the von Kossa stain (Figs 5.9a-c), was found in 59% of the 182 maculae over 33 years old (Fig 5.10, Table 5.2). These calcifications were localized in the elastic layer of Bruch's membrane, ranging from small patches in class 1 to long continuous plaques in class 3, and exhibited many breaks. Breaks without evidence of cell ingrowth presumably can be attributed to the postmortem processing and sectioning of the tissue.
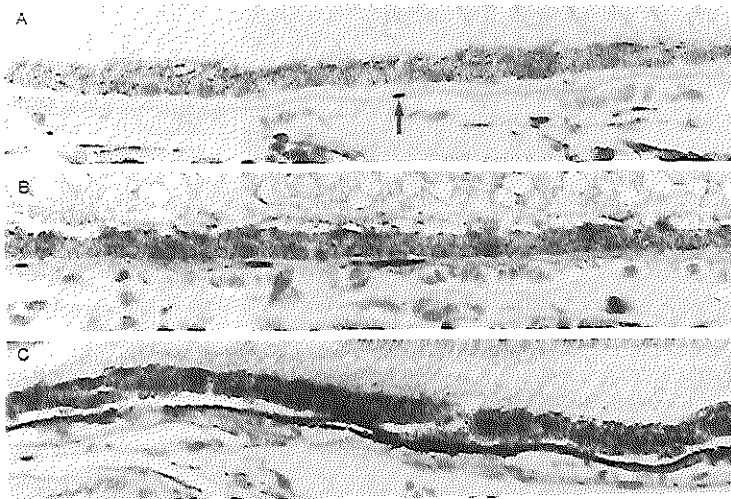
Fig 5.9) Sections of maculae stained with von Kossa, which stains the calcifications in Bruch's membrane brown-black.
a) class 1: small calcification (arrow, x400).
b) class 2: a few calcifications are visible, (x400).
c) class 3: almost the entire Bruch's membrane is calcified, (x250).

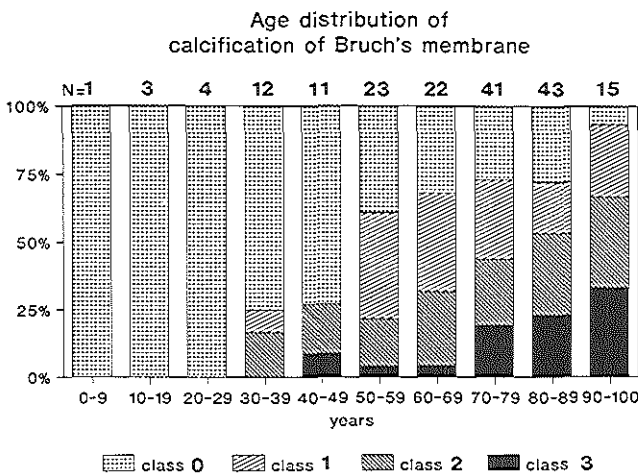Age distribution of calcification of Bruch's membrane

Fig 5.10) Age distribution and classification of calcification of Bruch's membrane in the maculae of 175 eyes.

Geographic atrophy was found in 9 (4.9%) out of 182 eyes at a mean age of 78 years (Fig 12.1). Seven of these eyes were from subjects older than 70 years, which is 6.6% of the total number of subjects 70 years or older. Seven of these eyes also showed persisting BLD in varying amounts, but only 2 had drusen.

Atrophy of photoreceptor outer segments in combination with the presence of BLD was hard to determine in a systematic way because of frequent displacement of the retina during tissue processing. In the maculae with geographic atrophy, the photoreceptor cell layer was atrophic, as indicated by flattening of the outer nuclear layer, due to the disappearance of the cell nuclei, and the disappearance of the photoreceptor inner and outer segments.

Subretinal neovascularization was found in the maculae of 5 (2.7%) out of 182 eyes at a mean age of 79 years. Four of these 5 eyes were from subjects older than 70 years, which is 3.8% of the total number of subjects 70 years or older. Three of these 5 eyes contained no drusen at all. However, all 5 eyes had BLD class 2 or 3. A disciform scar was not observed in this study.

The choriocapillaris showed no specific abnormalities that could be correlated directly with the presence of BLD or drusen in one part of the macula and the absence of BLD and drusen in an adjacent part.

Table 5.3 Classification of changes in the maculae of 45 paired eyes.

	BLD		hard drusen		thickening BM		calcif. BM	
	left/right		left/right		left/right		left/right	
class 0	22	26	27	26	1	5	17	17
class 1	8	10	11	15	14	10	7	10
class 2	11	5	5	3	13	12	12	9
class 3	1	1	2	1	16	17	5	5
not available	3	3	0	0	1	1	4	4
total	45	45	45	45	45	45	45	45

The number of soft drusen in this series was too small to represent here. The numbers are the absolute number of eyes. Left and right refer to the left or right eye. Not available refers to unclassifiable or missing sections.

The classification for the presence of BLD and drusen and changes in Bruch's membrane is given in Table 5.3 for the 45 paired eyes. The 45 contralateral eyes were only used for this table and are not included in the above mentioned percentages. The number of soft drusen in this series was too small to

represent here.

In the peripheral retina, a material similar to BLD was found between the RPE and Bruch's membrane (Fig 5.11). This BLD-like material had a more compact structure than BLD in the macula. The staining properties were similar. In most eyes, the difference between drusen and this material was distinct. The overlying RPE cells were flattened and had an irregular shape. The drusen in the peripheral retina were all hard drusen with the same shape and staining properties as hard drusen in the macula. The classification for BLD-like material and the number of hard drusen in the peripheral retina is given in Table 5.4. This BLD-like material was found in 44%, and hard drusen were present in 78% of the peripheral retinas of the 50 subjects. Soft drusen were not found. Notice the positive association between the amount of BLD and the mean age, and between the number of drusen and the mean age.
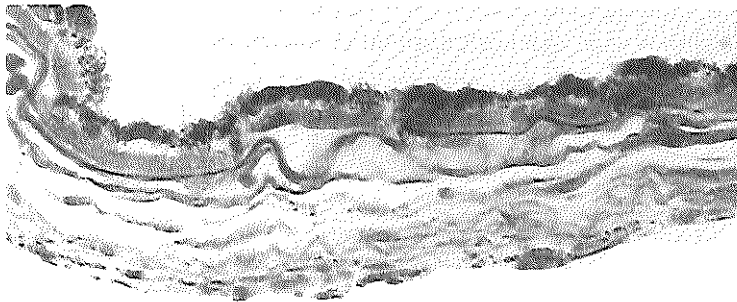
Fig 5.11) Section of the equatorial part of the eye stained with Mallory (x500). A thick continuous layer of BLD-like material can be seen under the RPE. Note the more compact structure of this material, but the same staining properties as BLD.

Table 5.4) Classification of BLD and drusen in the peripheral retina of 50 unpaired eyes. Note the positive association between the amount of BLD and the mean age, and the number of hard drusen and the mean age. Hard drusen were frequently found in the peripheral retina. SD = standard deviation. N = absolute number of eyes.

	BLD			hard drusen		
	N	age mean	(SD)	N	age mean	(SD)
class 0	28	67	18	11	52	19
class 1	6	78	9	13	74	8
class 2	9	80	6	14	79	14
class 3	7	85	5	12	81	8
total	50			50		

Of the four maculae of which serial sections were made, a mean of 62 classifications per macula was made. The results are given in Table 5.5. The numbers in the Table are percentages of how many times a certain classification was made for drusen, BLD and thickening of Bruch's membrane. The smaller the spreading in a column, the larger the representativeness of each triplet of sections for the macula. Comparison between these four maculae or between this Table and other Tables may not be made. The variation in the classification of BLD was mainly due to local differences in the amount of BLD. The distribution of drusen in the macula was more homogeneous. The thickness of Bruch's membrane was more pronounced in the center of the macula and decreased towards the edges.

Table 5.5) Results of serial sectioning of four maculae. The eyes were aged 76, 90, 92 and 93 years. A mean number of 60 classifications was made of each macula, each classification based on groups of three sections with the same in-between distance of 140 μm as was done in the sections of the 227 maculae. The numbers in the table are percentages of how many times a certain classification was made for drusen, BLD and thickening of Bruch's membrane. The smaller the spreading in a column, the larger the representativeness of each triplet of sections for the macula. Comparison between these four maculae or between this table and other tables may not be made.

	hard+soft drusen				BLD				thickening BM			
age (yrs)	76	90	92	93	76	90	92	93	76	90	92	93
	%	%	%	%	%	%	%	%	%	%	%	%
class 0	0	0	0	0	0	18	44	0	0	0	0	0
class 1	8	94	0	0	79	12	56	0	0	16	0	0
class 2	92	6	58	0	21	41	0	0	74	56	86	37
class 3	0	0	42	100	0	29	0	100	26	28	14	63

Statistical analysis

The correlations between the variables studied are given in Table 5.6. The presence of BLD, hard and soft drusen, thickening and calcification of Bruch's membrane was strongly correlated with age (P< 0.0001). No correlation was found between these variables and sex or left or right eye. A positive correlation was found for BLD with geographic atrophy (P = 0.0017) and BLD with subretinal neovascularization (P = 0.001) and for soft drusen with geographic atrophy (P = 0.0004). There was no correlation with the period between death and fixation and the presence of BLD in the macula.

Between paired eyes, a strong correlation was found for the presence of BLD (corr.coeff. 0.57; P<0.001), drusen (corr.coeff. 0.7; P<0.001), thickening (corr.coeff. 0.7; P<0.001) and calcification of Bruch's membrane (corr.coeff. 0.75; P<0.001).

Table 5.6 Cross table showing Spearman rank correlations between histological changes in the macula. Corr.coeff. refers to correlation coefficient. P values are given in parentheses. N.S. = not significant.

	BLD	hard drusen	soft drusen	thickening	calcif.
BLD corr.coeff.	1.0	.20	0.31	.50	.38
(P values)		(.004)	(<.001)	(<.001)	(<.000)
hard drusen		1.0	.26	.17	.14
			(<.001)	(.012)	(.037)
soft drusen			1.0	.26	-.003
				(<.001)	N.S.
thickening				1.0	.36
					(<.001)
calcification					1.0

There was a positive correlation between the presence of BLD-like material in the peripheral retina and BLD in the macula of the same eyes (corr.coeff. 0.39; P=0.003) and between the presence of drusen in the peripheral retina and in the macula of the same eyes (corr.coeff. 0.42; P<0.001). The presence of both BLD-like material and drusen in the peripheral retina correlated significantly with increasing age (P< 0.0001).

Interobserver and intraobserver variations were good to excellent with weighted kappa values > 0.6, except for classification of the thickening of Bruch's membrane (Table 5.7).

Table 5.7 Interobserver and intraobserver variation in the histological classification of the changes in the macula, presented as percentage agreement and as the weighted kappa value.

	BLD		drusen		thickening BM		calcif.BM	
	%	kappa	%	kappa	%	kappa	%	kappa
interobserver	69	0.61	69	0.63	46	0.33	71	0.71
intraobserver	77	0.77	72	0.70	54	0.38	76	0.81

DISCUSSION

The results of our study demonstrated in a quantitative way that the presence of BLD and both hard and soft drusen as well as the thickening and calcification of Bruch's membrane are attributable to aging and that the extent of these changes increases with age. However, the significant correlations between these aging changes do not necessarily signify a causal relationship. That means that we do not know if one aging change that begins at an earlier age (e.g., the thickening of Bruch's membrane) necessarily is the cause of other changes that are found at a later age. The exact pathogenesis of these changes still remains unclear[58,193]. The early start of these changes is, however, surprising.

In contrast to BLD, hard drusen and the thickening of Bruch's membrane, no correlation was found between the presence of soft drusen and calcification of Bruch's membrane in the macula. There is probably no causal relationship between these two aging changes. Another possibility is that the number of maculae in which soft drusen were found was too small to determine the correlation.

The absence of a significant correlation between the presence of BLD and the time between death and fixation of the eyes implies that BLD is not a postmortem artefact.

In 59% of the eyes examined in this study, calcification of the elastic layer of Bruch's membrane was present in varying amounts. The origin and the significance of these calcifications remain unclear. It has been stated that degeneration of elastin induces calcification[112], which might explain the location of these calcifications in the elastic layer of Bruch's membrane. Breaks in Bruch's membrane facilitate ingrowth of choroidal capillaries[112]. There is, however, no reason to believe that calcification of Bruch's membrane, which was seen in a high percentage of the maculae, increases the risk of breaks in Bruch's membrane with subsequent subretinal neovascularization. Breaks without cellular ingrowth were assumed to be artefacts. In our study, almost all breaks seemed to have developed during postmortem tissue processing.

Sarks[199] found that 14% (6 of 42) of the patients with BLD class 3 had histologic evidence of subretinal neovascularization. In our study, subretinal neovascularization was found in 5 eyes (2.7%). These 5 eyes contained remarkably large quantities of BLD, classes 2 and 3, in contrast to drusen, which were seen in only 2 of these eyes. In one case, a soft druse was infiltrated by a bloodvessel

coming from the choriocapillaris. It may suggest that vessel ingrowth might be more closely related to large quantities of BLD rather than the presence of hard drusen. This is confirmed by our results, which show a positive correlation between BLD and subretinal neovascularization and geographic atrophy. Also a positive correlation between soft drusen and geographic atrophy was found. However, neither BLD nor drusen necessarily lead to subretinal neovascularization or geographic atrophy.

In paired eyes the amount of BLD, number of drusen and extent of the changes in Bruch's membrane were the same, as has been described by others[29,166]. This is in accordance with clinical findings that visual loss in one eye will be followed by a drop in visual acuity in the contralateral eye[50,120]. The similar results in paired eyes also point to a good reproducability of the technique, since these eyes were processed and examined independently.

The correlation between the presence of BLD in the macula and the BLD-like material in the peripheral retina suggests that their pathogenesis is similar.

Care must be taken not to interpret the age distribution of the eyes in this study as epidemiologic data because eye bank eyes are not representative of the entire population.

The aim of the study was not to determine the total number of drusen in the macula or the total amount of BLD. Therefore, sections of only three levels of the macula and the peripheral retina of each eye were examined histologically. From Table 5.5 we can conclude that the chance of underestimation or overestimation of the classification of drusen and the thickening of Bruch's membrane was relatively small. For the classification of BLD, larger differences were seen.

The poor interobserver and intraobserver variation in the classification of the thickening of Bruch's membrane was due to the marked local differences within one macula. The classification of this thickening was related to the capillary diameter of the choriocapillaris, which is the most constant structure in the vicinity of Bruch's membrane, although this diameter tends to decrease slightly with age[199].

In conclusion, we can state that the presence of BLD, drusen and changes in Bruch's membrane are related to age, and are seen not only in the macula but also in the peripheral retina and are comparable in paired eyes. All of these changes in the macula start at a relatively young age, especially thickening of Bruch's membrane, and increase during life. Although we have observed these macular changes in a large percentage of cases, more advanced stages of ARMD were very scarce. Probably more factors are needed for the development of ARMD.

CHAPTER 6

Are Basal Laminar Deposits Unique for Age-related Macular Degeneration?

Theo L. van der Schaft,[1] MD; Wim C. de Bruijn,[2] PhD; Cornelia M. Mooy,[1,2] MD; Diane A.M. Ketelaars,[2] BSc; Paul T.V.M. de Jong,[1] MD

From the Institutes of Ophthalmology (1) and Pathology (2)
Erasmus University Rotterdam,
the Netherlands

INTRODUCTION

Visual loss due to ARMD is an increasing problem in the Western world, owing to a rise in the average age of the population[111,120]. In patients with clinical signs of ARMD, postmortem light microscopic (LM) examination has shown progressive accumulation of extracellular material at the basal side of the retinal pigment epithelium (RPE) in the macular area[199]. This has led to the postulation that these deposits might be a precursor of ARMD[199]. These basal deposits have been called basal laminar deposit(s)[192], basal linear deposit(s)[131,199] and linear basal deposit(s)[45]; all indicating identical materials. The basal deposits can be seen by LM as a linear band, actually representing a lamina between the RPE and Bruch's membrane. We prefer the singular expression basal laminar deposit (BLD).

Ultrastructurally, BLD is located between the RPE cell membrane and its basement membrane[122] and has a characteristic banded pattern, with a periodicity of about 120 nm.

A second type of BLD has been observed in eyes with long-standing macular atrophy[192]. It has been described as a mixture of amorphous clumps, fibrillar material and a small amount of fibrous long-spacing collagen (FLSC). It was called flocculent BLD, because of the multilaminar or flocculent arrangement at the base of the RPE.

It is assumed, that BLD might be a waste product of the RPE cells, and is secreted at the basal side of the cells[131].

The prevalence of BLD increases with age[75,131,199,260]. A mild visual loss has been reported in patients with postmortem histopathological evidence of a moderate amount of BLD in the macular area[199]. All patients with a large amount of BLD had serious visual loss during the last part of their life, and 14% had histopathological evidence of subretinal neovascularization[199].

We studied the structure and distribution of BLD in postmortem human eyes by transmission electron microscopy (TEM), emphasizing advanced age groups.

MATERIALS AND METHODS

We obtained 145 randomly collected postmortem human eye bank and autopsy eyes. Nothing was known about the ocular history. The age of the patients ranged from 0 to 94 years, with an average of 70 years (S.D. = 15,8 years). Time between death and fixation ranged from 2 to 22 hours. Only one eye of each patient was used for this study. After removing the cornea, the eyes were either fixed with a mixture of glutaraldehyde (1% vol/vol) and a (4% vol/vol) formaldehyde solution or a 4% formaldehyde solution in a 0.1 m/L. phosphate buffer at pH 7.2.

After horizontal sectioning of the globe with a razor, the eyes were examined with a Zeiss binocular preparation microscope at x4 magnification. Only eyes without macroscopically gross pathological changes, apart from macular degeneration or drusen, were used as BLD formation might be stimulated by various pathological conditions such as trauma or infection. The macular area was removed and cut into two equal parts. Half of the macula was embedded in paraffin following routine procedures for LM, to select the eyes with BLD. The other half of the macula was divided into three equal parts for TEM and stored in fixative until use.

To compare the ultrastructure of maculae with and without BLD and of maculae of all age groups, we selected 42 maculae; 16 maculae with LM evidence for the presence of BLD between the RPE and Bruch's membrane and 26 maculae without LM evidence for the presence of BLD; these were distributed over all decades. One part of these maculae was, without osmium tetroxide postfixation, embedded in epoxy resin (LX 112, Ladd Research Industries, Inc, Burlington, Vermont), after dehydration with grading acetone. Semithin sections (1 μm thickness) were made for LM with a glass knife and stained with toluidine blue (1% wt/vol). Ultrathin sections (70-to 80 nm thickness), made on a LKB IV Ultrotome with a diamond knife, were mounted on unfilmed mesh 300 copper grids. After staining for 30 minutes with uranyl acetate and 2 minutes with lead citrate, the ultrathin sections were examined with a Zeiss EM 902 transmission electron microscope (TEM), with an acceleration voltage of 80 kV. Micrographs were made using a Kodak SO 163 film (Eastman Kodak, Rochester, New York). An image-

analyzing system (IBAS 2000 Zeiss/Kontron, Oberkochen, FRG) was connected directly to the TEM for ultrastructural measurements.

Immediately after sectioning, ultrathin sections of 2 eyes with a large amount of BLD were additionally stained immediately after sectioning for 6 hours with phosphotungstic acid (10% wt/vol), a selective collagen stain.

In addition we embedded a piece of the anterior segment of 3 eyes obtained at autopsy, 59, 82 and 84 years of age, including a small part of the cornea, trabecular system and ciliary body.

RESULTS

BLD was located between the RPE cell membrane and its basement membrane as a complex of extracellular material (Fig 6.1). The most prominent part of the BLD appeared as irregularly oriented, small, trapezoidal or spindle-shaped pieces of material. Its most remarkable feature was the fingerprintlike cross-banding (Fig 6.1).
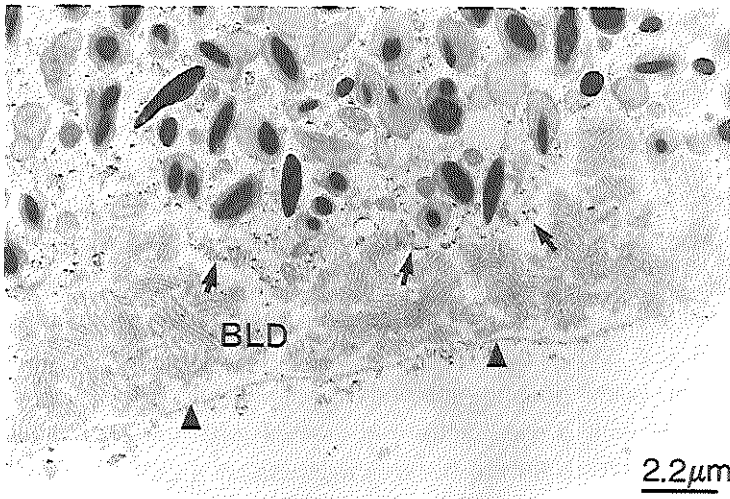

Fig 6.1. Electron micrograph of the RPE (top) and a large amount of BLD between the cell-membrane (closed arrow) and its basement membrane (arrow heads). Note the fingerprint-like banded pattern and the irregular orientation of the material. (uranyl acetate, lead citrate)

This banding pattern consisted of electron-dense bands with an average width of about 50 nm and electron-lucent interbands with an average width of about 80 nm (Fig 6.2). The electron-dense bands consisted of two parallel electron-dense bands, each of about 15 nm wide, and an electron-lucent band of about 20 nm in between. This electron-lucent band was not always clearly visible

(Fig 6.2). Within the interbands, a much finer striation was observed perpendicular to the electron-dense bands.

The bands ran in a strictly parallel fashion, although there was a marked variety in width of the banding pattern, within and also between the different patches of BLD. Its periodicity ranged from 115 to more than 140 nm. Above 140 nm, the demarcation of the electron-dense bands became so indistinct, that it was difficult to measure its periodicity (Fig 6.2). Scattered between the banded material were pieces of the same size and shape, with a homogeneous, moderate electron density, sometimes exhibiting the beginning of a banded pattern at one of the edges (Fig 6.2). This material seemed to consist of bundles of fibers sectioned perpendicularly and thus not exhibiting the banded pattern.
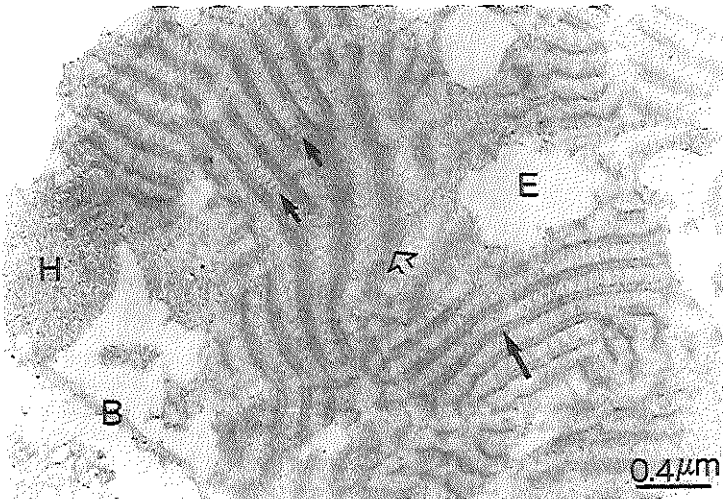

Fig 6.2. Higher magnification of BLD with the epithelial basement membrane (B), the banded material, homogeneous material (H) and electron-lucent spaces (E). Note the electron-dense bands, with the electron-lucent centre (closed arrow) and the lighter interbands with the longitudinally oriented fine striation (small arrows). Some bands seem wider, probably owing to the angle of sectioning (open arrow). The homogeneous material seems to consist of a bundle of fibers, sectioned perpendicularly, and merges gradually into a banded pattern. (phosphotungstic acid, uranyl acetate, lead citrate)

Most of the BLD was located close to the RPE basal cell membrane and between its basal infoldings. BLD-like material was not found within the RPE cytoplasm or within the lipofuscin granules found in the RPE. Between the banded material were areas filled with fibrils and electron-lucent spaces which seemed "empty" with uranyl acetate-lead citrate and phosphotungstic acid staining procedures (Fig 6.2). The fibrils were sometimes seen to be connected with the banded material (Fig 6.3). A small number of vesicles and occasionally a melanin granule were found between the banded material.
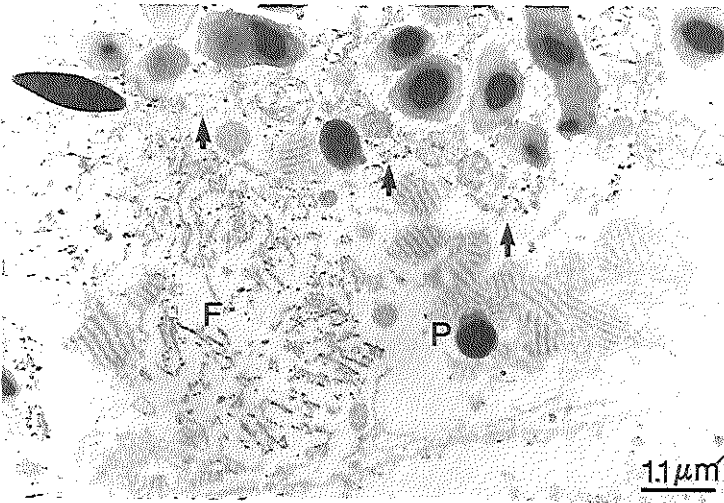
Fig 6.3. BLD between RPE cell (top) and its basement membrane (bottom). Note the fibrillar material (F) between the banded pieces of BLD. Excreted pigment granule (P), and cell membrane (closed arrows). (uranyl acetate, lead citrate)
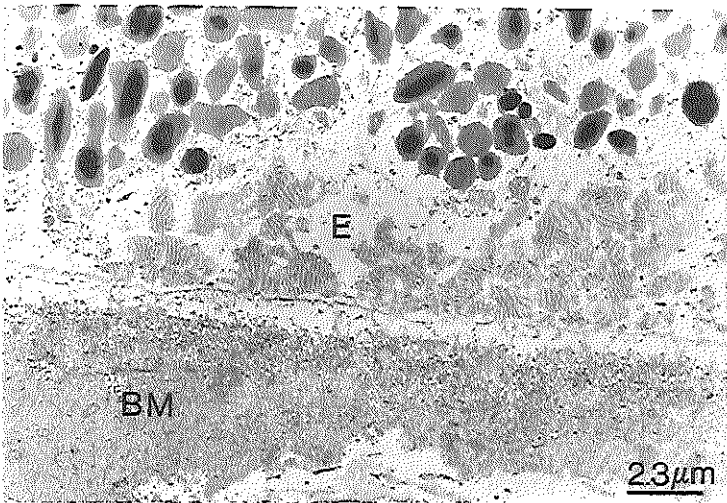

Fig 6.4. Electron micrograph of the RPE (top), BLD and Bruch's membrane (BM). The BLD and Bruch's membrane are heavily stained. The electron-lucent spaces (E) between the BLD are still unstained. (phosphotungstic acid, uranyl acetate and lead citrate)

The phagocytized discs of the photoreceptor outer segments in the RPE had a clearly different shape; the discs did not run exactly parallel, the striation was more dense and electron-lucent interbands were absent.

After staining with phosphotungstic acid, the collagen fibers of the sclera were heavily stained. In Bruch's membrane, however, only a moderate amount of collagen fibers was visible. The BLD stained faintly and was hard to distinguish from the RPE cytoplasm. After counter staining with uranyl acetate-lead citrate,
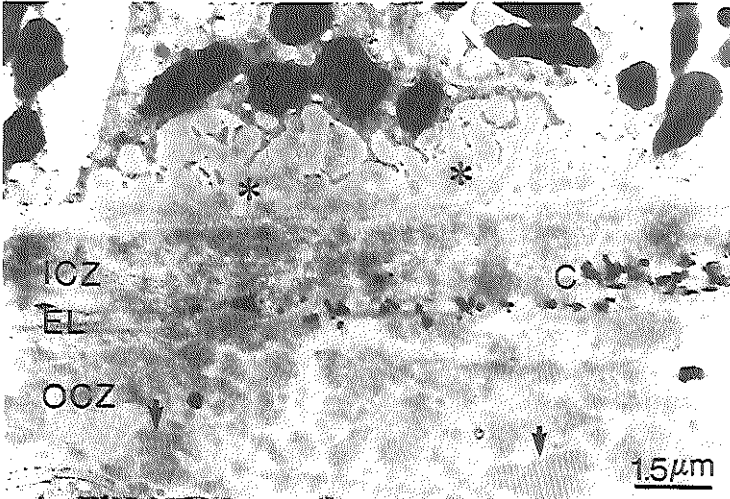
Fig 6.5. Electron micrograph of the RPE (top), Bruch's membrane with the inner collagenous zone (ICZ), elastic layer (EL) and outer collagenous zone (OCZ). Between the coarse basal infoldings of the RPE and the basement membrane is a relatively large amount of an early stage of BLD (asterisks) with a relatively small amount of banded material. Within the OCZ on the choroidal side, there is a large amount of banded material (arrows), which has the same structure and banding pattern as BLD. Note calcifications (C) in Bruch's membrane.
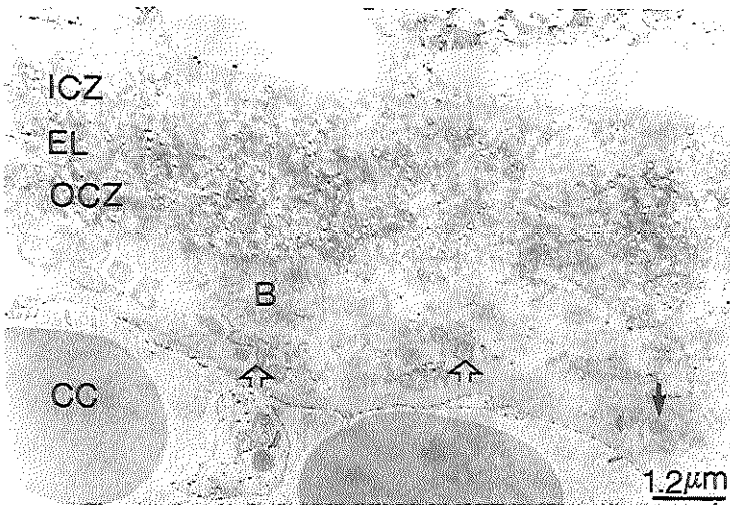
Fig 6.6. Electron micrograph of Bruch's membrane and the chorio-capillaris (CC) of an 86-year-old person. The difference between the layers of Bruch's membrane is not clearly visible in the macular area. The ICZ and OCZ are filled with small vesicels between the collagen fibers. Within the OCZ, especially on the choroidal side one may see banded material (B) similar to BLD, trilaminated curly membranes (open arrows), and an electron-dense granule (closed arrow). (uranyl acetate, lead citrate)

the BLD stained heavily, but the formerly described electron-lucent spaces remained electron-lucent (Fig 6.4). Also, the thickened part of the outer collagenous zone (OCZ) of Bruch's membrane was more electron-dense with this staining procedure.

Banded material, structurally similar to BLD and with the same periodicity

of about 120 nm, was interspersed in the OCZ of Bruch's membrane, especially on the choroidal side (Figs 6.5 + 6.6). In 33 (79%) of the 42 maculae examined, this BLD-like material was present in the OCZ (Fig 6.7), in some maculae in even larger amounts than between the RPE and its basement membrane (Fig 6.5). In 20 (48%) of the maculae, this BLD-like material was found in the OCZ, although no deposits could be found at the base of the RPE. The structure and periodicity of these deposits on the choroidal side of Bruch's membrane were similar to those between the RPE and its basement membrane. The amount of BLD in the OCZ increased with age and was seen at age 19 already. BLD between the RPE and its basement membrane was first seen at age 70 years.
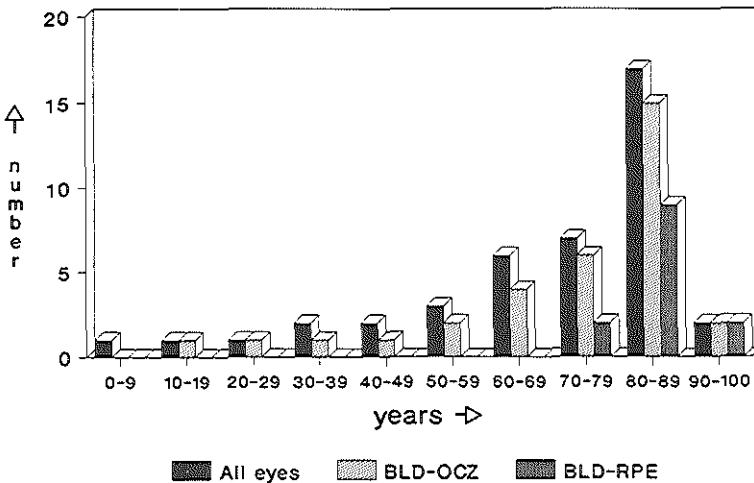

Fig 6.7. Age distribution of the 42 patients and the ultrastructural distribution of BLD in the macula. BLD-RPE indicates the BLD, between the basement membrane of the RPE and its cell membrane. BLD-OCZ indicates the BLD located in the OCZ of Bruch's membrane. Note the presence of BLD in the OCZ in young persons, in contrast to BLD between the RPE and its basement membrane.

In none of the eyes examined was BLD present on the capillary side of the endothelial basement membrane of the choriocapillaris. In seven maculae, small amounts of similar banded material were found in the inner collagenous zone (ICZ) of Bruch's membrane.

In seven maculae, an early stage of BLD was found between the basal infoldings of the RPE cell membrane and the RPE basement membrane (Fig 6.5). This consisted of globular deposits with a homogeneous, moderate electron density. In most cases these deposits were confluent. Interspersed between these deposits were found a few small pieces of 120 nm banded material, small amounts of fibrillar material, and nonhomogeneous, granular material in varying amounts.

The flocculent type of BLD was not seen in our study, probably because none of the eyes examined exhibited an advanced stage of macular degeneration.

No connection was observed between the presence of BLD and the location of other aging changes of the macular area, such as the amount of accumulated lipofuscin granules in the overlying RPE cells, loss of retinal pigment granules or calcifications within Bruch's membrane. No relation was found between the fixation delay and the prevalence of BLD.

In the trabecular system (Fig 6.8), a varying amount of BLD-like, banded deposits was found in the trabeculae of all three eyes, located close to the basement membrane of the trabecular endothelial cells. The periodicity of the banding pattern was also about 110-120 nm and was morphologically similar to the banded material of the BLD in the macular area, especially when sectioned obliquely. Only the electron-lucent center of the electron-dense bands was lacking in the deposits of the trabecular system.

In the ciliary body, no banded material was found in relation with the pigment epithelium, its basement membrane, or the superficial stroma.
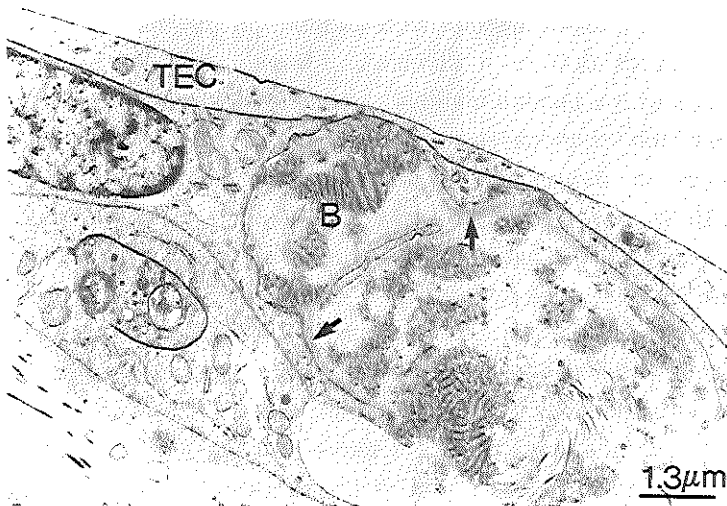

Fig 6.8. Tangential section through a trabecular fiber near the limbus of a 82-year-old patient. Two layers of endothelial cells (TEC) with a basement membrane (arrows) are covering the connective tissue core. Adjacent to this basement membrane, banded material (B) with a periodicity of 110 to 120 nm is seen. (uranyl acetate, lead citrate, osmiumtetroxide)

DISCUSSION

Sarks[199] showed that the amount of BLD is positively correlated with visual loss and is a good indicator of the degree of RPE degeneration. However, BLD cannot be detected directly by ophthalmoscopy or fluorescein angiography. The first clinically visible signs of ARMD are pigment changes in the macular area, due to alterations in the RPE cells. In this stage, there is already a slight visual loss[199].

It is generally assumed that BLD is produced by the RPE cells [75,131,199,260] probably owing to the fact that BLD was initially found between the RPE and its basement membrane. However, in this study, BLD was also found by TEM within the ICZ and OCZ and between the OCZ and the basement membrane of the choriocapillary endothelium, as has been mentioned by others[74]. This might be explained by diffusion of precursor material from the RPE through the layers of Bruch's membrane, before polymerization into BLD. However, in 20 maculae we found BLD located only between the OCZ and the endothelial basement membrane of the choriocapillaris, without evidence of BLD in relation to the RPE. This could be an argument against BLD production by the RPE and suggests a multifocal origin of BLD or a complete diffusion through Bruch's membrane of the precursors of the banded material. Also, the idea that BLD might originate exclusively from the choriocapillaris seems unlikely, because in the trabecular system, which is avascular, banded deposits have also been described[52,90,144,233]. In our study, the trabecular deposits were located adjacent to the trabecular endothelial basement membrane and were structurally similar to BLD in the macular area. The periodicity of the banded pattern in both was about 110 to 120 nm. The trabecular banded material was located in an area of a homogeneous and slightly electron-lucent substance, from which it seemed to originate (Fig 6.8). The longitudinally directed striations were, however, more pronounced than in BLD, and the electron-lucent center of the electron-dense bands was absent. As in the BLD, deposits with a higher periodicity were also seen here, coupled with broader and more indistinct striations. This is probably due to a different angle of sectioning. We can assume that when the periodicity is smallest and the bands are most distinct, the angle of sectioning is approximately 90 degrees.

Table 1. Organs and tissues in which the presence of fibrous long spacing collagen has been described under normal and pathological conditions.

Organ	Normal	Pathological
eye	Descemet's membrane	Descemet's membrane in -cornea guttata -Kayser-Fleischer rings -Fuch's dystrophy -desquamatory endotheliopathy -posterior keratoconus cornea in Scheie's syndrome interstitial keratitis
	trabecular meshwork	trabecular meshwork in -exfoliative syndr. -Sanfilippo syndr. -glaucoma
ear	macular region of the utricle	
heart	myocard	rheumatic carditis
neuronal	cauda equina	nerve trauma schwannomas neurofibromatosis astrocytomas Raynaud's phenomenon
skin		tuberous sclerosis angiofibromas melanomas lepromatous leprosy blue naevus scleroderma basal cell carcinoma squamous cell carcinoma
muscle		Duchenne's dystrophy
skeletal	nucleus pulposus articular cartilage (aged mice)	osteosarcoma Ewing sarcoma
lymphatic		lymph node in Hodgkin disease lymphadenitis thymomas
systemic		glomeruli in amyloidosis kidney with multiple myeloma extrapulm. silicotic lesions systemic hyalinosis

In the trabecular system, both the RPE and blood vessels are absent. This suggests another origin of the banded material or the uptake of precursor molecules from the chamber fluid, followed by polymerization into banded deposits. McMenamin et al[144] found large amounts of banded material in the trabecular system of eyes of aged patients, but this material has also been described in small amounts in patients from age 6 years old on[90,91].

Ultrastructurally, BLD resembles FLSC [45,50,67,91,96,107,131, 150,215,248]. Ghadially[67] mentioned four types of FLSC all of which can be made in vitro, but only FLSC III resembles in vivo FLSC[32,103,133]. Influences such as pH, oxygen pressure, and the concentration and type of glycosaminoglycans may be the reason that only type III is formed in vivo. This might also be influenced by age and pathological or traumatic changes in the tissue. FLSC III has been found thus far in a variety of normal and pathological tissues and organs, listed in Table 6.1 [2,51,67,117,189,220,228,258,263]. The slightly different ratio of collagen to glycosaminoglycans and other external factors may determine the small differences of length and width of the FLSC in the various tissues[50,107,117,263].

Authors have used confusing names for FLSC in TEM images, such as *banded structures, curly collagen, wide banded collagen, long spacing collagen, broad banded striated bodies, lattice collagen, sheath collagen, kollagenoid, gitterkollagen and Luse bodies*[67]. This might be due to its diverse TEM appearances as a result of the diversity in fixation techniques, staining procedures, and measuring methods of the periodicity of the banding pattern, or it might be due to the kind of tissue examined.

Our findings suggest that the most characteristic substance of BLD, the banded material found between the RPE and its basement membrane, within Bruch's membrane, and within the trabecular system, is the same as FLSC III. Structurally, BLD is similar to FLSC III, with a banding periodicity of 100 to 120 nm. Both have an extracellular location, often close to an epithelium with an adjacent basement membrane. Both BLD and FLSC III are found in tissue with aging or degenerative changes (Table 6.1).

Electron microscopically, BLD is surrounded by electron-lucent material, which is referred to by Loeffler and Lee[131] as "empty space, possibly in vivo filled with fluid" (Fig 6.5). Another explanation might be that this is electron-lucent material that does not stain with routine TEM staining techniques nor with phos-

photungstic acid.

In conclusion, we think that the formation of BLD is neither a unique process nor a purely ocular disease. In the eye, it is most often found in the vicinity of Bruch's membrane in the macular area, but it can also be found elsewhere, as in the trabecular system. The location of BLD in the macula, not only between the RPE cell membrane and its basement membrane but also within Bruch's membrane on the choroidal side, suggests a multifocal origin or a polymerization of smaller particles, eg, tropocollagen or basement membrane material. This may diffuse through the tissue and polymerize to collagen or to BLD, depending on the microenvironment. The production of an excessive amount of glycosaminoglycans might be a determining factor. Therefore, BLD might be a symptom of general degenerative changes.

Further research is needed to investigate the role of the RPE and the exact composition of BLD.

CHAPTER 7

Element Analysis of the Early Stages of Age-related Macular Degeneration

Theo L. van der Schaft[1], MD; Wim C. de Bruijn[2], PhD;
Cornelia M. Mooy[1,2], MD; Diane A.M. Ketelaars[2], BSc;
Paul T.V.M. de Jong[1], MD, PhD, FcOphth

Institutes of Ophthalmology (1) and Clinical Pathology (2)
Erasmus University Rotterdam,
the Netherlands

INTRODUCTION

With an increasing population of older persons, age-related macular degeneration (AMD) has become an increasingly important cause of reduced vision in the western countries[111,120]. The exact cause of AMD still remains unclear. Several authors[131,199] have emphasized that basal laminar deposit (BLD) is often seen in both the exudative and the geographic type of AMD. The possible role of zinc deficiency[121,156,157,256] and zinc toxicity[209] in the development of AMD has been discussed.

BLD is extracellular material, located between the retinal pigment epithelial (RPE) cell membrane and its basement membrane (Fig 7.1), which forms the inner layer of Bruch's membrane[131,192,199,202]. Ultrastructurally, the major component is long-spacing collagen, but fibrillar material, vesicles and, occasionally, some calcifications or a melanin granule, probably derived from the RPE, are also found[131,192,199,202]. The exact composition and origin of BLD are still unclear.
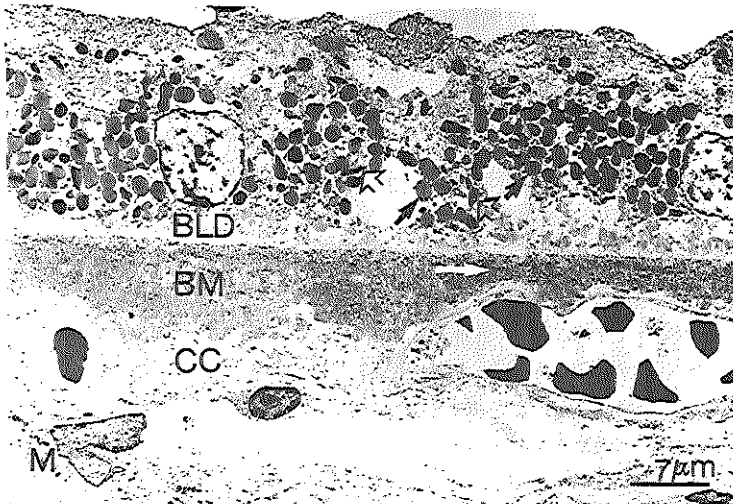

Fig 7.1. Electron micrograph of the macula of a 93-year-old person. The RPE (at top) contains pigment granules (open arrows) and lipofuscin granules (closed arrows). Between the RPE cell membrane and its basement membrane, a moderate amount of BLD is present. Bruch's membrane (BM) is thickened, especially between the capillaries of the choriocapillaris (CC). Calcifications (white arrow) are frequently seen in Bruch's membrane. Melanocyte (M) is shown in the choroid. The photoreceptors were lost during processing. (uranyl acetate and lead citrate)

The aim of this study was to analyze the matrix-bound elements in BLD and adjacent structures by means of electron-probe X-ray microanalysis (EPMA) to learn more about the composition of BLD and its relationship to the presence or absence of zinc.

MATERIALS AND METHODS

We obtained 118 unpaired eye bank and autopsy eyes. The selection and preparation have been described elsewhere[202].

Paraffin sections of each macula (thickness, 7 μm) were stained with hematoxylin and azophloxin, periodic acid-Schiff, Mallory's and von Kossa's stains and examined with light microscopy. The eyes were selected on the basis of age and the presence of BLD for ultrastructural examination and element analysis. For this study, one part of the stored maculae was embedded, without osmium tetroxide postfixation, in epoxy resin (LX 112, LADD Research Industries Inc. Burlington, Vermont) after dehydration at room temperature with graded acetone.

To check the influence of the fixation and dehydration of the tissue on the results of the element analysis, three maculae, obtained from persons aged 40, 71 and 87 years, were cryofixed on a metal-mirror fixation device (CF 100, LifeCell Corp, The Woodlands, Texas) within one hour after enucleation for ocular melanoma and stored in liquid nitrogen[130]. Molecular distillation drying (Polaron, Bio-Rad, Richmond, California) was performed in an ultrahigh vacuum with temperatures slowly raised from -180 $^{\circ}$C to 20 $^{\circ}$C, followed by paraformaldehyde vapor fixation and embedding in Spurr's resin (Taab, Berkshire, England) in vacuum[127].

Semithin sections (thickness, 1 μm) were cut with a glass knife and stained with toluidine blue (1% wt/vol). Ultrathin sections (thickness, 60-70 nm) for transmission electron microscopy were made as described elsewhere[202]. Sections (thickness, 100-120 nm) were mounted on carbon-coated formvar copper one-hole grids for element analysis. For detection of copper in the macula unfilmed molybdenum grids were used. The sections of the freeze-dried maculae were mounted on filmed nylon and carbon grids.

The EPMA was performed on a scanning transmission electron microscope (Philips STEM 400, Philips, Eindhoven, the Netherlands) with an X-ray microanalyzer (Tracor Northern 2000, Bilthoven, the Netherlands)[18,164,255]. The specimen was placed in a low-background specimen holder at an angle of 108° relative to the electron beam (tilt = 18^{0}). Each point of interest was measured for 100 seconds with an electron-probe (diameter, 400 nm) at an acceleration voltage of 80 kV. The X-ray spectra were either photographed directly from the monitor using a standard 35-mm camera or were printed. The geometry of the

system has been described elsewhere[188].

If present in the specimen, an area with BLD and/or calcifications in Bruch's membrane was selected as far away from the grid edge as possible. To monitor the instrumental background noise, spectra of the embedding resin of each section and from each formvar film, adjacent to the specimen, were recorded. The minimal detectable amount of an element was about 10^{-16} - 10^{-19}g, depending on the type of element[164]. With our detector, all elements with an atomic number of 11 or more could be detected[164]. Peaks were identified by the computer program Ident (Tracor Northern Software). Peak deconvolution was continuously performed by software using a "top hat filter". Net intensities above 25 counts/100 seconds were considered to be indicative of the presence of an element.

In our study this technique was not used to determine absolute weights or concentrations of the elements, but to detect and identify matrix-bound elements in the various tissue components. This method is not reliable for detection of free electrolytes reliably. Peaks in the EPMA spectra can be compared, by means of their net intensity values, within the same section. However, comparison between different sections is restricted to indications about the absence or presence of the various elements.

For statistical analysis, the Mann-Whitney-U test and the Wilcoxon Rank-Sum W test were used. P values below 0.05 were considered significant.

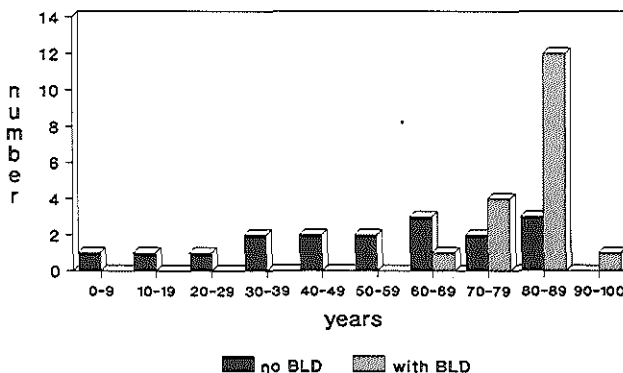Age distribution of eyes selected for electron probe X-ray microanalysis

Fig 7.2 Age distribution for the 38 eyes selected for EPMA, divided into two groups. There was one group of 20 eyes without LM evidence of BLD between the RPE and its basement membrane (closed bars). The second group consisted of 18 eyes with BLD (open bars). None of the younger eyes (age, <60 yrs) contained BLD.

RESULTS

With light microscopy, 38 eyes were selected from the 118 eyes. In 18 eyes BLD was present in varying amounts, i.e. Sarks' classification groups II to IV[199]. In 20 eyes, no light microscopic evidence of BLD was found. The age distribution is given in Fig 7.2.

A schematic drawing of a photoreceptor outer segment, a RPE cell, Bruch's membrane, the choriocapillaris and the choroid is presented in Fig 7.3.
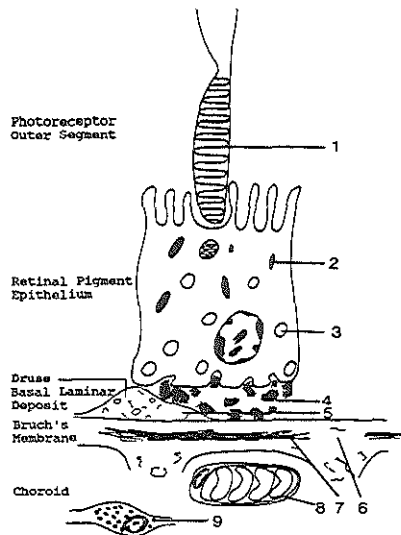

Fig 7.3. Schematic drawing of a photoreceptor outer segment (1), a retinal pigment epithelial cell with melanin granules (2) and lipofuscin granules (3), basal laminar deposit (4), a druse (5), Bruch's membrane (6) with calcifications (7), the choriocapillaris (8) and the choroid with a melanocyte (9). The numbers indicate the morphologic structures subjected to element analysis and correspond to the numbers given in the Table.

Table. Relative frequency of the presence of elements for various structures in the human macula.

location	macula	analysis	Ca	P	S	Zn	Cl	Fe	Na	K
	N =	N =	%	%	%	%	%	%	%	%
1 photoreceptor	9/38@	17	37	72	–	–	61	–		
2 pigment RPE	38/38	112	81	–	100	50	–	59	84*	56*
3 lipofuscin	38/38	128	62	48	80	9	58	–	87*	50*
4 BLD	9/18	17	–	–	–	–	59			
5 drusen	6/12	15	61	37	–	–	83	–		
6 Bruch's memb.	36/38	68	40	–	86*	28*	86	–	28*	28*
7 calcification	11/16	24	100	100	–	53	77	59		
8 choriocapill.	21/38	34	–	–	–	–	81	–		
9 melanocyte	35/38	50	80	–	100	36	–	68	100*	16*

Table. Results of the EPMA of 38 human maculae. For explanation of the calculation of the percentages, see text (results section). @: the numerator indicates the number of maculae in which that specific structure could be found during the EPMA. The denominator indicates the number of maculae in which this structure was seen with light microscopy. Differences between numerator and denominator are due to the absence of that structure in that specific section or the low visibility in the uncontrasted sections. * Results of freeze dried and vapor fixed maculae only. Analysis (column 2) indicates the number of spectra made of that structure. N are absolute numbers.
Ca = calcium, P = phosphorus, S = sulfur, Zn = zinc, Cl = chlorine, Fe = iron, Na = sodium, K = potassium

In the Table, a percentage represents the frequency with which a given element was found in relation to the number of macular specimens that were examined. For example, if the number of points measured in Bruch's membrane of macula X was three, and two of these spectra showed calcium, then the percentage of occurrence for calcium in this macula was 66%. The percentages for all maculae examined were added: the mean values are given in the Table.

Representative spectra, obtained by EPMA of the various structures of the aldehyde-fixed and acetone-dehydrated maculae, are shown in Figs 7.4a-h.

The range of elements in similar morphological structures was basically the same at all ages. However, BLD, drusen and calcifications in Bruch's membrane were not present in the younger eyes. In the macula of a stillborn child, only sporadic lipofuscin granules were found, whereas they were abundant in the maculae of the older eyes, but the elemental composition remained more or less stable.

The composition of drusen was very inhomogeneous, depending on whether they were calcified. The globular-shaped calcifications consisted of calcium and phosphorus only. The noncalcified parts of the drusen exhibited high peaks of chlorine (not shown).

The EPMA of the freeze-dried and vapor-fixed maculae showed the same elements but with addition of sodium and potassium in all structures. In the uncalcified Bruch's membrane sulphur and zinc were sometimes detected. Sulfur and zinc were not seen at this location in the aldehyde fixed and acetone dehydrated maculae.
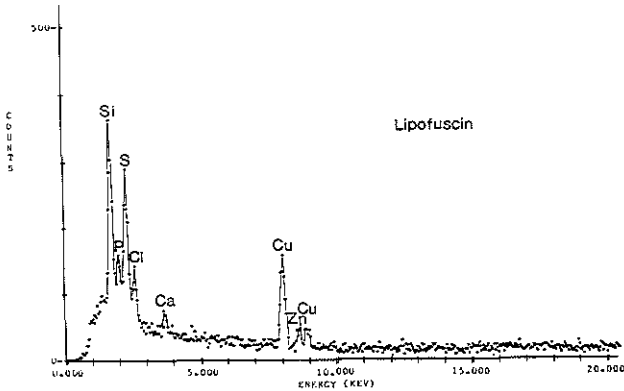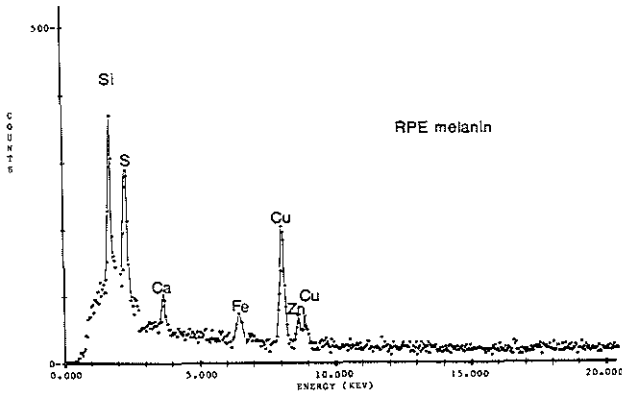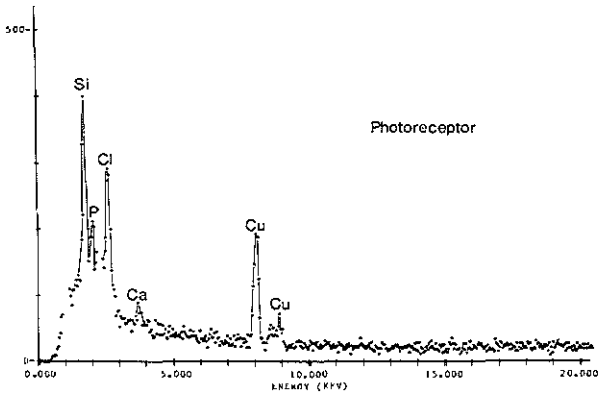
Figs 7.4a-c. Each spectrum represents one measurement in one structure. Silicon (Si) and copper (Cu) are artefacts.

a) photoreceptor; the small zinc (Zn) peak (not labeled) between both copper peaks is not significant in relation to the background i.e. less than 25 counts/100 seconds . P=phosphorus, Cl=chlorine, Ca=calcium.

b) RPE melanin; in sections mounted on molybdenum grids, high copper peaks were found only for the melanin granules (not shown). S=sulfur, Fe=iron.

c) lipofuscin granules; zinc was only seldomly found in lipofuscin granules

BLD

Si
Cl
Cu

COUNTS

ENERGY (KEV)

Bruch's membrane

Si Cl
Ca
Cu

COUNTS

ENERGY (KEV)

Ca

P

Ca

Bruch's membrane
calcification

Zn Cl
Fe Cu Zn

COUNTS

ENERGY (KEV)
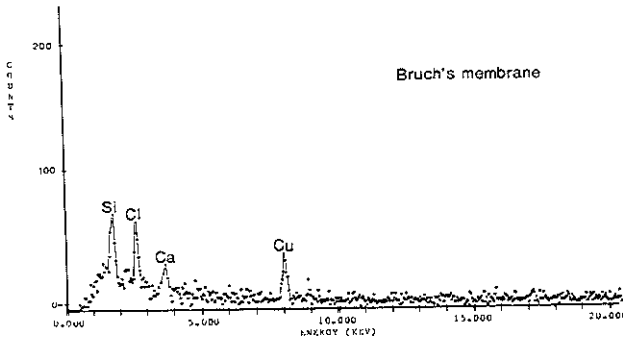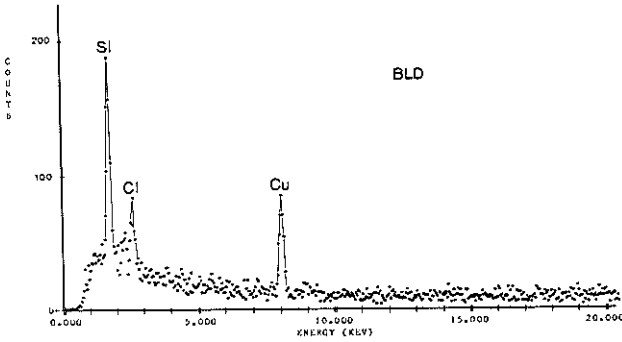
d) BLD; the second copper peak (Cu K$_\beta$) does not rise above the background.

e) Bruch's membrane; ultrastructurally, no calcification was seen in Bruch's membrane

f) The calcium : phosphorus atomic ratio for the calcifications in Bruch's membrane was on the average 1.88 : 1. Hydroxy apatite crystals were not found.

73
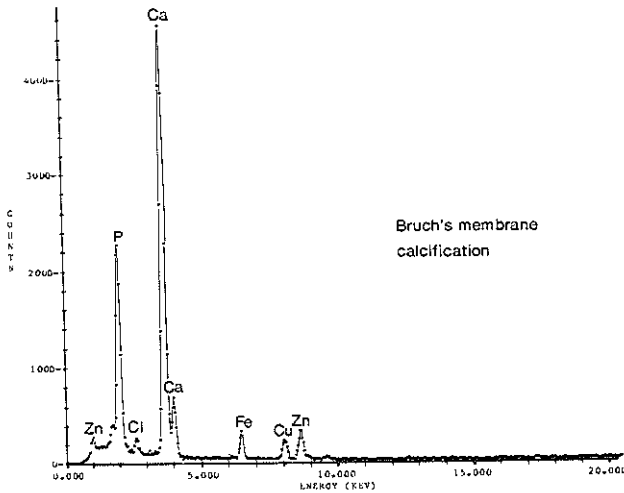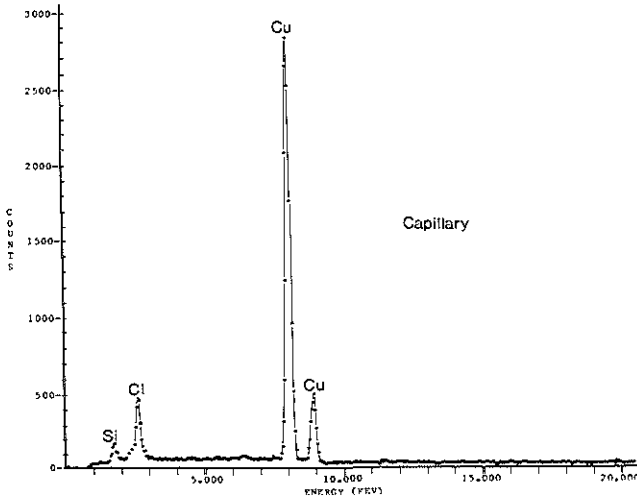
g) capillary; the high
copper peaks due to the
copper grid do not
influence the detection of
other elements.
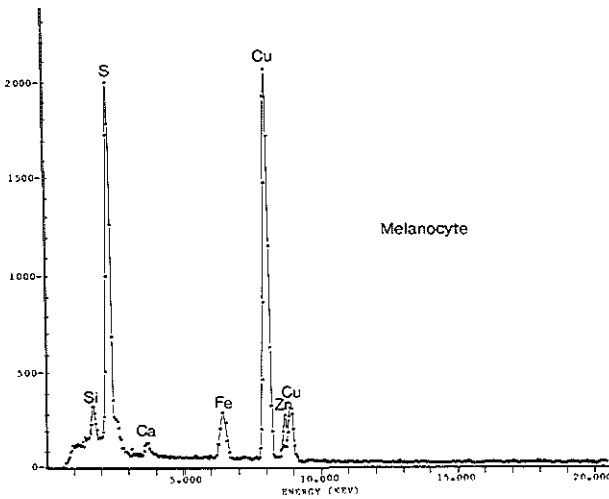
h) melanocyte; in sections
mounted on molybdenum
grids, high copper peaks
were found only for the
melanin granules (not
shown).

Between eyes with and without BLD, there was no difference in the mean zinc frequency in the pigment granules (P = 0.17) and in Bruch's membrane (P = 0.42). There was no correlation between the frequency with which zinc was found in the pigment granules of the RPE and in Bruch's membrane (P = 0.68). A rise or decrease in the detection frequency of zinc with increasing age was not seen. The eyes with and without BLD did not differ in the absence or presence of calcifications in Bruch's membrane (P = 0.94) or the absence or presence of zinc

within these calcifications (P=0.53). No correlation was found between the presence of calcifications in Bruch's membrane and the presence of calcium and phosphorus in lipofuscin granules (P=0.27 and P=0.68, respectively).

The control spectra that were taken of the embedding resin and formvar film and mounted on copper grids showed substantial amounts of chlorine, which is one of the constituents of the epoxy resin (LX 112), and copper from the specimen holder and copper grids. The silicon peak was probably due to the silicon in the X-ray detector.

The element analysis could not be performed at every location in each specimen of all 38 maculae, mainly because these structures were not always present but also because some structures were difficult to localize with certainty in uncontrasted specimens.

DISCUSSION

Most authors[75,131,199,260] assume that BLD is secreted by the RPE and consists of an excessive amount of basement membrane material, produced by the RPE for unknown reasons[75,131,192,202,260]. However, up to now, this has not been confirmed with immunotechniques. Another possibility could be that the precursor material of BLD originates from the choriocapillaris[58,202]. BLD is not derived from lipofuscin granules of the RPE, because these granules are not released from the RPE[46].

The analysis of BLD and the choriocapillaris vessel wall showed no specific elements at either location, except for a higher frequency of occurrence of chlorine compared to the embedding resin within the same section.

The element analysis of BLD and the basement membranes of the RPE and the choriocapillaris could not be compared by means of the present method, due to the small dimensions of the basement membranes and their low electron-scattering capacities.

We compared the frequency with which elements were found in the photoreceptor outer segments, lipofuscin granules of the RPE and Bruch's membrane. All of these structures contained calcium and chlorine. There were, however, more different elements in the lipofuscin granules than in the photoreceptor outer segments and Bruch's membrane, which might be due to accumulation of elements in the lipofuscin granules. The absence of elements in

BLD, except for chlorine, confirms that it is unlikely that BLD consists of incompletely digested photoreceptor outer segment discs originating from the lipofuscin granules.

BLD has been considered to be a precursor of AMD and a good marker for the degree of RPE cell degeneration[199], which is accompanied by a loss of pigment granules. It seems unlikely, however, that BLD is just formed out of degenerated pigment granules, because the elements in the two are quite different.

The elements in the pigment granules of the RPE and the choroidal melanocytes were roughly the same. In the sections mounted on the molybdenum grids, copper was detected in pigment granules only, which confirmed the results of other studies[208,239] in which the presence of copper in the RPE was investigated. We used these molybdenum grids for only one macula, because the peak of molybdenum overlaps those of sulfur and phosphorus. The high frequency with which calcium was detected in the pigment granules confirmed findings from other reports[165] that cells that contain pigment granules sequester calcium under physiologic conditions. This might be related to calcification of Bruch's membrane with increasing age. These calcifications were mainly located in the elastic layer of Bruch's membrane and consisted of calcium and phosphorus, as previously described[35]. Phosphorus, however, was only present in the photoreceptor outer segments and in the lipofuscin granules of the RPE and not in the melanocytes.

Several structures in our specimens contained zinc, as has been reported earlier for the retina and choroid[105,165,209]. Zinc is a component of several metalloenzymes[105,156,157,208]. RPE melanin is known to act as a heavy metal scavenger[190]. This could explain the presence of zinc in the pigment granules. Elevated serum zinc levels have been found in patients with AMD[209]. Other studies have reported that the administration of zinc inhibits visual loss in patients with AMD[156,248]. In our study, no relationship was found between the frequency of occurrence of zinc in RPE pigment granules or calcifications in Bruch's membrane and the presence of BLD in the maculae.

Zinc and iron were also frequently found in the calcifications in Bruch's membrane. These elements might be derived from the pigment granules of the RPE and/or choroidal melanocytes in which calcium, zinc and iron were also detected, although the renewal of pigment granules is very slow[185,250]. Degeneration and depigmentation of the RPE might play a role in the deposition of these metals in Bruch's membrane. In the globular calcifications in drusen, no zinc could be

demonstrated.

We realize that elements might have escaped detection as a result of aldehyde fixation and dehydration, which presumably does not occur in freeze-dried and vapor-fixed specimens[164,188]. Our results of the EPMA of the freeze-dried and vapor-fixed maculae were comparable with the results of the EPMA of the conventionally fixed and dehydrated maculae. We must emphasize, however, that we did not intend to measure the elements in metalloenzymes or free electrolytes: only matrix-bound elements were investigated.

The question remains wether BLD and drusen are formed because of degeneratives changes in the RPE or that the RPE degenerates due to the mechanical barrier of the BLD, drusen and the calcification of Bruch's membrane. BLD and drusen have been considered to be early stages of AMD, which are related to depigmentation and degeneration of the RPE. Since this process is relatively slow it will probably not elevate serum zinc levels as seen after laser treatment of the retina[208]. In our study, we found no correlation between the presence of zinc in the melanine of the RPE and in calcified Bruch's membrane and the presence of BLD. Thus, it seems unlikely that the formation of BLD is related to wether or not zinc is detected in the macula.

CHAPTER 8

Immunohistochemical Light and Electron Microscopy of Basal Laminar Deposit.

Theo L. van der Schaft,[1] MD; Cornelia M. Mooy,[1,2] MD;
Wim C. de Bruijn,[2] PhD; Fred T. Bosman,[2] MD, PhD,
Paul T.V.M. de Jong,[1] MD, PhD, FCOphth.

From the Institutes of Ophthalmology (1) and Pathology (2),
Erasmus University Rotterdam, The Netherlands

(submitted)

INTRODUCTION

Basal laminar deposit (BLD), one of the histopathological changes in the aging human macula[192,203], is assumed to be an early stage of age-related macular degeneration (ARMD)[131,199]. BLD is considered to be a marker of the degree of retinal pigment epithelial (RPE) degeneration and the presence of a BLD is accompanied by a decrease in visual acuity[199]. It precedes the atrophic as well as the exudative type of age-related macular degeneration[199]. In previous studies the prevalence of BLD at various ages as well as the light and electron microscopical structures of BLD and the chemical composition was described [131,192,199,202,203,204].

The location of BLD between the RPE plasma membrane and its basement membrane and in the outer collagenous zone (OCZ) of Bruch's membrane, close to the basement membrane of the choriocapillaris, and its largely amorphous structure suggest that a BLD is composed of relatively large amounts of basement membrane material. This might be produced by the RPE and the choriocapillaris endothelial cells[202].

Ultrastructurally, BLD consists of two main components: banded material, called long-spacing collagen[67], and homogeneous, finely granular material with the same electron density as basement membranes[131,202]. These two components can be intermixed in different ratios depending on the type of BLD. Ultrastructurally early type BLD, often found in small patches, contains relatively more finely granular material than long-spacing collagen. In the late type BLD, which can be seen as a linear band between the RPE and Bruch's membrane, the main component is long-spacing collagen[202]. A flocculent type BLD, which is often seen in long-standing geographic atrophy, is also composed mainly of homogeneously stained material. It is called flocculent BLD because of the cumuliform or flocculent arrangement of this deposit when examined by light microscopy[192].

Previously it has been suggested that under certain conditions long-spacing collagen, with a periodicity of 100-120 nm, can be formed through direct polymerization of basement membrane material[27,103]. There are indications that these deposits, which accumulate in the region of the basement membranes, are a manifestation of gradual degeneration of the associated cells[199].

The main components of the basement membranes of most tissues are type IV collagen, heparan sulfate proteoglycans (HSPG) and laminin[1,13,23]. Labelled antibodies against these components can therefore be used for the identification and localization of basement membrane material by means of immunohistochemistry. Fibronectin, an important factor in cell adhesion [23,113], is also found in basement membrane and thus might also be one of the components of BLD.

Ultrastructural studies have revealed lateral arrangement of the approximately 100-nm beaded filaments of type VI collagen[19,20,88]. This might be an alternative explanation for the formation of long-spacing collagen, the main component of late type BLD.

The aim of this investigation was to determine whether or not a BLD is composed of basement membrane material, as disclosed by the presence of type IV collagen, laminin or HSPG. If so, this would support the hypothesis that BLD can be produced by both the RPE and the choriocapillaris endothelium.

Furthermore we tested for the presence of type VI collagen and fibronectin.

MATERIALS AND METHODS

We obtained 76 eyes from 68 human subjects at autopsy or after surgical enucleation for anteriorly located choroidal melanoma. Age at time of enucleation ranged from 29 to 95 years (mean 73, SD = 20). Time between enucleation of the eye or death of the subject and fixation ranged from ½ to 10 hours.

After enucleation the macula lutea was dissected from the globe and hemisectioned in the direction of the optic disc. One half was fixed in formaldehyde (4% vol/vol, pH 7.4, for 24 hrs, room temp.) and embedded in paraffin for light microscopy and immunohistochemical studies. The other half of the macula was hemisectioned again. One part, without aldehyde fixation, was snap frozen in isopentane at -70 °C and subsequently stored in liquid nitrogen for immunohistochemical studies. The other part was fixed in paraformaldehyde (2% wt/vol, pH 7.4, for 1½ hrs, room temp.) and was either infiltrated with 2.3 M sucrose and frozen in liquid nitrogen for immuno electron microscopy of ultrathin frozen sections or dehydrated with a graded series of ethanol and embedded in LR-White for immunoelectron microscopy on semithin and ultrathin plastic sections.

To determine the influence of fixation on immunoreactivity one macula was divided into three parts. One part was fixed in 4% formaldehyde, one part in 2% paraformaldehyde and one part in a mixture of 4% formaldehyde and 1% glutaraldehyde (pH 7.4, for 2 hrs, 4 °C).

To determine the influence of the duration of fixation on immunoreactivity, two maculae were each divided into 6 equal parts and all parts were simultaneously fixed in 2% paraformaldehyde at 4 °C, 1 h after enucleation. After 1, 1½, 2, 2½, 3, and 24 h, respectively, fixation was terminated and the tissue specimens were washed and stored until further processing in phosphate-buffered saline (PBS), pH 7.2, at 4 °C.

To determine the influence of time between enucleation of the eye or death of the subject and fixation of the macula on immunoreactivity, one macula was divided into 4 equal parts and stored at 4 °C in a few drops of vitreous fluid of the eye. One, 2, 3 and 24 hrs, respectively, after enucleation, specimens were fixed in paraformaldehyde (2% at 4 °C). All tissue specimens were subsequently processed for immunohistochemical analysis.

Light microscopy

For immunohistochemical analysis of unfixed macular tissue with alkaline phosphatase and peroxidase-labelled antibodies, cryostat sections (5 μm) were cut and mounted on glass slides coated with 3-aminopropyl 3-aethoxy silane (AAS), (Sigma Chemical Co, St.Louis, USA) and air dried. Cryostat sections were further treated as described for paraffin sections.

Paraffin sections (6 μm) were mounted on glass slides and after deparaffinization and rehydration, endogenous peroxidase was blocked with hydrogen-peroxide (3% H_2O_2 in methanol, for 25 min, room temp). After rinsing with water and PBS the sections were incubated with pronase (0.1 % in PBS, for 10 min, 37 °C, pH 7.4). The reaction was stopped with cold PBS and the slides were washed several times with PBS at room temperature. Before treatment with pronase several sections were incubated for 30 minutes with either 6 M guanidine-hydrochloride (Sigma Chemical Co, St.Louis, USA) in 50 mM sodium-acetate (pH 6.5, 10 min, room temp.) or 0.1% sodium-borohydride (Sigma, USA) in order to restore immunoreactivity after aldehyde fixation[13]. The slides were placed in a Sequenza immunostaining workstation (Shandon Scientific Ltd, Astmoor Rancorn Cheshire, England) and incubated with primary antibodies. These included rabbit

anti-human collagen type IV (1:50 dilution, AKZO Organon Teknica, Boxtel, the Netherlands), mouse anti-human collagen type VI (1:20 dilution, Heyl, Berlin, Germany), rabbit anti-EHS mouse sarcoma laminin (1:50 dilution, AKZO Organon Teknica, Boxtel, the Netherlands), rabbit anti-human fibronectin (1:1200 dilution, Dakopatts, Glostrup, Denmark) and mouse anti-human HSPG (1:2 dilution, Chemicon International, Temecula, USA). After washing and incubation with biotinylated secondary antibodies, sections were incubated with avidin-biotin-horseradish-peroxidase complex (1:1200 dilution, ABC, Dakopatts, Denmark). Finally immunoreactivity was visualized with 0.02% 3,3 diaminobenzidine (DAB) tetrahydrochloride (Fluka, Hilversum, the Netherlands) in PBS with 0.05% hydrogen peroxide. Other sections were used to visualize immunoreactivity with alkaline phosphatase labelled secondary antibodies and a phosphatase substrate (Vector Laboratories Inc. Burlingame, USA). Sections of 24 maculae were stained with peroxidase, those of 44 maculae with alkaline phosphatase-labelled secondary antibodies. The sections were counterstained with Mayer's hematoxylin for 1 minute. For negative controls, normal rabbit or mouse serum replaced the primary antibodies. Basement membranes of the capillaries of the retina and choriocapillaris served as internal positive controls. Antigen retrieval methods for formalin-fixed paraffin embedded tissue[207] were tested but were not suitable for macular tissue.

Electron microscopy

Macular tissue from 3 eyes was fixed with paraformaldehyde (2%, pH 7.4, for 1½ hrs at 4 °C); the tissue was dehydrated with 50% ethanol for 2 x 1 hr followed by 70% ethanol for 2 x 1 hr and embedded in LR-White (TAAB, Berkshire, England). The LR-White was polymerized at 50 °C for 24 hrs[155,231]. A part of the similarly fixed and dehydrated maculae from 5 eyes was embedded in Lowicryl-K_4M (Balzers, Maarssen, the Netherlands). Polymerization took place under ultraviolet light at -35 °C for 24 hrs and at room temperature for an additional 48 hrs. Semithin sections (1 μm) were cut with a glass knife and mounted on AAS-coated glass slides.

Colloidal gold immunolabeling on semithin plastic sections was performed as described below for ultrathin plastic sections, with an additional silver enhancement reaction (15 min, room temp, in darkness) (Aurion, Wageningen, the Netherlands). These semithin sections were examined by reflection-contrast

microscopy (Axioplan, Zeiss, Oberkochen, Germany), which allows detection of very delicate immunogold/silver-staining.

Ultrathin sections (50-60 nm) were cut with a diamond knife and mounted on unfilmed 200-mesh copper grids. Immunostaining for electron microscopy was performed as previously described[33]. Sections were incubated with primary antibodies, diluted in PBS/BSA/glycine (for 2 hrs at room temperature). Dilutions of primary antibodies of 1:10 and 1:20 were used for type IV collagen, laminin, HSPG and fibronectin. Transmission electron microscopy was performed (Zeiss TEM 902, Oberkochen, Germany) and electron micrographs were made on sheet film (Kodak SO 163, Rochester, New York, USA).

For immunoelectron microscopy of frozen sections, tissue was first fixed with paraformaldehyde (2% wt/vol, pH 7.4 for 1½ hrs, 4 °C) and subsequently infiltrated with 2.3 M sucrose for 1 hour. Ultrathin frozen sections were prepared on a cryostat (Cryo-Nova, LKB, Stockholm, Sweden) with a glass knife and mounted on formvar-filmed, 200-mesh copper grids. Immunoreactions were performed as previously described[33], although incubation times were shortened to 1 hour and blocking of background staining with normal goat serum was omitted. The basement membranes of the choriocapillaris and the capillaries in the retina served as positive internal controls.

RESULTS

Table 1. Results of immunohistochemical analysis of human maculae examined by light and electron microscopy.

	BLD	B-RPE	B-CC	Ch	drusen	BM	ret.cap
type IV collagen	++*/+†	++/±	++/++	++/	-/	-/-	+/
laminin	+*/±	++/±	++/+	++/	-/	-/-	+/
HSPG	++*/	-/	±/	+/	-/	-/	++/
fibronectin	-/-	±/-	±/-	+/	-/	++/+	/
type VI collagen	-/	-/	±/	±/	-/	-/	/

*early type- and flocculent BLD † homogeneous component only
++ strongly positive, + positive, ± faintly positive, - negative.
B-RPE=basement membrane of the retinal pigment epithelium, B-CC=basement membrane of the choriocapillaris, Ch=choroid, BM=Bruch's membrane, ret. cap. =retinal capillaries.

The light microscopy results of immunostaining cryostat sections with antibodies against type IV collagen, laminin, fibronectin and HSPG revealed specific staining of the capillaries of the retina and choriocapillaris and the choroidal vasculature. Bruch's membrane, the RPE basement membrane and drusen were not stained. At places a BLD would be faintly positive for type IV collagen and laminin. Treatment of the cryostat sections with pronase prior to immunostaining did not affect the results.
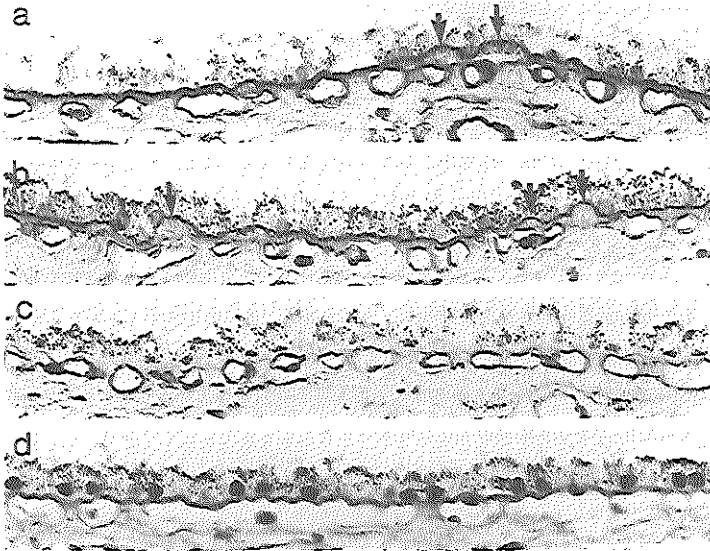

Figure 8.1 Immunohistochemical analysis of paraffin sections of a human macula. a) antibodies against type IV collagen. The basement membranes of the RPE and the vessels of the choriocapillaris and choroid are stained. Notice the hard drusen between the basement membrane of the RPE and the inner collagenous zone of Bruch's membrane, which show no immunoreactivity (arrows). b) Antibodies against laminin. Positive staining of the vascular and RPE basement membranes is seen. Several unstained hard drusen are present (arrows). c) Antibodies against type VI collagen. Only the basement membranes of the capillaries are positive. d) Antibodies against fibronectin. The inner and outer collagenous zones of Bruch's membrane are strongly positive. Basement membranes are faintly positive. (immunoperoxidase staining, magnification 400x).

Immunohistochemical studies on paraffin sections, after pretreatment with pronase, showed that the basement membranes of the RPE and the choriocapillaris, as well as the retinal and choroidal vessels were intensely positive for type IV collagen and laminin (Fig 8.1). BLD was not positive for either type IV collagen or laminin except for a thin layer directly adjacent to the RPE plasma membrane. This positive immunoreaction was exhibited by both flocculent BLD

(Fig 8.2a) and a thin layer of BLD (Fig 8.2b). Hard and soft drusen were not positive (Figs 8.1 + 8.2).
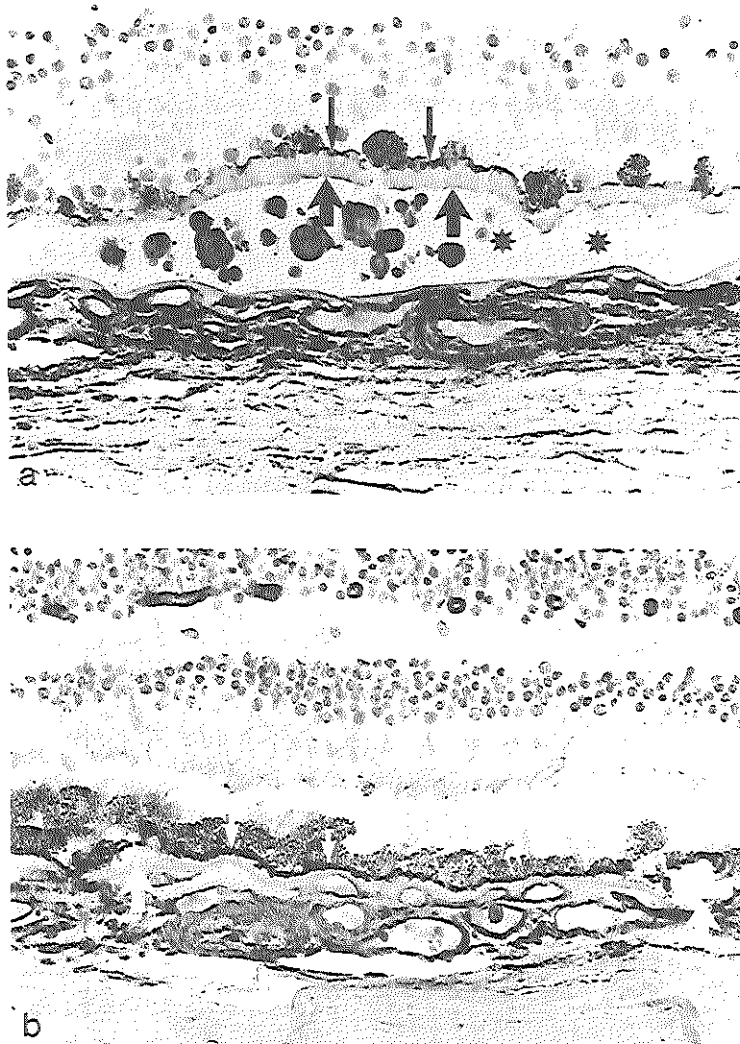
Figure 8.2 Paraffin section of a human macula. a) with a flocculent BLD (large arrows) overlying soft drusen (asterisks) with calcifications, stained with antibodies against type IV collagen. Notice that only a small rim of the BLD adjacent to the RPE cells is stained (small arrows). b) Section of the same macula, just outside the fovea, stained with antibodies against laminin. A thin layer of a late type BLD is stained (small white arrows). Two hard drusen (large white arrows) are not stained. (immunoperoxidase, magnification 400x).

Immunostaining for type VI collagen on frozen as well as on paraffin sections revealed no immunoreactivity in BLD, the basement membrane of the RPE, hard drusen and Bruch's membrane(Fig 8.1c).

For fibronectin, immunoreactivity was diffuse in Bruch's membrane (Fig 8.1d). and negative in BLD and hard drusen.

Pretreatment of the deparaffinized and rehydrated sections with guanidin-hydrochloride or sodium-boronhydride did not further enhance the immunoreactivity.

Semithin sections of LR-White-embedded tissue examined by the immunogold-silver technique using reflection-contrast light microscopy showed that the BLD and the basement membranes of the RPE and the choriocapillaris were positive for type IV collagen and laminin (Fig 8.3). Drusen did not stain.

Figure 8.3 LR White (1 μm) section of a human macula, stained with antibodies against type IV collagen labelled with 10 nm colloidal gold particles with silver enhancement. top) Normal light microscopy: the part of the BLD closest to the RPE cells is the most densely stained (arrows). bottom) Reflection-contrast microscopy of same section shows staining of a large portion of a late type BLD (small white arrows) and the choriocapillaris (large white arrows). (magnification 630x).

Immunoelectron microscopy of ultrathin frozen sections and ultrathin sections of LR-White embedded tissue showed intense type IV collagen-specific staining of the basement membrane of the choriocapillaris and only very weak staining of the basement membrane of the RPE in the same section (Fig 8.4). Aspecific background staining was virtually absent. The staining pattern for laminin was similar but less intense. Antibodies against fibronectin produced only

diffuse staining of Bruch's membrane. The long-spacing collagen component of BLD between the RPE plasma membrane and the RPE basement membrane and in the outer collagenous zone of Bruch's membrane did not exhibit positivity for type IV collagen, laminin (Fig 8.4+8.5) or fibronectin. However, the homogeneous material close to the basement membrane of the choriocapillaris was positive for type IV collagen and laminin (Fig 8.4+8.5).

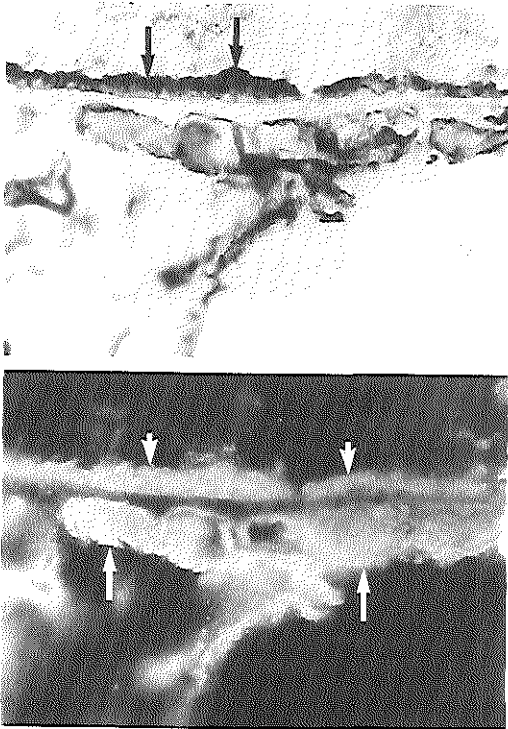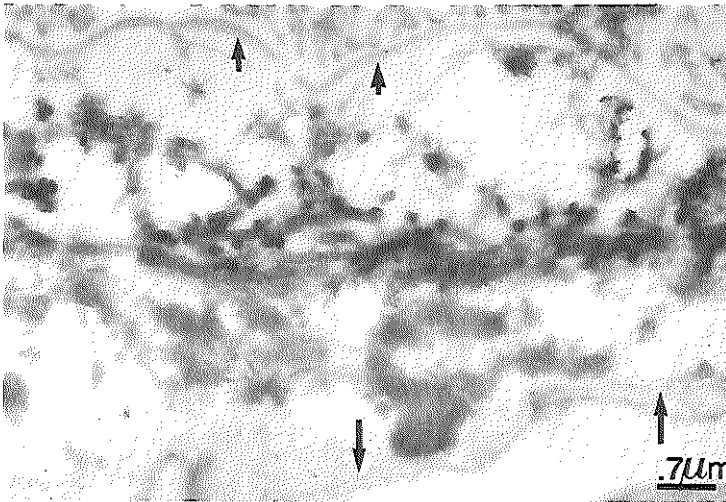*Figure 8.4 Electron micrograph of an ultrathin frozen section of a human macula, stained with antibodies against type IV collagen labelled with 10 nm colloidal gold particles. a) The RPE basement membrane is lightly stained (short arrows) in contrast to the chorio-capillaris basement membrane (long arrows). The long-spacing collagen component of BLD in the outer collagenous zone of Bruch's membrane is not stained.*
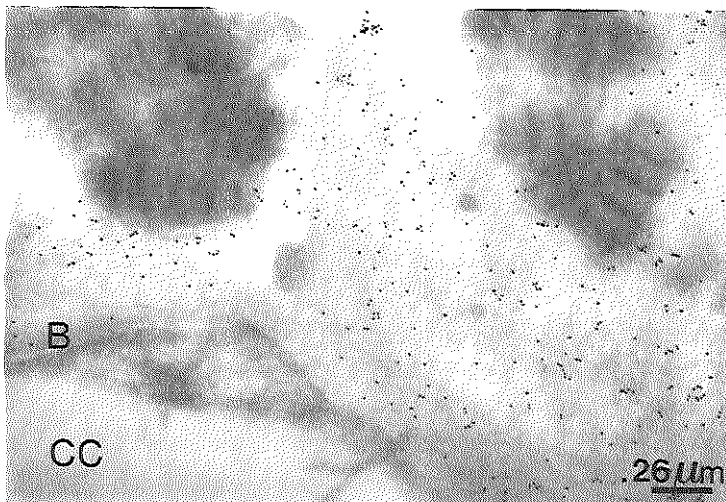
b) higher magnification of the basement membrane (B) of the choriocapillaris (CC) and the outer collagenous zone of Bruch's membrane with BLD. Notice the labelling of the homogeneous material. The long-spacing collagen is not stained.

Figure 8.5 LR White (50 nm) sections of a human macula with a BLD in the outer collagenous zone of Bruch's membrane. a) The homogeneous (H) material is positive for type IV collagen, but the long-spacing collagen is not stained.
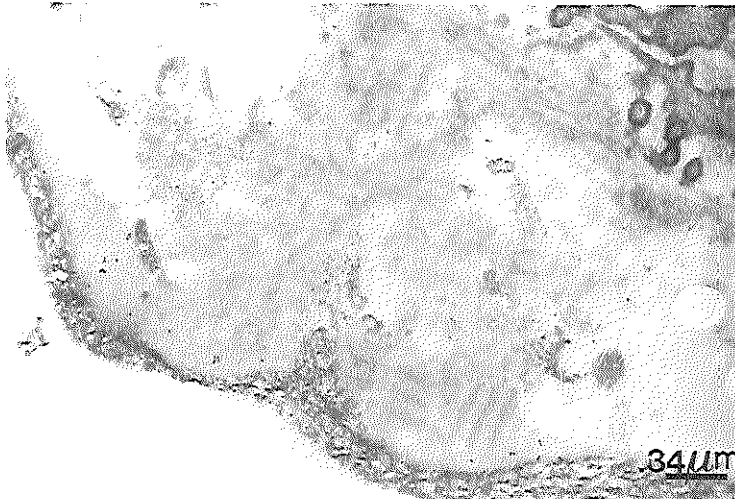
b) Similar labelling is seen with antibodies against laminin.

Fixation in 2% paraformaldehyde preserved immunoreactivity best, but this mild fixation resulted in a loss of preservation of the ultrastructure. A fixation time of 1½-2 hrs ensured an acceptable ultrastructure for 1 mm^3 cubes of tissue and optimum immunoreactivity. With increasing time between enucleation of the eye and fixation of the macula only a slight reduction in immunoreactivity was seen.

Short fixation delays yielded the best results, but even after storage for 24 hrs at 4 °C, immunoreactivity was still acceptable.

DISCUSSION

The localization and ultrastructure of a BLD suggest that it is partly composed of basement membrane material, which is probably produced by the RPE and/or endothelial cells from the choriocapillaris due to either an increase in age or degenerative changes in the macula[202]. However, definite proof that basement membrane components are involved has not been published. It is known that various basement membranes differ in composition[13,140a], but all basement membranes contain type IV collagen, HSPG and laminin[1,232]. Therefore positive staining for these components would be expected in the BLD. Immunoreactivity for these components was best with short post-mortem/post-enucleation times (a maximum of about 4-6 hrs) and mild fixation such as 2% paraformaldehyde or 4% formaldehyde, for short periods, the optimum being 1½-2 hrs.

Demasking techniques, such as antigen retrieval with guanidin-hydrochloride or sodium-borohydride, were not successful. Partial digestion of proteinaceous material in paraffin sections with pronase gave a remarkable improvement in specific immunostaining without an increase in background staining.

The results of our study indicate that the basement membranes of the choriocapillaris and the RPE differ in composition; staining for type IV collagen and laminin was intensely positive in the basement membrane of the choriocapillaris and relatively weak in the RPE basement membrane in the same sections (Fig 8.4)[13,33].

Staining of BLD for type IV collagen and laminin seemed to vary with the type of BLD and with the technique used to detect the antigen-antibody reaction. The results of immunostaining of cryosections and paraffin sections prepared for light microscopy were variable for type IV collagen and laminin but after a prior demasking treatment of paraffin sections with pronase, small portions of an early type BLD, as well as that part of a flocculent BLD which was in close contact with the RPE cells, were clearly positive. Morphologically both early type BLD and

flocculent BLD were composed mainly of homogeneously stained material, which ultrastructurally resembled basement membrane material (Fig 8.5)[192]. If it is assumed that a BLD is deposited by the RPE cells, then the immunoreactive edge of flocculent BLD adjacent to the RPE cells suggests that configurational changes in the antigens, which occur after deposition, reduce or abolish immunoreactivity. The late type BLD, which ultrastructurally consists mainly of long-spacing collagen, was positive only when the immunogold-silver technique was used. This suggests that in this material a lower concentration of type IV collagen-reactive material was present or that the antigens partially were not recognized by antibodies against type IV collagen.

With immunoelectron microscopy positive staining for type IV collagen of the homogeneous component of BLD, close to the basement membrane of the choriocapillaris, was confirmed. The long-spacing collagen component remained unstained, as was described previously[33a,140a]. This could explain the diffuse weak staining of late type BLD achieved with the immunogold-silver technique, as seen by light microscopy, as being due to the relatively small amount of homogeneous component dispersed between the long-spacing collagen.

Immunostaining of all types of BLD for collagen type VI was negative. Thus the hypothesis that BLD could be composed of laterally arranged 100-nm beaded type VI collagen filaments, which would then form long-spacing collagen, becomes unlikely. Fibronectin, a substance which is important in cell adhesion, also was not a component of BLD.

We can conclude that the homogeneously stained component of a BLD, which ultrastructurally resembles basement membrane material, contains type IV collagen, HSPG and laminin and is thus probably composed of excess basement membrane material derived from the RPE and the choriocapillaris. The long-spacing collagen component of BLD did not stain. This is probably due to a difference in composition or an altered antigenicity resulting from polymerization of the material into long-spacing collagen. Type VI collagen and fibronectin were not present in BLD.

ACKNOWLEDGEMENTS

Chapter 9

Early Stages of Age-related Macular Degeneration:
An Immunofluorescence and Electron Microscopical Study

Theo L. van der Schaft,[1] MD; Cornelia M. Mooy,[1,2] MD;
Wim C. de Bruijn,[2] PhD; Paul T.V.M. de Jong,[1] MD, PhD, FCOphth.

From the Institutes of Ophthalmology (1) and Pathology (2),
Erasmus University Rotterdam, The Netherlands
(submitted)

INTRODUCTION

Age-related macular degeneration (ARMD) is the most common cause of severe visual loss in the elderly in the western world[120]. Two end-stages are known: geographic atrophy and disciform macular degeneration. The exact cause still remains unknown, but a multifactorial process is considered most likely[120].

The presence of a basal laminar deposit (BLD), which is a sub-RPE deposition of extracellular material[199,202,203], or numerous large hard drusen can eventually lead to the development of atrophy of both the retinal pigment epithelium (RPE) and photoreceptor cells, so-called geographic atrophy[75]. Soft drusen and BLD are often associated with subretinal neovascularization [29,75,199], which eventually results in the development of the exudative end-stage of ARMD and leads functionally to a deterioration of central vision.

Light microscopically, BLD has been found in aged maculae and is often referred to as abundant basement membrane material[199,202,203], based upon its localization between the RPE cell membrane and its basement membrane. A thick layer of BLD is usually seen in maculae with RPE degeneration, geographic atrophy or disciform macular degeneration[131,199,203].

In subretinal neovascularization, capillaries originating from the choriocapillaris must cross Bruch's membrane, which normally forms a firm and continuous mechanical barrier in the macula, to reach the sub-RPE space[75]. Therefore breaks in Bruch's membrane have to be formed prior to neovascularization. Histologic examination of eyes with subretinal neovascularization or disciform scars has shown macrophages adjacent to the thin areas and ruptures in Bruch's membrane[108]. This has been interpreted as the breakdown of Bruch's membrane by these macrophages[108,160,170].

In general, macrophages are attracted by foreign bodies or chemical substances such as immune complex deposits[44,254]. Phagocytic action of macrophages has been described in eyes with ARMD[180], where they digested the OCZ of Bruch's membrane, preferentially when BLD or drusen were present[170]. However, it is unknown why macrophages are attracted to, and apparently digest, Bruch's membrane in patients with early stages of ARMD.

The purpose of this study was to investigate whether immune complex deposits can be detected in maculae with early stages of ARMD and to explain the

assumed macrophage reaction prior to the disciform reaction. We examined a series of human maculae by direct immunofluorescence light microscopy using antibodies against immunoglobulins, fibrinogen and complement factors. Transmission electron microscopy was performed to identify the macrophages.

MATERIALS AND METHODS

The maculae of 20 human eyes from 13 subjects were obtained at autopsy or after surgical enucleations for intraocular melanoma. The ages of the subjects ranged from 41 to 96 years (mean 74, SD = 19,6)

The maculae were dissected from the globes and divided into two equal halves in the direction of the optic disc. One half was snap frozen in isopentane (-70 °C) and stored in liquid nitrogen for immunofluorescence studies. Three series of frozen sections (5 μm) taken at 50-μm intervals were prepared and mounted on cleaned glass slides. After fixation with acetone the sections were air-dried. The slides were placed in a Sequenza immunostaining workstation (Shandon Scientific Ltd, Astmoor Rancorn Cheshire, England). Primary antibodies included fluorescein isothiocyanate-conjugated (FITC) goat anti-human IgG (dilution 1:800, De Beer Medicals bv, Hilvarenbeek, the Netherlands), FITC-conjugated goat anti-human IgA (dil. 1:800, De Beer Medicals), FITC-conjugated goat anti-human IgM (dil. 1:800, Kallestad Lab. Inc. Chaska, Mn, USA), mouse anti-human IgE (dil.1:50, Central Lab. Red Cross Bloodtransfusion Service (CLB), Amsterdam, the Netherlands), rabbit anti-human complement (C_{3c}, C_{3d}, C_4; dil. 1:50, CLB), rabbit anti-human C_1Q (dil. 1:50, CLB) and rabbit anti-human fibrinogen (dil. 1:50, CLB). As negative controls normal rabbit serum (Dakopatts, Denmark) and sections of a macula from a 41-year-old subject, which did not exhibit any abnormalities by conventional light microscopy, were used. As positive controls frozen sections of human skin and kidney from subjects with known immune complex diseases were routinely used at regular time intervals. After incubation with the primary antibodies, the slides were washed and if necessary incubated with FITC-conjugated horse anti-rabbit secondary antibodies by the indirect method (polyclonals: complement, fibrinogen, C_1Q, C_3) or with FITC-conjugated rabbit anti-mouse antibodies(monoclonal: IgE). After washing, the sections were covered with glycerin-phosphate buffer. The

sections were examined with a fluorescence microscope (Zeiss, Oberkochen, FRG) with epi-illumination (excitation: BP 450-490nm; dichroic mirror: CBS 510nm; emission: BP 520-560nm). The immunoreaction was considered to be positive when a bright extracellular granular fluorescence was present in a linear or patchy fashion. Three sections of every macula were stained with hematoxylin-azofloxin (H & A) for normal light microscopy to detect BLD and drusen.

To reveal the possible presence of immune complexes, seen as dense deposits, and to confirm the presence of macrophages and ruptures in Bruch's membrane, we fixed the opposite half of several maculae with a mixture of 4% formaldehyde/1% glutaraldehyde (for 24 hours, pH 7.4). After fixation the tissue was divided into three smaller parts and embedded in epoxy resin (LX 112, Ladd Research Industries Inc, Burlington, VT) for transmission electron microscopy, as previously described[202]. Semithin sections (1 μm thick) were cut with a glass knife and stained with Toluidine blue for light microscopy. Ultrathin sections (30-40 nm thick) were cut with a diamond knife on an ultrotome (LKB, Stockholm, Sweden) and mounted on unfilmed 200-mesh copper grids. After staining with uranyl acetate and lead citrate, the ultrathin sections were examined with a transmission electron microscope (Zeiss TEM 902, Oberkochen, Germany), with an acceleration voltage of 80 KV. Micrographs were made on sheet film (Kodak SO 163, Eastman Kodak, Rochester, N.Y., USA).

RESULTS

In 16 of the 20 maculae hard drusen and BLD of varying thickness (class 1 to 3 [203]) were present in the H & A-stained frozen sections. All sections exhibited thickening of Bruch's membrane (class 2 to 3)[203]. In two maculae geographic atrophy was present and in one macula a disciform scar was seen.

Hard drusen remained unstained with antibodies against IgG, IgA, IgE, IgM, fibrinogen, C_1Q and C_{3c}. In three sections some of the drusen exhibited partial faint granular or homogeneous staining for complement factors. The BLD showed a local faint granular staining for complement factors in three maculae and for fibrinogen in two other maculae.
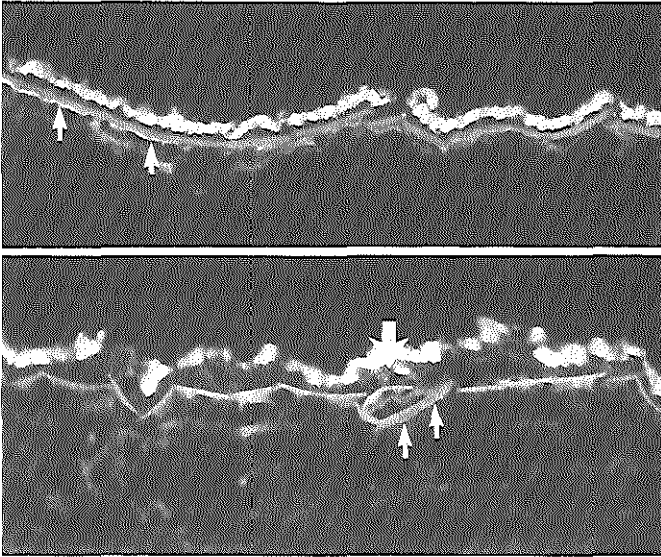
Fig 9.1) a) Immunofluorescence of macula with a BLD between the retinal pigment epithelium (RPE) and Bruch's membrane. Both the RPE and Bruch's membrane exhibit autofluorescence. Specific staining with antibodies against fibrinogen on the outer side of Bruch's membrane (arrows) (magnification 125x).
b) Immunofluorescence on a section of a macula with a BLD between the RPE and Bruch's membrane. Specific staining with antibodies against complement factors on the outer side of Bruch's membrane (small white arrows). Patches of fluorescence are present in the BLD (large arrow) (magnification 250x).
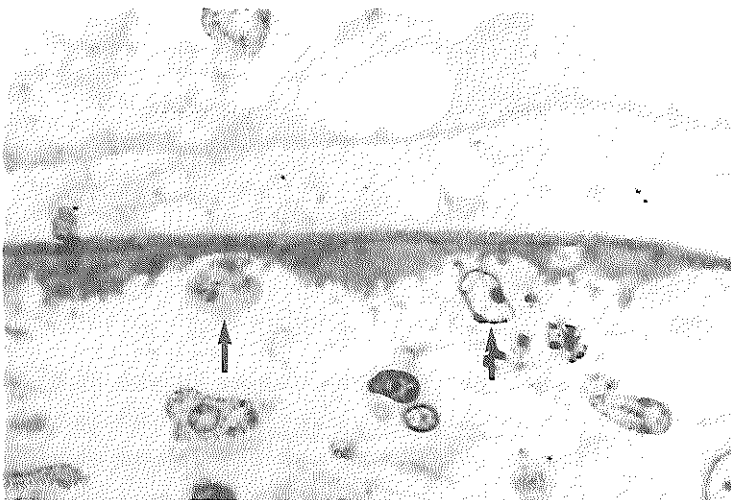
Fig 9.2) Light microscopy of a (1 μm) plastic section of a macula with a fibrovascular scar. Macrophages, heavily loaded with phago-lysosomes and residual bodies can be seen on the outer side of Bruch's membrane (arrows), especially where Bruch's membrane is thinner than normal for that age. On the right a break in Bruch's membrane has almost developed. The RPE has degenerated completely and the photoreceptors have disappeared. (Toluidine blue, 630x).

Fig 9.3) Electron micrograph of a macrophage, filled with phagolysosomes adjacent to Bruch's membrane (top) on the side of the choriocapillaris. On the left Bruch's membrane has disappeared up to the elastic layer (EL). The material seen between the pseudopodal extensions of the cell is mostly long-spacing collagen (arrows), which has loosened from the outer collagenous zone of Bruch's membrane.

Fig 9.4) Electron micrograph of a macrophage, which envelops material from Bruch's membrane (top) from the side of the choriocapillaris (arrows).

In one macula there was a combination of staining of the BLD for complement factors and fibrinogen. Bruch's membrane and the lipofuscin granules of the RPE exhibited autofluorescence, which was also seen in the negative controls.

A linear rim of the OCZ of Bruch's membrane adjacent to the choriocapillaris was positive for fibrinogen (16/20 maculae)(Fig 9.1a), complement (12/20

maculae) (Fig 9.1b), C$_1$Q (1/20 macula), C$_{3c}$ (1/20 macula) and IgM (1/20 macula). The latter three positive reactions were in different maculae. In the macula with a disciform scar light microscopic observations of semithin sections revealed several breaks and abnormally thin areas in Bruch's membrane (Fig 9.2).
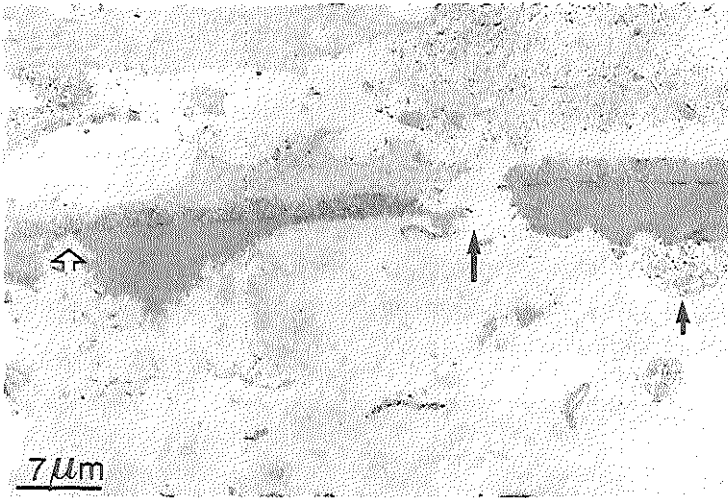
Fig 9.5) Electron micrograph of a complete break in Bruch's membrane in a macula with a disciform scar. Notice the thin area in Bruch's membrane on the left (open arrow), the total break in the middle (large arrow) and a macrophage on the right (small arrow). The RPE is totally degenerated.

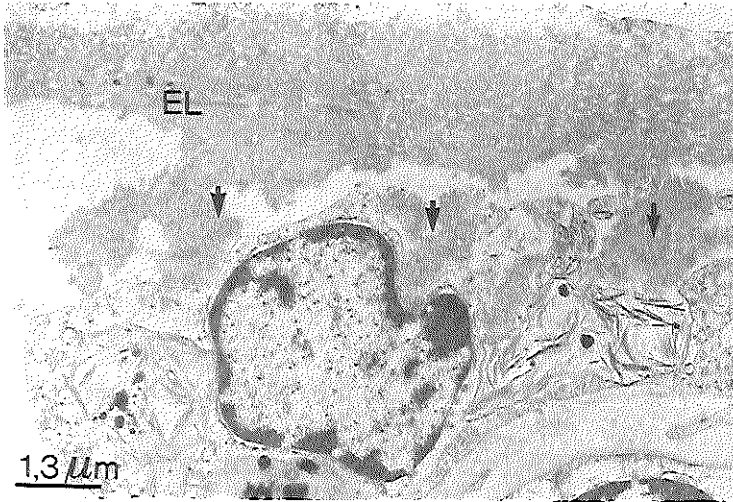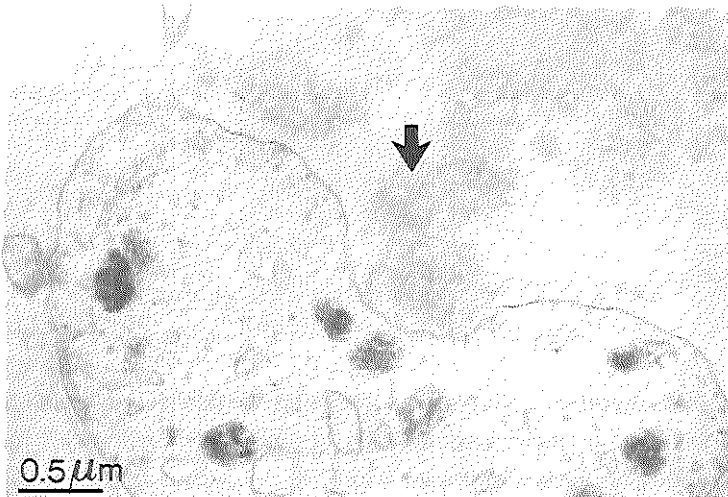*Fig 9.6) Electron micrograph of a macrophage adjacent to Bruch's membrane (top) on the side of the choriocapillaris. The phagocytized material consists mainly of long-spacing collagen (arrow).*

On electron microscopical observation, cells with morphological characteristics of macrophages were seen in the vicinity of these places. These cells contained phagolysosomes with digestion products. The images are suggestive of phagocytosis of the OCZ of Bruch's membrane by these cells (Fig 9.3 + 9.4). Bruch's membrane was destroyed from the side of the choriocapillaris on, up to the elastic layer. Calcifications in the elastic layer seemed to have stopped the phagocytic cells, but several complete breaks were seen (Fig 9.5).

Between the infoldings of the plasma membranes of the phagocytic cells, material which resembled that of the outer collagenous zone could be seen; it consisted mainly of long-spacing collagen (Fig 9.3, 9.4, 9.6). Unfortunately this macula with macrophages was aldehyde-fixed. Therefore immunoreactions could not adequately be investigated. Thus the negative results of immunofluorescence found for this single macula were unreliable.
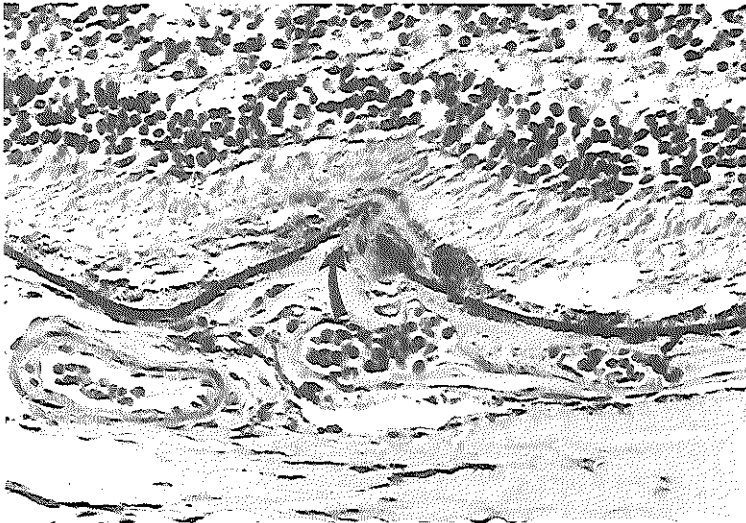
Fig 9.7) Light microscopic image of a paraffin section of a macula stained for calcium phosphates (Von Kossa). Notice the break in the highly calcified Bruch's membrane, with vascular ingrowth from the choriocapillaris into the sub-RPE space (curved arrow). (magnification 400x)

In another macula, electron microscopy revealed a clear example of diapedesis of an endothelial cell of the choriocapillaris. A cytoplasmic sprout of the cell pointed in the direction of Bruch's membrane (Fig 9.8).

DISCUSSION

Circulating immune complexes are in general associated with many systemic immune diseases, such as certain types of arthritis, glomerulonephritis or systemic vasculitis syndromes[44]. Patients with ARMD usually do not exhibit systemic manifestations of immune complex diseases[120].

Humoral immunity against BLD, drusen or deposits of cellular debris in Bruch's membrane with circulating immune complexes and elevated levels of serum IgG, IgA, IgM, IgE or complement has, to the best of our knowledge, not been investigated in eyes with early or advanced stages of ARMD.

Immune complex deposits within the drusen or BLD could not be demonstrated unequivocally, because of the faint and only local staining. Almost all sections, including those from younger subjects, revealed linear deposits of complement and fibrinogen in the OCZ of Bruch's membrane, adjacent to the choriocapillaris, suggesting deposition derived from the choriocapillaris, possibly as a result from leakage through the fenestrated endothelium. The presence of complement and fibrinogen without immunoglobulins is not considered to be a sign of immune complex disease.

Human vascular endothelial cells synthesize and secrete complement factors. Both activators (C_3) and inhibitors (factors H) are produced and regulated by cytokines (interleukin 1, gamma interferon)[44,170]. Therefore the observed deposits of C_3 probably originated from the circulation. This explains the linear deposition of complement along the choriocapillaris. The fibrinogen was probably derived from leakage of the capillaries.

Lysosomal destruction of complement and immunoglobulins has been described. Lysosomal enzymes, such as elastase and collagenase from neutrophilic granulocytes and maybe also from macrophages[108], may cause tissue destruction as well as removal of the immune complexes [254]. Hence, these complexes cannot be detected with immunofluorescence techniques. Only the remnants of the deposits, such as tissue-bound C_3 fragments and precipitated fibrinogen, can be observed, as was found in our study. However, to remove all of this material more macrophages or neutrophilic granulocytes should be present in this tissue. Moreover, in the macula of the 41-year-old subject similar deposits of complement and fibrinogen were found. This is an argument against the theory of

immune complexes as a causal factor in the development of ARMD.

Our electron micrographs show phagocytic cells close to perforations in Bruch's membrane in a macula with a fibrovascular scar, as has previously been described by others[108]. These cells exhibited the morphological characteristics of macrophages, with numerous phagolysosomes and residual bodies[108]. The electron micrographs clearly suggest that these cells participate in the digestion of Bruch's membrane from the side of the outer collagenous zone. Thus, a pathway for subretinal neovascularization, which is the initial phase in the formation of a fibrovascular scar, is formed. There appeared to be a preference for phagocytosis of the long-spacing collagen, which is often seen in the outer collagenous zone of Bruch's membrane[107,202]. However, the presence of this material in a high percentage of the maculae[202] compared to the low prevalence of disciform macular degeneration[203] makes it questionable whether that this is the only causal factor involved in the formation of gaps in Bruch's membrane. Changed proteins, which are not recognized as autologous material, are another explanation for this phagocytic action.

Other factors for macrophage attraction, such as immune complex deposition or foreign substances in Bruch's membrane could also be involved. With electron microscopy, immune complexes can be identified[254] but were not seen in this study. Moreover, the presence of macrophages is not a consistent finding in early and advanced ARMD.

Other causes of gaps in Bruch's membrane are mechanical breaks in a highly calcified Bruch's membrane (Fig 9.7) or perforation of the basement membrane of the choriocapillaris by endothelial cells (Fig 9.8), as described previously[86,108,173,179]. Even single RPE cells have been shown to be able to penetrate Bruch's membrane (Fig 9.9) [78,170]. The initial cause of this endothelial outgrowth could be the absence of vascular inhibiting factors, which are normally produced by the RPE cells[23,69], the presence of angiogenic stimulating factors from macrophages[171,173,179] or a reaction to ischemia in the outer retina or choroid.

0,6 μm
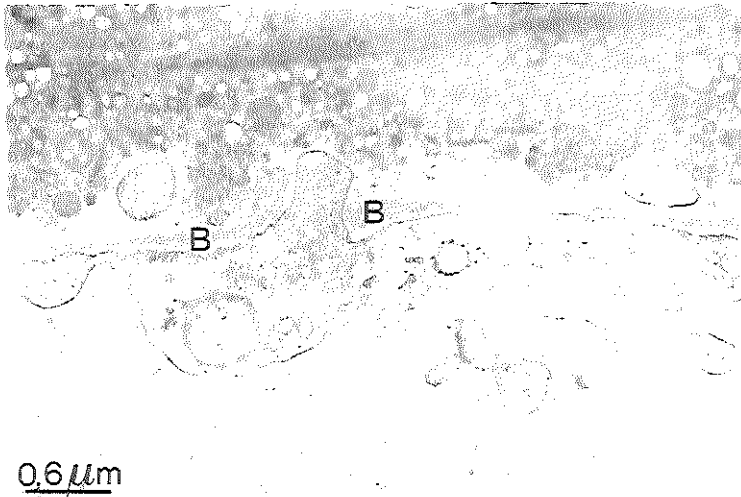
Fig 9.8) Electron micrograph of an endothelial cell of the choriocapillaris (bottom), which has penetrated its basement membrane (B) and projects a cytoplasmic sprout towards the OCZ of Bruch's membrane (top).

Fig 9.9) Light microscopic image of a paraffin section of a human macula. Notice the RPE cell, which seems to have penetrated Bruch's membrane and is now located halfway to the choriocapillaris (arrows). (Mallory stain, magnification 400x).

From our study we can conclude that definite immune complex deposits cannot be found in maculae with BLD or drusen. Linear deposition of fibrinogen and complement was found on the choriocapillaris side of the outer collagenous zone of Bruch's membrane. These deposits are considered to be aspecific and not typical for immune complex disease. Accumulation of unknown or changed proteins in the outer collagenous zone of Bruch's membrane might be a cause of activation of macrophages, which were seen in the vicinity of perforations in Bruch's membrane. However, the presence of macrophages was not a consistent finding in early and late stages of ARMD and thus they are not likely to be the sole factor in the development of ARMD.

ACKNOWLEDGEMENTS

CHAPTER 10

Basal Laminar Deposit in the Aging Peripheral Human Retina.

Theo L. van der Schaft[1], MD; Wim C. de Bruijn[2], PhD;
Cornelia M. Mooy[1,2], MD; Paul T.V.M. de Jong[1], MD, PhD, FCOphth

From the Institutes of Ophthalmology (1) and Pathology (2),
Erasmus University Rotterdam, the Netherlands

INTRODUCTION

Post-mortem light microscopic examination of eyes from patients with clinical signs of age-related macular degeneration (ARMD) has shown an accumulation of extracellular material between the retinal pigment epithelial (RPE) plasma membrane and the inner side of Bruch's membrane in the macular area [199]. This material is called a basal laminar deposit (BLD)[192,199,203]. The presence of a BLD in the macula has been associated with RPE degeneration and decreased visual acuity[192,199]. Light microscopically, a BLD appears as a dis-continuous layer in the early stage of ARMD and as a linear band or a continuous layer between the RPE and Bruch's membrane in a more advanced stage[203].

Ultrastructurally, a BLD is located between the RPE plasma membrane and its basement membrane[131,202] in contrast to drusen, which lie between the basement membrane of the RPE and the inner collagenous zone of Bruch's membrane[216]. The early type of BLD is distributed in a patchy fashion between the RPE and Bruch's membrane and consists ultrastructurally of homogeneously stained, finely granular material interspersed with small amounts of banded material, called long-spacing collagen (LSC)[67]. The late type of BLD, which generally occurs as a thick continuous layer between the RPE and Bruch's membrane, is composed mainly of LSC, which displays a characteristic fingerprint-like banded pattern with a periodicity of about 120 nm and is embedded in small amounts of homogeneously stained, finely granular material[202,204]. Furthermore, some fibrillar material can be seen as well as a few vesicles. Material morphologically similar to that of a BLD has also been found in the inner and outer collagenous zones of Bruch's membrane in the macular region[45,202].

A third type of BLD has been observed in eyes with long-standing macular degeneration at the edges of geographic atrophy. This is called a flocculent BLD, because of its multilaminar or cumuliform arrangement at the base of the RPE[192]. The ultrastructure has been described as a mixture of amorphous clumps, fibrillar material and small amounts of banded material[192].

In a previous light microscopical study[203], the equatorial retina was found to contain sub-RPE deposits, which had the same staining properties as a BLD in the macula but exhibited a slightly more compact structure. These deposits extended farther than hard drusen normally do and, in most eyes, they could be

distinguished from drusen by both their shape and the difference in staining properties.

Most studies on ARMD focus on the degenerative changes in the macula[74,75,90,258,260] since these changes have more important implications as far as function is concerned. Because the exact pathogenesis of ARMD as well as the exact origin of a BLD is still unknown, we examined the ultrastructure of BLD-like sub-RPE deposits and differences in ultrastructure of the RPE and Bruch's membrane in peripheral parts of the retina and choroid of eyes with a BLD in the macula.

MATERIALS AND METHODS

We selected 10 eyes from a larger series of 50 post-mortem human eye-bank and autopsy eyes described previously[203]. These 10 eyes were selected because light microscopy revealed the presence of a BLD class 2 (a thin continuous layer) or class 3 (a thick layer measuring at least half the height of the RPE) between the RPE and Bruch's membrane in the peripheral retina[203]. The age of the subjects ranged from 72 to 90 years. The eyes were fixed with formaldehyde (4% vol/vol, in buffer, pH 7.4). In 5 of these 10 eyes tissue was taken from the stored but not embedded part adjacent to tissue in the paraffin block. Macroscopically, BLD cannot be recognized. In the remaining 5 eyes, the parts of the retina and choroid containing these deposits, as seen light microscopically, were excised from the paraffin blocks. These blocks were subsequently deparaffinized with toluol and rehydrated in graded alcohols. After additional post-fixation with osmium tetroxide (1% wt/vol in buffer, pH 7.4, room temp., overnight) and subsequent dehydration with graded acetone, all tissue samples were embedded in LX 112 (Ladd Research Industries, Inc, Burlington, Vermont, USA) as previously described[202]. Semithin sections (1 μm thick) were cut with a glass knife and stained with toluidine blue for light microscopy. Ultrathin sections (30-40 nm thick) were cut with a diamond knife on an ultrotome (LKB, Stockholm, Sweden) and mounted on unfilmed 200-mesh copper grids. After staining with uranyl acetate and lead citrate, the ultrathin sections were examined with a transmission electron microscope (Zeiss TEM 902, Oberkochen, Germany), with an acceleration voltage of 80 kV. Micrographs were made on sheet film

(Kodak SO 163, Eastman Kodak, Rochester, N.Y., USA). The ultrastructure of the sub-RPE deposits in peripheral retinas was compared with some micrographs of the ultrastructure of BLD in maculae from different eyes from a previous study[202].

RESULTS

The ultrastructure of the RPE and Bruch's membrane in the peripheral retina differed in some aspects from the ultrastructure of similar structures in the macula.

The RPE in the peripheral part of the eye (Fig 10.1a) was more attenuated and contained fewer melanin, melanolipofuscin and lipofuscin granules than that in the macula. These granules are mainly located in the apical parts of the RPE cells (Fig 10.1a). The mitochondria were more evenly distributed throughout the cytoplasm of the RPE cells and not merely in the basal part of the cells (Figs.10.1a + 10.2), as in the macula (Fig 10.1b). The apical villi were long and numerous and often appeared to have branches and connections (Fig 10.2). Basal infoldings of the RPE cells were numerous (Fig 10.1a), as can be seen in the macula (Fig 10.1b). In both the macula and the peripheral retina the basement membrane of the RPE did not follow the basal infoldings of the cell membrane but continued in a straight line (Fig 10.1a + b).

The most striking difference between Bruch's membrane in the macula and outside the macula was the presence in the periphery of a thick elastic lamina, which was often discontinuous (Fig 10.1a). In the macula this elastic lamina was composed of a very thin meshwork of elastic fibers (Fig 10.1b). The structure of both the inner collagenous zone (ICZ) and the outer collagenous zone (OCZ) of Bruch's membrane seemed to be more open in the peripheral retina than in the macula (Fig 10.1a + b). In the ICZ several types of small vesicles, dense granules and membrane fragments could be seen (Fig 10.1a) although these were not as abundant as in the macula (Fig 10.1b). The OCZ was often thinner in the peripheral retina than the ICZ and contained fewer vesicles and membrane fragments than the ICZ. In this series the OCZ in the periphery hardly seemed to have thickened with advanced age. In contrast the macular OCZ contained abundant cellular debris accumulated during life (Fig 10.1b) [45].

F. 10.1

.
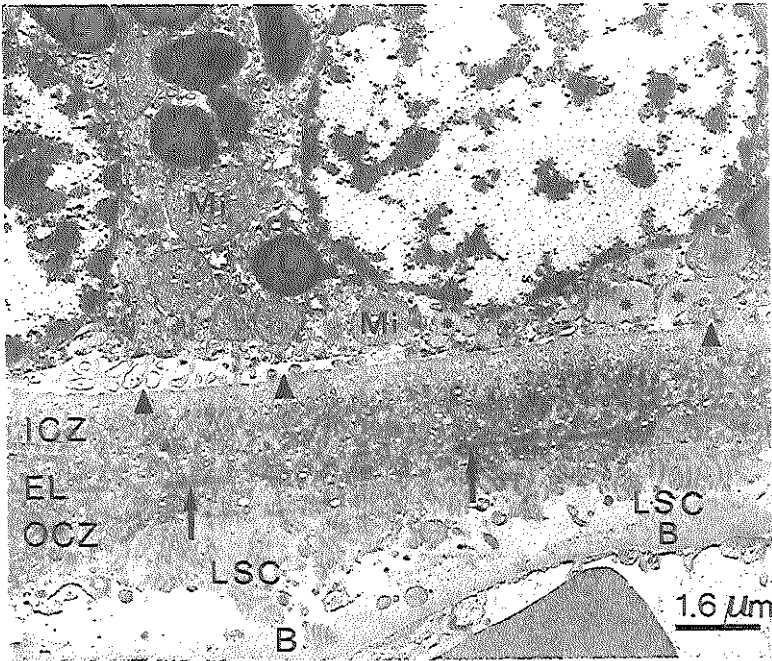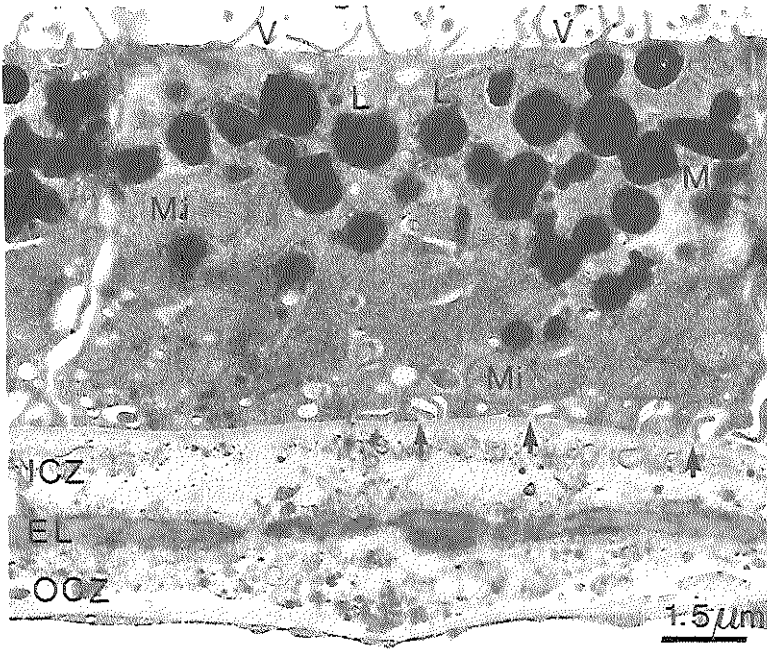
Fig 10.1a) Electron micrograph of the RPE (top) and Bruch's membrane (bottom) in the <u>equatorial</u> retina of an 84-year-old subject. Most apical villi (V) are seen tangentially or in cross-section. The melanin (M) (oval) and lipofuscin (L) (round) granules are located in the apex of the cells. Mitochondria (Mi) can be seen throughout the cytoplasm. At the base of the cells are numerous basal infoldings of the cell membrane. Note that the basement membrane (arrows) does not follow the basal infoldings. The inner collagenous zone (ICZ) of Bruch's membrane is slightly thickened. The thick elastic layer (EL) of Bruch's membrane is frequently interrupted. OCZ= outer collagenous zone.

b) Ultrastructure of the RPE (top), Bruch's membrane and choriocapillaris (bottom) in the <u>macula</u> of an 81-year-old subject. The elastic layer of Bruch's membrane(arrows) is very thin and indistinct. The ICZ and OCZ are filled with vesicles, membranous material and long-spacing collagen (LSC). LSC is mainly located close to the thickened basement membrane (B) of the choriocapillaris. The lipofuscin granules (L) in the RPE are less electron-dense, because this part of the macula was not post-fixed with osmium tetroxide. There are many basal infoldings (arrow heads), some of which are filled with basement membrane-like material (asterisks). Mi = mitochondra.

In 8 out of the 10 eyes, amorphous material was found at the location of the BLD-like deposits revealed by light microscopy in the paraffin sections. Ultrastructurally, it was localized outside the RPE cells between the basal infoldings of the cell membrane, which appeared wider when associated with these deposits (compare Fig 10.1a with Fig 10.2). This material was continuous with the RPE basement membrane and had the same electron density. When close to the RPE cell membrane, the deposits often had a fibrillar structure (Fig 10.2 inset).

In 5 of these 8 eyes banded material or long-spacing collagen was observed in the deposits (Fig 10.3). The proportion of the amount of banded material to the amount of finely granular material was low, as was found for the early type BLD in the macula (Fig 10.4). The late type BLD in the macula consisted almost entirely of long-spacing collagen (Fig 10.5).

Fig 10.2) Electron micrograph of the RPE and Bruch's membrane in the <u>equatorial</u> retina of a 72-year-old subject. The apical villi (V) of the RPE seem to branch out and connect with each other. An amorphous, finely granular deposit can be seen between the RPE cell membrane and the ICZ of Bruch's membrane. The basal infoldings have become wider than in the RPE cells without the deposit. Close to the basal cell membrane of the RPE, the deposit appears fibrillar (asterisks and inset).

Fig 10.3) Amorphous, finely granular deposit between the RPE (top) and Bruch's membrane <u>halfway between the macula and the equator</u> of a 90-year-old subject. Long-spacing collagen (LSC) is interspersed within this material. A second thin basement membrane can be seen along the basement membrane of the RPE (arrows). Adjacent to this basement membrane the deposit appears fibrillar (asterisks). The original basement membrane is still parallel to the ICZ of Bruch's membrane (arrow heads). (Ultrathin section recovered from paraffin-embedded material.

F.10.2

1.2 μm

F.10.3

1.3 μm
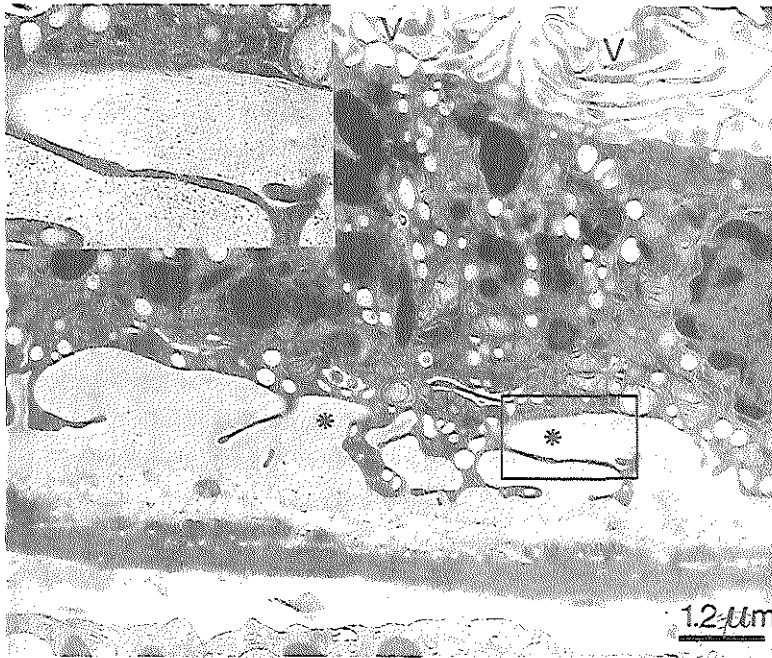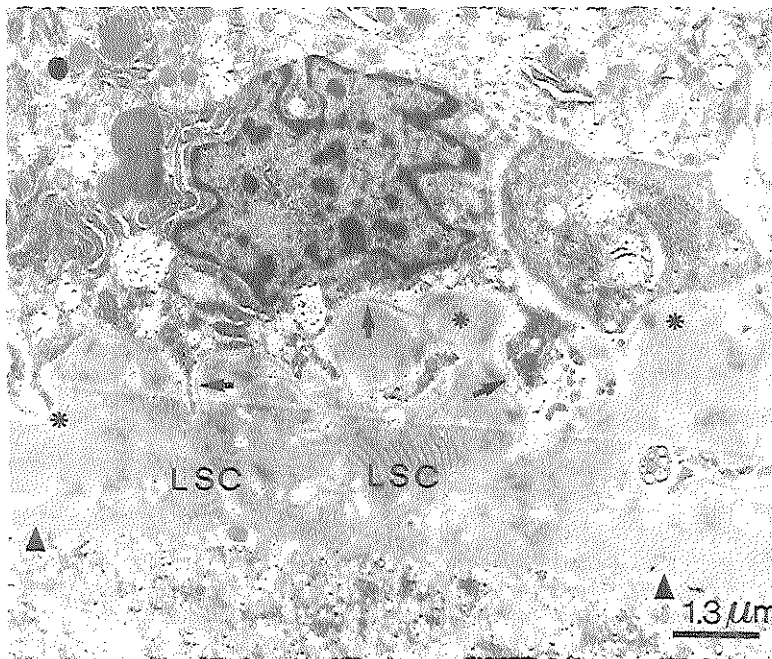
The extracellular deposits in 5 out of the 8 eyes contained randomly scattered and irregularly shaped clumps of amorphous, more electron-dense material (Fig 10.6a). These clumps consisted of a similar amorphous material but were more compact. This material was not surrounded by a membrane (Fig 10.6b).

Large vacuoles were found in the cytoplasm of several RPE cells in the peripheral retina (Fig 10.7). Some vacuoles were filled with a finely granular amorphous material, similar to that observed between the RPE cells and Bruch's membrane. Smaller vacuoles, filled with morphologically the same type of material, could be seen in the basal parts of the RPE cells. Frequently, these vacuoles were continuous with the extracellular RPE basement membrane (Figs 10.1b,10.7-10). Still other vacuoles were electron-lucent and seemed to be empty or were partially filled with even smaller vacuoles containing membranous cellular debris (Fig 10.7). Sometimes the deposits appeared to be lined with a basement membrane on the RPE side as well as on the side of Bruch's membrane (Fig 10.8).

In only 2 of the 8 eyes with sub-RPE deposits the long-spacing collagen component of BLD was found in the OCZ of Bruch's membrane in the peripheral retina (Fig 10.7+10.11). Only a few fragments of long-spacing collagen were sometimes seen in the ICZ (Fig 10.11).

In 2 of the 10 eyes the sub-RPE deposits, identified by light microscopy as being BLD-like, appeared ultrastructurally to be located between the RPE basement membrane and the ICZ of Bruch's membrane (Fig 10.9). These deposits consisted of the same mixture of cellular debris as can be seen in hard drusen (Fig 10.10) as well as in the thickened ICZ and OCZ of Bruch's membrane in the macula (Fig 10.1b), but long-spacing collagen was not found. Although the ultrastructure of these deposits was similar to that of hard drusen, light microscopy revealed that this material was deposited in an elongated and flat way, thus imitating a more extensive BLD. The ultrastructure of the RPE cells overlying the flat deposits was normal (Fig 10.9).

Fig 10.4) An early type BLD in the <u>macula</u> of an 88-year-old subject. The major component of this type of BLD is the homogeneous material (H). Small amounts of long-spacing collagen (LSC) are present. Basement membrane (arrow heads).

Fig 10.5) Large BLD in the <u>macula</u> of an 88-year-old subject. The major component is long-spacing collagen. Only small amounts of homogeneous material can be found (H). Basement membrane (arrow heads). Many lipofuscin (L) and melanolipofuscin (Ml) granules can be seen in the RPE cytoplasm.

F.10.4

F.10.5

F.10.6

a   1.7 μm

b   0.56 μ
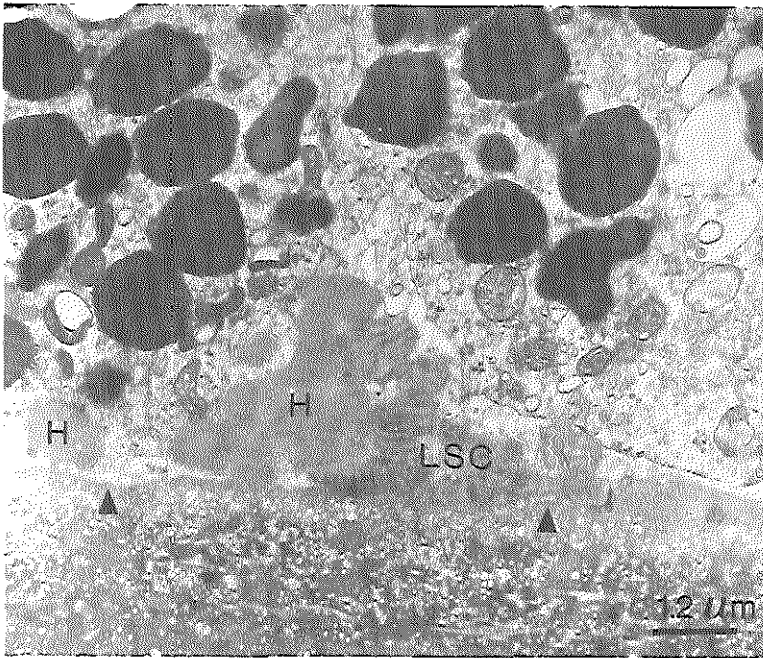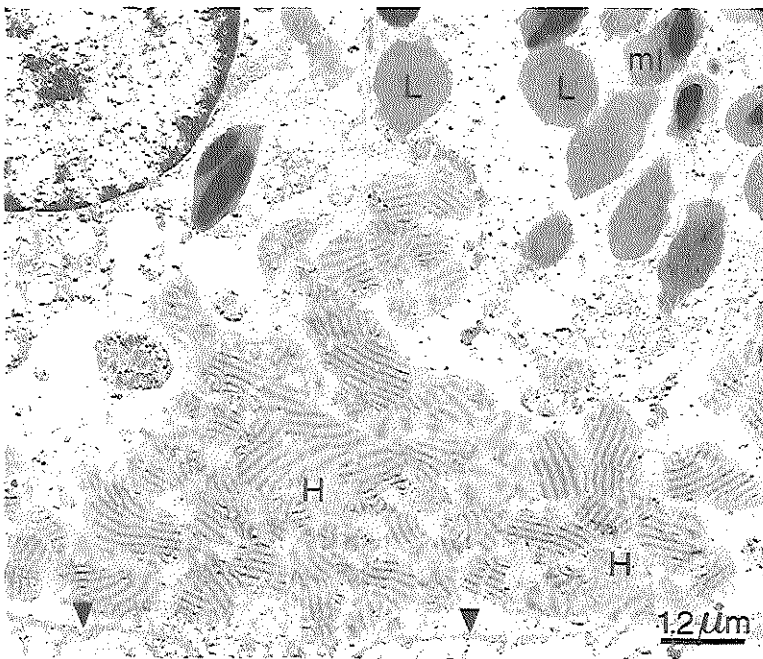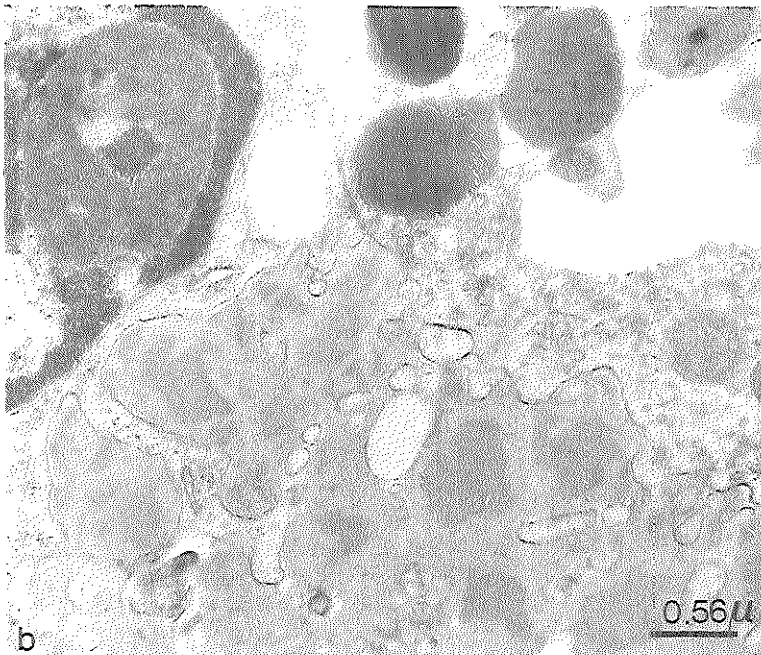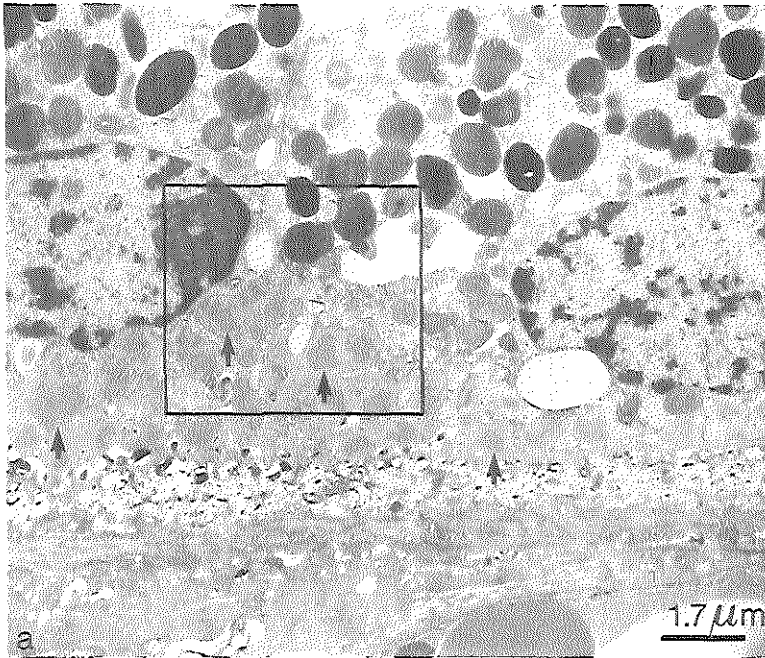
Fig 10.6) a) Deposit between the RPE cell membrane and Bruch's membrane in the <u>peripheral retina</u> of an 82-year-old subject, consisting of lightly stained amorphous material with electron-dense, irregularly shaped clumps (arrows).
b) Higher magnification of the deposit. The electron-dense parts are not surrounded by a membrane.

Several dome-shaped hard drusen were also found (Fig 10.10). These drusen were located between the RPE basement membrane and the ICZ of Bruch's membrane. The top of the druse in Fig 10.10 consisted of homogeneously stained, finely granular material with the same electron density as the RPE basement membrane and was continuous with this basement membrane. There was no long-spacing collagen in these hard drusen. The RPE cells on top of the more dome-shaped drusen contained less pigment. These RPE cells still exhibited basal infoldings.
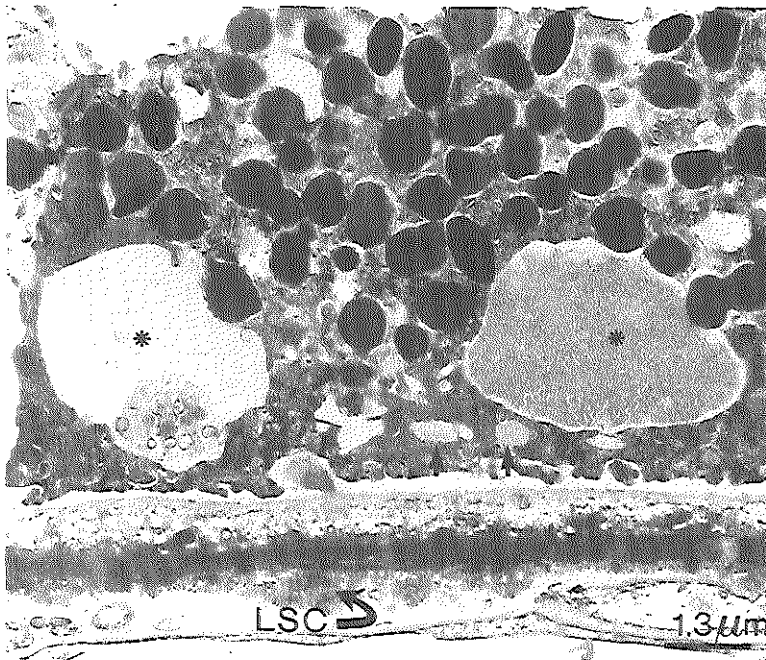
Fig 10.7) Two large vacuoles (asterisks) and several small vacuoles (arrows) in the RPE in the <u>equatorial</u> <u>region</u> of a 90-year-old subject. The right vacuole is filled with amorphous, finely granular material as are several small vacuoles (arrows). The large vacuole on the left is partly filled with membranous debris. Small sub-RPE deposit (open arrow) consisting of lightly stained material and electron-dense material. Small pieces of long-spacing collagen (LSC) can be seen in the outer collagenous zone of Bruch's membrane.

F. 10.8

ICZ

EL

OCZ

1.1 μm

F. 10.9

ICZ

EL

1.4 μm
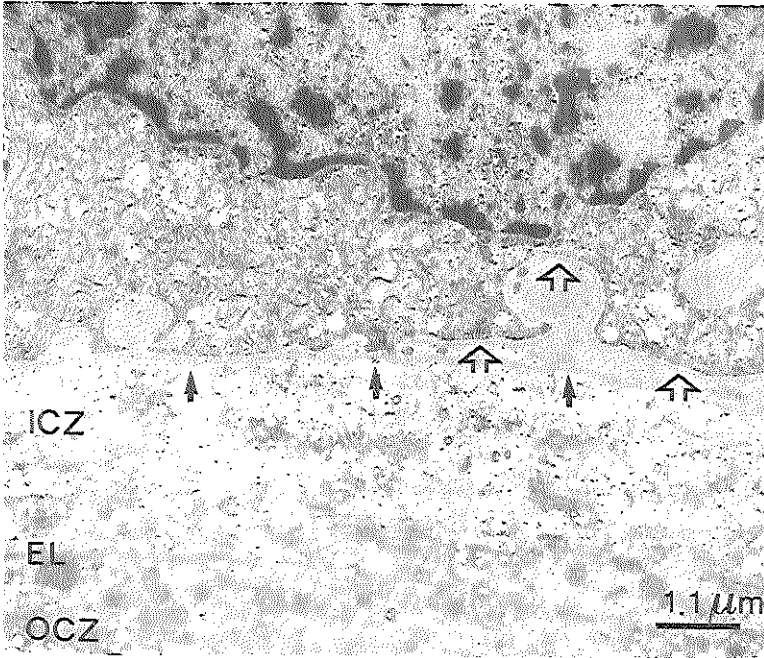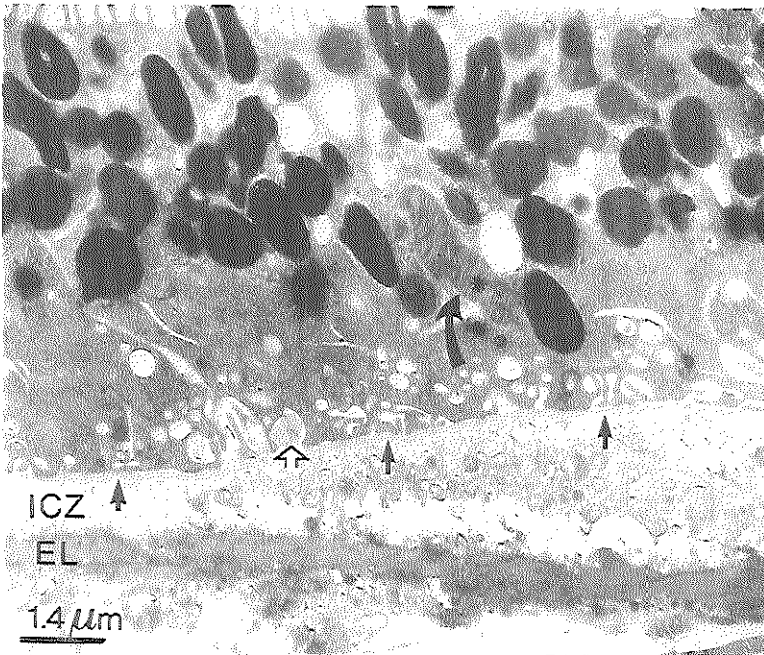
Fig 10.8) Small deposit between the RPE (top) and Bruch's membrane (bottom), just <u>outside the macula</u> of a 90-year-old subject. Note that the original basement membrane is still parallel to the ICZ of Bruch's membrane (closed arrows). A second, thinner basement membrane is adjacent to the RPE cell membrane (open arrows). The ICZ and OCZ of Bruch's membrane are markedly thickened. EL= elastic layer. (Ultrathin section of tissue recovered from paraffin-embedded material.

Fig 10.9) Elongated, drusen-like deposit (asterisk) between the RPE basement membrane (closed arrows) and the ICZ in the <u>peripheral</u> part of the retina of an 84-year-old subject. In the cytoplasm of a RPE cell is a vacuole filled with phagocytized discs of a photoreceptor outer-segment (curved arrow). Note the basal infoldings overlying the druse-like deposit; some are filled with material which is confluent with the basement membrane (open arrow).

DISCUSSION

As previously described in chapter 5 [203], sub-RPE deposits similar to a BLD in the macula can be seen by light microscopy in the peripheral retina; although their staining properties are similar, the deposits in the peripheral retina have a more compact structure than a BLD in the macula. A positive correlation between the presence of these deposits in the macula and the peripheral retina of the same eyes was found[203]. Ultrastructurally, both differences and similarities were found. The main component of the deposits in the peripheral retina was a homogeneously stained material, only rarely interspersed with long-spacing collagen. In contrast, a BLD in the macula consisted of small amounts of homogeneously stained material embedded in large amounts of long-spacing collagen[202] (Fig 10.5). However, an early type BLD in the macula closely resembled the deposits in the peripheral retina[202] (Figs 10.3 + 10.4).

It is not clear why there is a difference in the ratio of the two components of these deposits depending on site in the same eye. Several hypotheses have been proposed. The most striking difference between the macula and the peripheral retina is the distribution of rods and cones, with the cones dominating in the macular region. Because there are no indications that a BLD is comprised of degradation products of the photoreceptor outer segments[48,204], it is unlikely that this is the determining factor. Another difference between the macula and the peripheral retina is the difference in the structure of RPE cells. Although several authors think that the sub-RPE deposits are produced by the RPE [75,131,192,260, see also chapter 6], it is not clear why differences in cell morphology would result in a difference in the composition of the deposits. One might postulate that differences in the composition of Bruch's membrane between the macula and the peripheral retina could result in a more or less well-developed chemical and mechanical barrier between the RPE and the choriocapillaris in the peripheral part of the region[107]. This might lead to differences in the composition of the extracellular fluid and, subsequently, in the composition of the BLD. The OCZ in the peripheral retina contained only a few age-related deposits, such as curly membranes, vesicles of various sizes, dense granules and long-spacing collagen, in contrast to the OCZ in the macula. This does not support a

Fig 10.10) Typical dome-shaped druse between the RPE basement membrane and the ICZ in the *equatorial* retina of an 84-year-old subject. The basal infoldings of the RPE cells are still present. Some of them are filled with material which is continuous with the basement membrane (open arrows). The RPE overlying the druse is attenuated.
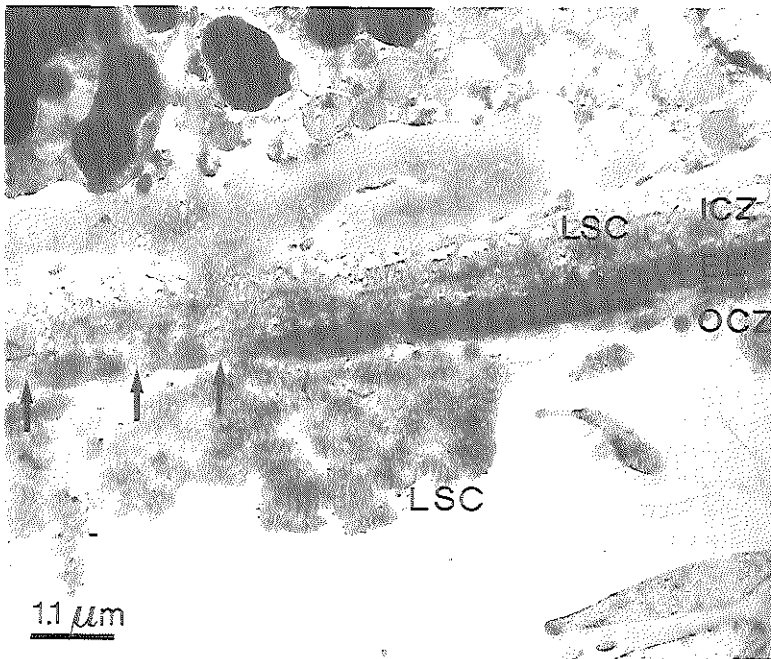
Fig 10.11) Amorphous deposit (asterisks) between the RPE cell membrane and the basement membrane (arrow heads)in the *peripheral* retina of a 90-year-old subject. Long-spacing collagen (LSC) in the ICZ and OCZ of Bruch's membrane. Note the gaps in the thick elastic layer of Bruch's membrane (arrows).

possible role of the choriocapillaris endothelial cells in the secretion of long spacing collagen in the peripheral retina, as was suggested for the macula[202].

The deposits in the macula as well as in the peripheral parts of the eye ultrastructurally seemed to consist partly of basement membrane material, which was often continuous with the basement membrane of the RPE. In the macula these deposits were also found adjacent to and sometimes connected with the endothelial basement membrane of the choriocapillaris[202]. The presence in these deposits of collagen type IV and laminin, which in general are the main constituents of basement membranes, is discussed in chapter 8.

The intracellular vacuoles in the RPE cells were filled with homogeneous material that was morphologically the same as that found directly outside the cytoplasm of the RPE cells (Fig 10.7). This can be interpreted as the production and possible secretion of this material by the RPE cells. It can also be a misleading image of very large basal infoldings, that are sectioned obliquely. A few vacuoles were filled with membranous material, which can also be found in aged Bruch's membrane and in soft drusen[192].

The more electron-dense, irregularly shaped material (Fig 10.6) has not been described in the macula. Perhaps this material condenses or polymerizes into the banded material, as is suggested in Figure 10.3.

The sub-RPE deposits sometimes seemed to be lined by two basement membranes, one on either side, suggesting first the deposition of material between the RPE cell membrane and the basement membrane and afterwards the production of a new basement membrane on the RPE side (Fig 10.8). This production of a new basement membrane has been explained as a defense mechanism of the RPE against macrophages and an attempt to repair breaks in Bruch's membrane[180].

The sub-RPE deposits in 2 of the 10 eyes were located between the RPE basement membrane and the ICZ of Bruch's membrane. Ultrastructurally they consisted of hard drusen, but they were flatter than normal and extended farther. Presumably, under the light microscope, these very flat drusen were confused with a BLD. Another possibility is that the deposits seen by light microscopy were not present in the adjacent tissue, embedded for electron microscopy.

From our observations we can conclude that the ultrastructure of the sub-RPE deposits in the peripheral retina is morphologically similar to that of basement

membrane material. Relatively large amounts of this homogeneously stained basement membrane material are interspersed with some long-spacing collagen, as in the early type BLD in the macula. This hypothesis is further supported by the fact that a statistically significant correlation between the presence of a BLD in the macula and the occurrence of these sub-RPE deposits in the peripheral retina has been established[203]. Therefore we postulate that the deposits found in the peripheral part of the retina can be classified as early type BLD. Because of the almost exclusive localization of these deposits in the peripheral retina between the RPE plasma membrane and the basement membrane, they seem to arise from the RPE cells. The differences in composition between the deposits in the macula and those in the peripheral retina cannot be explained. Light microscopically a BLD in the equatorial region can easily be confused with elongated, flat drusen. However, ultrastructurally the differentiation of these drusen is easy.

CHAPTER 11

Morphometric Analysis of Bruch's Membrane, the Choriocapillaris and Choroid in Normal Aging and Age-related Macular Degeneration.

Raan S. Ramrattan,[1] MSc; Theo L. van der Schaft,[1] MD;
Cornelia M. Mooy,[1,2] MD; Wim C. de Bruijn,[2] PhD;
Paul G.H. Mulder,[3] MSc; Paul T.V.M. de Jong,[1] MD, PhD, FCOphth.

From the Institutes of Ophthalmology (1), Pathology (2)
and Epidemiology & Biostatistics(3),
Erasmus University Rotterdam, the Netherlands.

(submitted)

INTRODUCTION

Age-related macular degeneration (ARMD) is considered to be multifactorial in origin[71,85,120,234,260]. However, the factors that initiate these changes have not yet been identified.

Histologically, ARMD has been described as the presence of multiple or confluent hard drusen, soft drusen, a thick layer of basal laminar deposit (BLD) between the retinal pigment epithelium (RPE) and Bruch's membrane (BrM) [131,199,202], atrophy of both the RPE and photoreceptors (geographic atrophy) or subretinal neovascularization with the subsequent formation of a disciform scar[75,199,203]. It has been postulated that atrophy of the choriocapillaris (CC) in the macula, characterized light microscopically by a decrease in the number and diameter of capillaries, might be an important factor in the pathogenesis of ARMD[58,167]. Histologically, it has been demonstrated that patches of atrophy of the retinal pigment epithelium (RPE) usually correspond to the lobular structures of the CC [137a,248a], which is functionally (but not anatomically) an endarterial system [116a,233a]. Atrophy of the CC with a reduced perfusion has been observed in eyes with geographic atrophy [27a,154]. Biochemical investigations have shown both a trophic and an inhibiting interaction between the RPE and the choriocapillaris[114,114a].

These observations make it conceivable that atrophy of the CC, possibly in combination with changes in the thickness [139a] or composition of BrM [87,166a], may initiate or aggravate impairment of metabolism in the RPE and subsequently in the photoreceptor cells. The degree to which changes in the CC and choroid[61a,199] can be attributed to normal aging and differ from those characteristic of the various stages of ARMD is still uncertain. Furthermore, the correlation between age-related atrophy of the CC and the choroid and thickening of BrM has not been examined systematically in a large group of eyes.

In this investigation, the range of variations in the thickness of BrM, atrophy of the choriocapillaris and the choroidal thickness and their mutual relationships were studied quantitatively in a series of 95 normal human maculae of all ages and 25 maculae with various histological stages of ARMD.

MATERIALS AND METHODS

We obtained 120 unpaired human eye bank and autopsy eyes, consisting of 112 phakic and eight pseudophakic eyes. Eyes from subjects with a history of diabetes mellitus or panretinal photocoagulation were excluded from this study.

The eyes were processed as previously described [203]. In short, after aldehyde fixation, a horizontal tissue block, including the optic disc and the macula, was cut from the hemisectioned globe, dehydrated with graded alcohols and embedded in paraffin. At least three sections (7 μm thick at 140 μm intervals) were cut and stained with the Mallory stain for light microscopy.

The histological changes in 95 of the 120 maculae were considered to be due to normal aging[199,203]. In these normal maculae the number of small hard drusen could be classified as class 0 (no drusen) or class 1 (1-3 drusen), as previously described[203]. There was either no BLD (class 0) or small patches of BLD were present (class 1). The age of the subjects ranged from 6 to 100 years (mean 61 yrs). In total, 25 of the 120 maculae were selected on the basis of histopathological changes associated with ARMD such as hard drusen class 2 or 3 (4 to 10 or many or confluent drusen), BLD class 2 or 3 (thin continuous layer or thick layer of half the height of the RPE), geographic atrophy or disciform scarring. This group of pathological maculae was subdivided into 7 maculae demonstrating only BLD class 3, 10 maculae exhibiting geographic atrophy and 8 maculae from pseudophakic eyes with disciform scarring. The age of the subjects ranged from 40 to 98 years (mean 85 yrs) in the group of pathological maculae from phakic eyes and from 65 to 90 years (mean 81 yrs) in the group of pathological maculae from pseudophakic eyes.

In each histological section, four variables were measured (Fig 11.1): the length of the lumen of each capillary in the CC (1), the luminal diameter of the capillaries (2), the thickness of BrM (3), and the choroidal thickness in the foveal area (5).

For each macula, the ratio of the sum of the lengths of the lumina of the capillaries to the length of the zone in which measurements were made was calculated (Fig 11.1 (1)). This ratio, which theoretically can range from 0 to 1, will subsequently be referred to as the capillary density of the CC. The capillary luminal diameter was measured perpendicular to BrM (Fig 11.1.(2)). The thickness of BrM was defined as the distance between the basement membrane of the RPE and the

basement membrane of the CC (Fig 11.1.(3)). Consequently, the thickness of BrM was not assessed in the intercapillary pillars, which have indistinct borders. The thickness of BrM and the capillary diameter were measured eight times in each histological section at regularly spaced intervals of 140 μm. These values were averaged. Choroidal thickness was defined as the distance between the outer border of BrM and the inner border of the sclera in the foveal area (Fig 11.1 (5)).
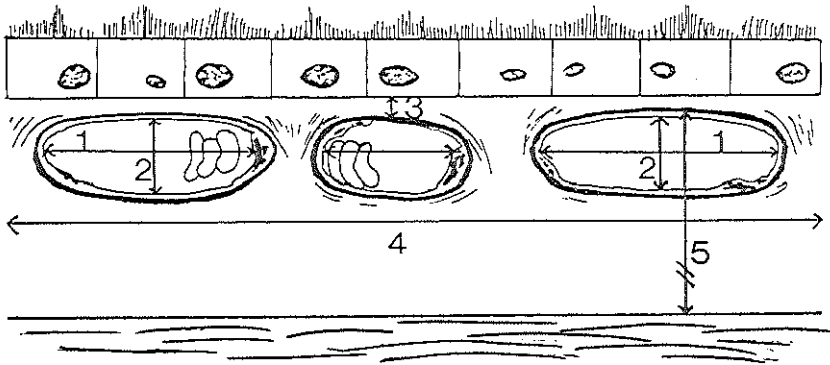
Figure 11.1. Diagram illustrating the way in which measurements were performed in histological sections of the maculae. 1 = length of capillary lumen measured parallel to BrM. 2 = cross-sectional diameter of capillary lumen measured perpendicular to BrM. 3 = thickness of BrM. 4 = total distance (1120 μm) along BrM within which measurements were made. 5 = choroidal thickness.

Measurements were performed using a digital image-processing system (IBAS 2000 system, Kontron, München, Germany) with a final on-screen magnification of 1295x and a spatial resolution of 0.2710 μm (inter pixel distance).

Measurements were taken exactly in the center of the sections of the maculae in a standardized zone measuring 1120 μm along BrM and including the foveola and the central part of the fovea. The distance of 1120 μm was chosen because of practical considerations involving the image-processing system.

Local variations in the four measured variables were determined by comparing the measurements obtained from two sections, with an interval of 140 μm, from 10 normal maculae, one representing each decade.

Intraobserver variation was assessed by comparing the results of measuring the same section from 10 normal maculae, one representing each decade, in a masked fashion twice at a three-month interval. To determine the interobserver variation, the same procedure was followed by the first two authors (RR and TvdS), independently of each other.

STATISTICAL ANALYSIS

For statistical analysis Spearman's rank-correlation test was used to determine the associations between age, thickness of BrM, capillary density, capillary diameter and choroidal thickness in sections from normal and pathological maculae. Partial correlation statistics, which separate the influences of two or more variables from that of a third variable, were performed to clarify observed rank correlations between variables. To eliminate the influence of age on the variables studied, multiple linear regression analysis was applied for the age-adjusted comparison of normal and pathological maculae. In the group of pathological maculae from phakic eyes, the data of the histologically abnormal part of the sections (i.e. BLD class 3, geographic atrophy) were first pooled before comparison with the measurements of normal maculae. The data on pseudophakic eyes with disciform scarring were analyzed separately from the data on the phakic eyes. P-values below 0.01 for Spearman's rank-correlation test and below 0.05 for the other tests were considered to be significant. Local variations in the measured variables and intraobserver and interobserver variation were expressed as the mean difference and the standard deviation of the differences. Intraobserver and interobserver variation could not be expressed as kappa-values because kappa-values only pertain to ordinal variables, while our measurements resulted in continuous variables.

RESULTS

Normal maculae

The results of linear regression analysis showed that the thickness of Bruch's membrane in normal maculae increased by 135% from approximately 2.0 μm in the first decade to a mean of 4.7 μm in the tenth decade with a skewed distribution towards higher values with increasing age (Fig 11.2). The variation in thickness also increased at high age.

The capillary density in normal maculae decreased in an almost linear fashion from approximately 0.75 in the first decade to almost 0.41 in the tenth decade (Fig 11.3). However, high age was not invariably related to low capillary density. With increasing age, the variability of the capillary density increased and in several aged subjects appeared to be comparable to that found for much younger subjects.
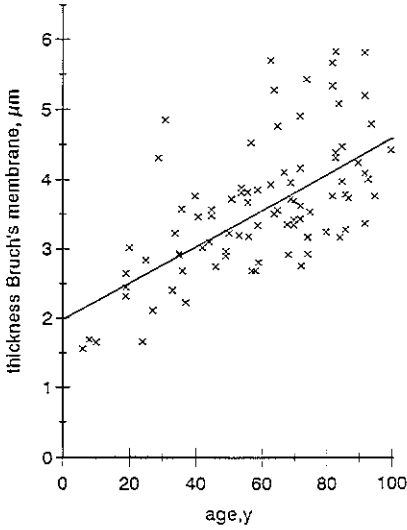
Figure 11.2. Thickness of BrM in 95 histologically normal maculae plotted against age. Notice the steep incline of the thickness. The solid line denotes the best linear fit to the data: the thickness of BrM = 1.99 + 0.027 x age, (R^2=0.42, P<0.00005).
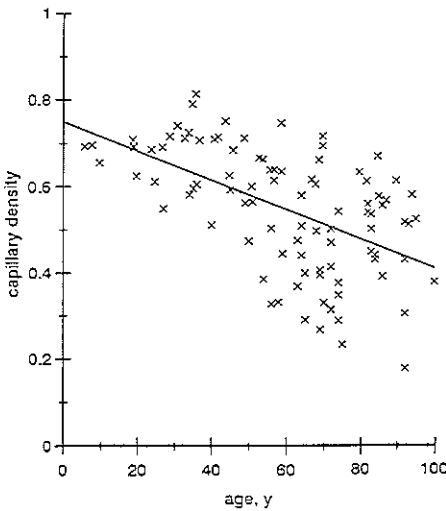
Figure 11.3 Capillary density in 95 histologically normal maculae plotted against age. A significant drop in mean capillary density starting in the sixth decade was found. The solid line denotes the best linear fit to the data: capillary density = 0.75 - 0.0034 x age, (R^2 = 0.31, P<0.00005).

The rank correlations between age, thickness of BrM, capillary density, capillary diameter and choroidal thickness in normal maculae are presented in Table 1. All variables were correlated with age. Capillary density was closely correlated with capillary diameter (r=0.64), which may reflect the fact that both parameters are affected by choriocapillary atrophy. Capillary density exhibited a negative correlation with the thickness of BrM (r=-0.36) and a positive correlation with choroidal thickness (r=0.34). Capillary diameter exhibited a negative correlation

with thickness of Bruch's membrane (r=-0.27) and a positive correlation with choroidal thickness (0.52).

Table 1. Rank correlation coefficients (r) for a number of variables in 95 normal maculae.

	capillary density	capillary diameter	thickness BrM	choroidal thickness
age	-0.58	-0.40	0.63	-0.48
capillary density		0.64	-0.36	0.34
capillary diameter			-0.27	0.52
thickness BrM				N.S.

For all correlation coefficients P<0.0005.
BrM = Bruch's membrane. N.S. = not significant

When partial correlation calculations were made, it appeared that changes in capillary density in normal maculae could only be explained by age (r=0.56, P<0.00005) and not by either thickness of BrM (r=-0.07, P=0.49) or choroidal thickness (r=0.15, P=0.16). The rank correlations of capillary density with thickness of the choroid and BrM were fully mediated by age, which consequently appeared to be the sole factor directly related to capillary density.

The capillary diameter in normal maculae decreased by 34% from approximately 9.8 μm in the first three decades of life to 6.5 μm in the tenth decade (Fig.11.4). Partial correlation calculations for capillary diameter showed a direct positive correlation with choroidal thickness (r=0.52, P<0.00005) and, to a much lesser extent, a direct negative correlation with age (r=-0.18, P=0.04). The thickness of BrM was not directly related to capillary diameter. The observed negative rank correlation (Table 1) between thickness of BrM and capillary diameter (r=-0.27) was thus confounded by choroidal thickness and age.

The choroidal thickness in normal maculae decreased by 56% from 194 μm in the first decade to 84 μm in the tenth decade (Fig 11.5). Variations in choroidal thickness were, however, large for all ages.
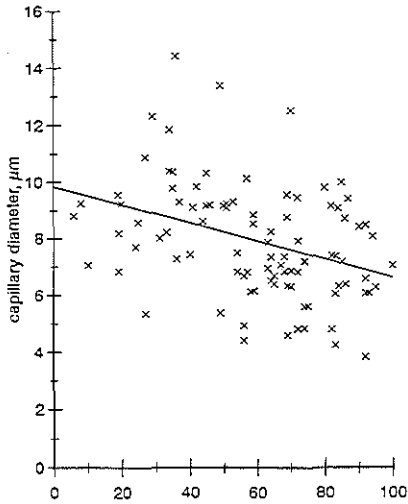
Figure 11.4 Capillary diameter in 95 histologically normal maculae plotted against age. The solid line represents the best linear fit to the data;
capillary diameter = 9.85 - 0.033 x age, (R^2 = 0.14, P = 0.0001).
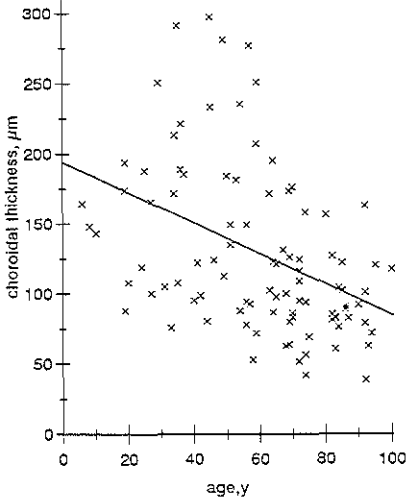
Figure 11.5 Choroidal thickness in 95 histologically normal maculae plotted against age. The solid line represents the best linear fit to the data;
choroidal thickness = 194 - 1.1 x age, (R^2 = 0.18, P < 0.00005).

Comparison with pathological maculae

In Table 2 the results of the age-adjusted comparison of normal maculae and pathological maculae are presented. The total number (N) of pathological maculae in table 2 exceeds the 25 maculae mentioned in Materials and Methods, because in several cases both BLD and geographic atrophy were present in one macula, although in different parts of the macula. Therefore the results of measurements related to BLD were not influenced by the measurements related to geographic atrophy. The capillary density was lower in areas with disciform scarring (43% of

Table 2. Age-adjusted mean values of measured variables for pathological maculae as a percentage of the mean values for normal maculae (=100%).

	pathological maculae		
	BLD (n=9)	geographic atrophy (n=13)	disciform scar (n=8)
	%	%	%
capillary density	63 (±11*)	54 (±10*)	43 (±10*)
capillary diameter	81 (±9.7)	73 (±8.7)	75 (±9)
thickness BrM	102 (±7.9) NS	100 (±6.9) NS	81 (±8)
choroidal thickness	85 (±18) NS	81 (±14) NS	89 (±15) NS

* = standard error of the mean.
BLD = basal laminar deposit. NS = not significant. BrM = Bruch's membrane. P-values for thickness of BrM all exceeded 0.31, except for disciform scarring (P = 0.02). P-values for choroidal thickness all exceeded 0.46.

normal) than in areas underlying geographic atrophy (54% of normal) or BLD (63% of normal). The capillary diameter was also significantly decreased, but to an equal extent in maculae with geographic atrophy or disciform degeneration and slightly less in maculae with a thick layer of BLD (class 3). In maculae with a disciform scar the thickness of Bruch's membrane was significantly reduced. In maculae demonstrating BLD, geographic atrophy or disciform scarring (Table 2), choroidal thickness was not found to be significantly different from that in normal maculae.

The local variation in capillary density between two sections of the same macula at 140 µm intervals (Table 3) was very small. The interobserver and intraobserver variations (Table 4) were small compared to the normal variability.

Table 3. Local variability in two sections from one macula in a series of 10 normal maculae.

	capillary density	capillary diameter (μm)	thickness BrM (μm)	choroidal thickness (μm)
mean difference	0.017 (±0.031*)	0.55 (±0.93)	0.13 (±0.40)	14.15 (±20)

* = Standard deviation of the differences. BrM = Bruch's membrane.

Table 4: Interobserver and intraobserver variation: mean differences between measured values.

	capillary density	capillary diameter (μm)	thickness BrM (μm)	choroidal thickness (μm)
Interobserver[1]	0.059 (±0.1[2])	0.22 (±0.84)	0.23 (±0.64)	7.03 (±23)
Intraobserver[1]	0.015 (±0.05)	0.13 (±0.99)	0.08 (±0.16)	4.76 (±25)

[1] : N = 10 normal maculae. BrM = Bruch's membrane.
[2] : Standard deviation.

DISCUSSION

In this study, we have assumed that the choriocapillaris is an almost two-dimensional structure, because of the negligible thickness compared to the area of the choriocapillaris (compare with a sheet of paper). Knowing that the normal choriocapillaris meshwork is regular in the entire fovea, we can draw conclusions on the density of the choriocapillaris meshwork within the fovea by measuring one dimension only.

We quantified the changes in capillary density of the CC for all decades and found that it diminished in a linear fashion from approximately 0.75 in the first decade to 0.41 in the tenth decade. Partial correlation calculations revealed only a close correlation with age (P<0.00005). Our results confirm a previous study, in which planimetric evaluation of choroidal casts was used for morphometry of the CC [162a]: the intercapillary space, was found to increase from 25% in four young

subjects (21-50 yrs) to 60% in four old subjects (80-97 yrs)[162a]. Absolute figures from this study may not be compared with our measurements.

The close correlation between the capillary density and capillary diameter (Table 1) is partially influenced by the fact that a decrease in diameter automatically results in a, relatively small, decrease in capillary density. Changes in diameter of the capillaries are relatively small compared to the total area of the fovea and therefore hardly influence the measurements of the choriocapillaris density.

The cause of the age-related decrease in capillary density of the CC is unknown. Apart from the skin [258a] and testes [1a,228a], for which an age-related decrease in capillary density has also been described, knowledge of the age-related changes in capillary meshworks in other tissues as well as the possible causes is very scarce. However, an increase in PAS-staining of capillary basement membranes and the surrounding extracellular matrix in the fifth decade has been reported for many body tissues, such as the brain, muscle, skin and intestinal wall [213]. In the macula, the age-related decline in choriocapillary density is also accompanied by an increase in PAS-staining of BrM and widening of the intercapillary pillars [60a,107,203a]. Thus the age-related drop in capillary density may have a systemic basis. The increase in the range of values of the capillary density with increasing age in normal maculae illustrates that a wide range in the age-related changes can still be considered normal. In the maculae with features of advanced ARMD, the capillary density was significantly decreased in the presence of BLD, geographic atrophy or disciform degeneration. This might be one of the causal factors in ARMD or it may be secondary to atrophy of the RPE. Biochemical alterations in the composition of the extracellular matrix between the choriocapillary endothelium and the RPE and in BrM could modify the diffusion characteristics of extracellular modulating factors produced by the RPE [115,69] and CC [23], thereby causing atrophy of the CC and damage to the RPE.

It has been postulated that a progressively thickened BrM could mechanically compress the choriocapillaries and cause a decrease in choriocapillary diameter [58,167,199]. The results of our study (Table 1) indicate, however, that the capillary diameter is directly correlated with choroidal thickness and age. Calculation of partial correlations showed that the thickness of BrM was of no importance in explaining the variation in capillary diameter. This is also consistent with our finding (Table 2) that in maculae with BLD, geographic atrophy or disciform degeneration, in which a decrease in capillary diameter was found, the thickness of BrM did not significantly differ from that in normal maculae of the

same age groups. If the presumed compressing properties of BrM could induce a decrease in capillary diameter in ARMD, a significant difference in the thickness of BrM is to be expected. This was not confirmed in our study.

Our observation that the thickness of BrM does not significantly differ between maculae with BLD or geographic atrophy and normal maculae, suggests that accumulation of cellular debris in BrM is not significantly increased in these stages of ARMD compared to normal aging. However, it might be possible that the chemical composition of substances in BrM are altered in ARMD, which could hamper the free diffusion of solutes between the RPE and CC [167].

The significant, age-adjusted, reduction in the thickness of BrM in disciform scarring compared to normal maculae, that has been suggested to result from the phagocytic action of macrophages directed against the outer collagenous zone of BrM (see chapter 9), confirms the histopathological observations made by others [108]. We must keep in mind that the maculae with a disciform scar came from pseudophakic eyes in which other processes are involved, such as the mechanical trauma of cataract extraction and implantation of the intraocular lens and the presence of a foreign body in the eye (see chapter 12). However, similar macrophage activity has been described in normal phakic eyes.

In normal maculae a progressive decrease in choroidal thickness was found with advancing age. We could not confirm previous observations [198,199] that the choroidal thickness is reduced in geographic atrophy and increased in disciform degeneration.

The small interobserver and intraobserver variations in the measurements were almost completely within the normal range of the measured parameters in several histologic sections from the same macula and are negligible in comparison with the normal variation between maculae of the same decade. The 1120-μm zone of the fovea, in which the measurements were taken, was sufficiently large to obtain representative and reproducible results.

In conclusion: with advancing age histologically normal maculae show a decrease in the density and diameter of the capillaries in the choriocapillaris, a decrease in choroidal thickness and an increase in the thickness of BrM. In eyes with various stages of ARMD the decrease in capillary density and diameter was significantly larger than in normal maculae (adjusted for age). In maculae with ARMD the thickness of both the choroid and BrM was not significantly different from that in normal maculae except for maculae with a disciform scar, which had a significantly thinner BrM.

CHAPTER 12

Increased Prevalence of Disciform Macular Degeneration After Cataract Extraction with Implantation of an Artificial Intraocular Lens.

Theo L. van der Schaft,[1] MD; Cornelia M. Mooy,[1,2] MD;
Wim C. de Bruijn,[2] PhD; Paul G.H. Mulder,[3] MSc;
Jan H. Pameyer,[1] MD, Paul T.V.M. de Jong,[1] MD, PhD, FCOphth.

From the Institutes of Ophthalmology (1), Clinical Pathology (2)
and Biostatistics (3)
Erasmus University Rotterdam, the Netherlands

INTRODUCTION

The most common cause of poor vision in the elderly is cataract[111,120]. In the United States of America more than 1 million cataract operations a year are performed, accounting for 12% of all Medicare payments[56,99]. After cataract extraction and implantation of an artificial intraocular lens (IOL), visual acuity is regained in a high percentage of the cases. Thus the second most common reason for visual loss in the western world has become more important: age-related macular degeneration (ARMD), which is now the leading cause of blindness in the elderly in the western world [111,120]. However, development of ARMD has previously been described shortly after cataract extraction and IOL implantation[68,240].

After the first two decades of life the original lens becomes yellower and partly filters out the harmful blue light and ultraviolet (UV) radiation of the sun [123,129]. With the development of cataract this filtering capacity of the lens increases, protecting the posterior pole of the eye against possible free radicals formed under influence of the blue and UV-light[123,129,138,183,261]. At cataract extraction this biological filter is removed and during the operation, the retina is exposed to the light source of the operating microscope, which has been proved to induce phototoxic damage to the macula[148]. The cataractous lens is replaced by a crystal-clear artificial IOL with or without an UV-filter, which results in a so-called pseudophakic eye. It has been postulated that increased UV- and blue-light radiation affects normal macular functioning and thus that cataract extraction might stimulate ARMD[229,252,261,265].

Advanced ARMD will become manifest as either geographic atrophy of the retinal pigment epithelium (RPE) and the photoreceptors (Fig 12.1) or as a disciform reaction, which consists of the ingrowth of new blood vessels from the choriocapillaris through Bruch's membrane under the RPE. A subsequent hemorrhage from these vulnerable vessels often results in disciform scar formation[216] (Fig 12.2).

Neovascularization can only reach the subretinal space through ruptures in Bruch's membrane[170,196]. These breaks can be caused by calcification of Bruch's membrane[63a], macrophages[108,170] or other factors. Pronounced calcification or thickening of Bruch's membrane probably increases the rigidity of

this membrane and thus makes it more fragile[170].
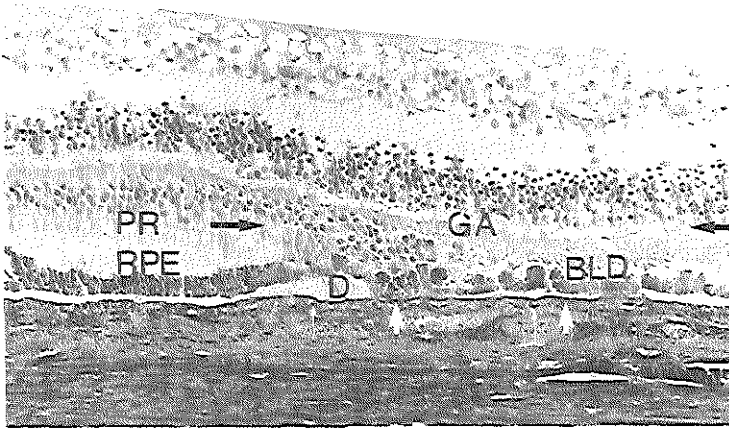
Fig 12.1. Light microscopic image of a human macula with geographic atrophy (GA, between black arrows). On the right the retinal pigment epithelium (RPE) and the photoreceptors (PR) are atrophic. Basal laminar deposit (BLD), grade 3, is present under the the remnants of the RPE. A soft drusen (D) can be seen between the RPE and Bruch's membrane (small white arrows). The choriocapillaris (arrow heads) is located under Bruch's membrane. (Mallory stain, magnif.125x).
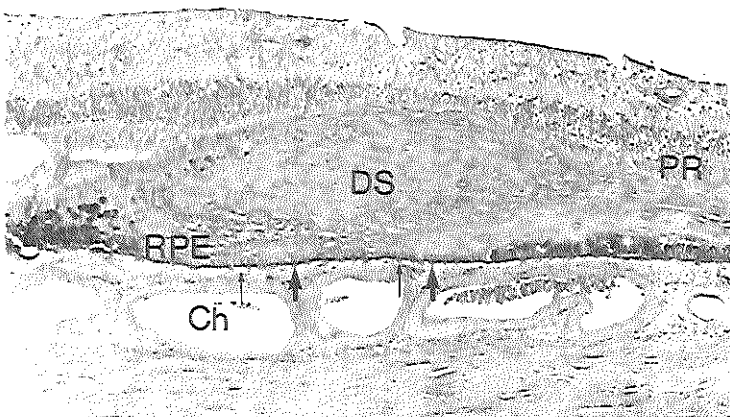
Fig 12.2) Light microscopic image of a human macula with a disciform scar (DS). The retinal pigment epithelium (RPE) and the photoreceptors (PR) are atrophic. Bruch's membrane (arrows), choriocapillaris (arrow heads), CH = choroid. (Mallory stain, magnification 80x).

One of us (PdeJ) had the impression from clinical practice that extra-capsular cataract extraction with implantation of an IOL in the elderly was sometimes followed, within a month, by the development of a subretinal hemmorrhage and a subsequent disciform reaction. The hypothesis was formulated

that ruptures in Bruch's membrane might be induced by sudden changes in intraocular pressure and in the volume of the eye during surgery, which would involve deformation of the eye.

The aim of this histological investigation was to study this hypothesis and to determine the possible role of the increased transmission of blue and UV-light in the development of ARMD and macular aging in pseudophakic eyes without an UV-filter compared to pseudophakic eyes with an UV-filter. Also the prevalence of ARMD in pseudophakic eyes with brown or blue irises was compared. Extensive literature on the histology of macular aging is available [75,108,192,196,199, 202,203,204,216,260], but to the best of our knowledge this is the first report on the histopathology of a series of human maculae after cataract extraction and implantation of an IOL.

MATERIALS AND METHODS

We obtained 89 post-mortem human caucasian pseudophakic eyes from a corneal transplantation bank and autopsies. At a later stage 7 pseudophakic eyes were excluded from this study because information on age and date of cataract extraction was not available. Otherwise no selection was made. The remaining 82 eyes included 21 pairs of pseudophakic eyes, 16 pseudophakic eyes of which the phakic fellow eye (eye with the original biological lens) was also available for this research and 24 single pseudophakic eyes with no fellow eye available for research. An age-matched series of 126 unpaired phakic eye bank or autopsy eyes was used as control group. The age distributions for the study group and the control group were similar (Fig 12.3). The control group was taken larger than the group of eyes with an artificial IOL in order to increase statistical power. For statistical reasons, the subject (and not the eye) was considered to be the experimental unit.

Age at the time of death ranged from 62 to 100 years for both the pseudophakic group (mean 81,3 years, S.D. = 7,6) and the control group (mean 78,5 years, S.D. =8,9). The time between IOL implantation and death ranged from 3 to 168 months (mean 52 months, S.D. =40, median =48).

The maculae were prepared for light microscopy as described in a previous study[203]. The presence of a basal laminar deposit (BLD), hard and soft drusen,
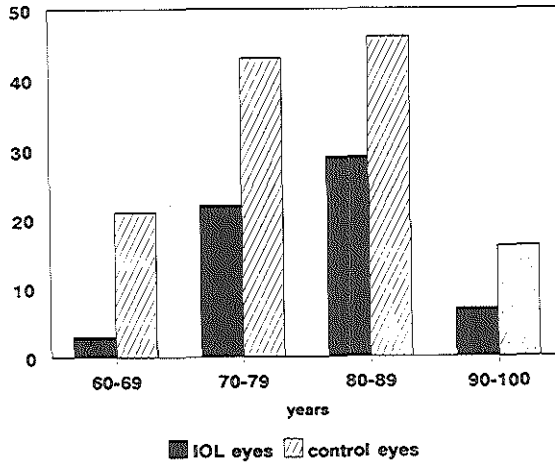
Fig 12.3. Age distribution of the 61 subjects with an artificial intraocular lens and the 126 phakic control eyes. Notice the similarity in distribution. For statistical reasons only one eye from each patient is included here. The control group was larger to increase the statistical power.

thickening and calcification of Bruch's membrane, geographic atrophy, subretinal neovascularization and a disciform reaction in the macula was assessed blind in a standardized way, using the classification system described before[203].

BLD was defined as amorphous, granular material located between the RPE and the inner layer of Bruch's membrane. It stained pale blue with the Mallory stain (Fig 12.1). Thickening of Bruch's membrane was assessed with the periodic acid-Schiff (PAS) stain. Calcification of Bruch's membrane was studied with the von Kossa stain, which stains calcium phosphates brownish-black.

Drusen are deposits of material between the basement membrane of the RPE and the inner collagenous zone of Bruch's membrane. The drusen were divided into hard drusen, which were usually dome-shaped with a hyalinized appearance and stained brownish-blue with the Mallory stain, and soft drusen, which were usually larger, had sloping edges, contained granular material which stained pale blue with the Mallory stain or appeared to be optically almost empty (Fig 12.1).

The absence or presence of UV-absorbing chromophores in the IOL's was

The absence or presence of UV-absorbing chromophores in the IOL's was measured with a spectrophotometer through the intact anterior segment of the eyes. As a control the anterior segments of five phakic aged eyes, one phakic eye of a six year old child, two aphakic eyes and a single IOL with and without UV-filter were measured.

For statistical analysis the Mann-Whitney U test and the exact trend test were used to compare the presence of BLD, hard and soft drusen and changes in Bruch's membrane, all scored from 0 to 3 in the study group and the control group[203]. Fisher's exact test was used to compare the absence (class 0) or presence (class 1) of geographic atrophy, subretinal neovascularization and disciform degeneration in the pseudophakic and control eyes. For these calcula- tions only one, randomly chosen, pseudophakic eye from each subject was used (61 eyes). The influence of the length of time between IOL implantation and death on the presence of BLD, drusen and changes in Bruch's membrane was determined with the Spearman rank correlation test. For geographic atrophy, subretinal neovascularization and disciform degeneration the Mann-Whitney U test was used. For comparison of macular degenerative changes between pseudophakic eyes with and without UV-filter, between eyes with brown and blue irises and between eyes which underwent an intracapsular or extracapsular cataract extraction, the Mann-Whitney U test was used for the classification of BLD, drusen and changes in Bruch's membrane. Fisher's exact test was used for the classification of geographic atrophy, subretinal neovascularisation and disciform degeneration. For the latter associations within the IOL study group, all 82 pseudophakic eyes were used. P-values below 0.05 were considered statistically significant. Two-sided P-values were used throughout. For comparison of the histological classification of fellow phakic eyes Wilcoxon's matched pairs signed rank test was used.

RESULTS

The prevalences of BLD, drusen and thickening and calcification of Bruch's membrane for both the study group and the control group are given in Table 12.1. No significant differences were found between the IOL group and the control group except for a significantly higher prevalence of hard drusen in the IOL group (Exact trend test and Mann-Whitney U test, $P=0.038$). The distribution of the

classification scores (ranging from 0 to 3) determined for the histological changes did not differ significantly between the study group and the control group (not shown).

Table 12.1. The prevalence of histological age-related changes in the maculae of 61 unpaired eyes with an artificial IOL and of 126 phakic eyes of the age-matched control group.

| | drusen* | | BLD* | Bruch's membrane* | |
	hard	soft		thickening	calcif.
IOL group	38(62%)†	9(15%)	40(66%)	55(90%)	49(80%)
control gr.	57(45%)†	18(14%)	69(55%)	122(97%)	96(76%)

*The scoring scale with a range of 0 to 3 was dichotomized into 0 (absent) and larger than 0 (present).
† Mann-Whitney U test and Exact trend test, P=0.038 (significant!)

In Table 12.2 the prevalences of geographic atrophy, subretinal neovascularization and disciform degeneration are given. No significant differences were found in geographic atrophy and subretinal neovascularization between the two groups. A significantly higher percentage exhibited disciform degeneration in the IOL group than in the control group (Fisher's exact test, P=0.007).

Table 12.2. Prevalence of histological macular degeneration in 61 unpaired eyes with an artificial IOL and 126 phakic eyes of the age-matched control group.

	geographic atrophy	subretinal neovasc.	disciform scar
IOL group	4 (7%)	5 (8%)	5 (8%)‡
control group	7 (6%)	4 (3%)	0 (0%)‡

‡ Fisher's exact test, P=0.007 (significant!)

In three of the five maculae the disciform scar was flat and in one of them the overlying RPE was only partially atrophic. The other two maculae had a thick scar which clearly elevated the retina (Fig 12.2). The overlying RPE was again partially atrophic in only one macula.

In three of the five maculae with a disciform scar Bruch's membrane was

locally abnormally thin, alternating with the normally thickened membrane for that age (chapter 5 and 11).

The time between IOL implantation and death of 4 of the 5 subjects with disciform macular degeneration was 6, 42, 60 and 126 months (mean 58 months). For one eye this information was not available. However, the exact time between IOL implantation and the development of a disciform scar could not be retrieved. The mean age of the patients with a disciform reaction at the time of enucleation was 83 years.

The differences between the IOL and the control group for geographic atrophy and subretinal neovascularization were not statistically significant. None of these changes exhibited a significant correlation with the length of time between implantation of the artificial IOL and death.

The signed ranks test revealed no significant difference in age-related changes or degeneration of the macula between the eyes of pairs consisting of one pseudophakic and one phakic eye.

No significant differences in histological macular changes could be found between eyes for pairs of pseudophakic eyes, even when the eyes with an IOL implant for the longest period of time were compared with the fellow eye with an implant of shorter duration (mean time difference 28 months, range 6 to 78 months).

In 43% of the pseudophakic eyes the IOL had an UV-filter, whereas in 41% of the eyes an IOL without UV-filter was implanted. The anterior segment of the remaining 16% was not available for measurement of the UV-light transmittance. The UV-filtering chromophores blocked nearly all light with a wavelength of less than 400 nm, thus including the absorption of UV-B (290-320 nm), $UV-A_1$ (320-340 nm) and $UV-A_2$ (340-400 nm), but letting violet and blue light (400-500 nm) through. The cornea absorbed all light with a wavelength shorter than 310 nm. The biological lens of the six year old child had a sharp absorbtion threshold at 390 nm in contrast to aged lenses, which had a sloping absorption curve, starting at 600 nm and inclining to a relative total block at 500 nm.

No significant differences in macular aging or degenerative changes were found between pseudophakic eyes with or without UV-filter, nor between pseudophakic eyes after intra- or extracapsular cataract extraction. Of the five eyes with a disciform scar, three IOL's had an UV-filter. In four of the five pseudopahkic eyes with a disciform scar the IOL's were implanted after

extracapsular cataract extraction. No statistically significant differences were found between pseudophakic eyes with brown or blue irises.

DISCUSSION

In this study we found a significantly higher prevalence of histological disciform macular degeneration after cataract extraction and subsequent implantation of an IOL than for an age-matched control group of phakic eyes. This is further confirmed by the observation of subsequent disciform macular degeneration in one of the 7 pseudophakic eyes that were excluded from the series because of a lack of information about age. It is assumed that the longer an artificial lens is in situ, the longer free radicals can be formed in the eye by photic energy, a process which can damage the retina[229]. However, there was no significant correlation between the period of time between IOL implantation and death and the histological degree of aging or degeneration of the macula. The absence of UV-blocking chromophores in the IOL's was not associated with an increase in macular aging or degeneration. Iris color did not influence macular aging either. Therefore our findings do not support the assumed increase in both the formation of free radicals and macular aging or degeneration.

The results of several studies on the prevalence of cataract and ARMD are rather contradictory. Some authors think that the development of a cataract protects the eye from harmful UV-light which might stimulate the development of ARMD [240,261]. Others conclude that cataract and ARMD are age-related changes which develop simultaneously in the same person [68,120]. The results of another study indicate a direct correlation between ARMD and cortical cataract and an inverse correlation between ARMD and nuclear cataract [129]. Aphakic eyes exhibited a two-fold increase in the prevalence of ARMD with respect to phakic eyes without lens opacities[129].

Our results suggest that the incidence of disciform macular degeneration is higher after cataract extraction with an IOL implant than would be expected for a normal population. However, we must keep in mind that a single new vessel or a single cell layer, considered to be the beginning of a disciform scar, can only be seen by the pathologist and not by the ophthalmologist with his ophthalmoscope. Clinically a disciform scar is first visible when it comprises 5 or 6 cell layers [196].

Therefore clinical data on disciform macular degeneration might represent an underestimation compared to our histological data. In the Food and Drug Administration (FDA) report on intraocular lenses, postoperative macular degeneration was not considered as an adverse reaction but as a confounder and these eyes (number not mentioned) were excluded from the results[219].

For the development of disciform macular degeneration there must be an ingrowth of new vessels, originating from the choriocapillaris, into the sub-RPE space. Normally Bruch's membrane forms a firm continuous mechanical barrier between the choriocapillaris and the RPE. Thus a pathway through Bruch's membrane must be created.

One possibility is that the surgical trauma causes ruptures in Bruch's membrane, which is known to be more fragile when thickened and calcified (Fig 9.7) [216]. The subsequent passage of new vessels from the choroid into the sub-RPE space is followed by exudation of serous fluid or hemorrhage and the formation of a disciform scar. In the four eyes with a disciform scar, Bruch's membrane was not more calcified than in either the other pseudophakic or the control eyes. In the fifth eye Bruch's membrane was markedly calcified, like an eggshell, and exhibited many breaks. If we assume that calcification is the main indicator for fragility of Bruch's membrane, our findings do not confirm the hypothesis that breaks in a calcified Bruch's membrane are a major cause of post-operative subretinal neovascularization, but can be one of the causes.

A second explanation might be that macrophages, coming from the choroid, create a pathway for neovascularization by breaking down the layers of Bruch's membrane (see chapter 9). Usually the thickness of Bruch's membrane increases with age [203], but in our study Bruch's membrane in three maculae with a disciform scar was abnormally thin (see chapter 11) and sometimes even showed breaks, which were covered by the scar tissue. Adjacent to these breaks, at the side of the choriocapillaris, histiocytic cells were seen in two of these eyes (see chapter 11). Others described that after experimental laser coagulation of the retina, Bruch's membrane first remained intact[179]. However, macrophages were attracted, probably by released chemotactic factors, and created gaps in Bruch's membrane after several days or weeks[179]. Macrophages can also induce angiogenesis [173]. This laser-induced chemo-attraction of macrophages might be similar to the mechanism in eyes with an IOL, in which the cataract extraction or more generally the surgical trauma acted as the initiating factor for release of

chemotactic factors that attract macrophages.

A third explanation is based on the differences, seen in Table 12.2, in subretinal neovascularization between the control group of normal phakic eyes (3%) and the IOL group (8%). It is well known that these new vessels easily leak or bleed, even under physiological conditions[196]. During surgery several non-physiological conditions occur, such as the rise in orbital pressure during peribulbar anesthesia, the drop in intraocular pressure after incision and mechanical forces arising from manipulation of the eye, irrigation and aspiration of lens material, and nowadays the highly energetic ultrasound waves used for phacoemulsification. All of these non-physiological conditions might weaken possible pre-existing new vessels or provoke further outgrowth or hemorrhage and thus subsequent disciform reaction.

Other possibilities are the infiltration of Bruch's membrane by endothelial cells and pericytes of the choriocapillaris without pre-existing breaks (see Fig 9.8) [108]. Even the infiltration of Bruch's membrane by single RPE cells has been reported (see Fig 9.9) [78]. The importance of the latter two possibilities is unknown.

The prevalence of large confluent soft drusen, clinically often associated with neovascularization, was similar for both the IOL and the control group so it is unlikely that soft drusen are responsible for the difference in the prevalence of disciform reactions [75,192].

The higher prevalence of hard drusen in pseudophakic eyes compared to phakic eyes could not be explained. However, the presence of hard drusen is not correlated with serious loss of vision[120] or with the development of a disciform reaction[75,199] and a causal relationship is thus unlikely.

There was no significant relationship between the presence of cataract and the development of age-related changes in the macula. Thus there was no indication that protection of the retina against UV-light by the cataractous lens in the years before cataract extraction had prevented aging or other degenerative changes in the macula.

The best reference for assessment of the changes in a pseudophakic eye after age-related cataract surgery is the non-operated phakic fellow eye, because the only difference between the fellow eye and the pseudophakic eye is the cataract extraction with the implantation of an IOL and the resulting change in conditions. No differences were found between the sixteen pairs of pseudophakic

and phakic eyes. However, the number of pairs was relatively small so that no reliable conclusions can be drawn from this finding.

We can conclude that in this study increased prevalences of histological disciform macular degeneration and hard drusen were found after cataract extraction with implantation of an IOL. The exact cause remains unclear, but a direct relationship with either an increase in UV-light on the retina due to IOL's without UV-filter or the duration of an increased amount of UV-light could not be demonstrated. Concerning the disciform scars it seems more likely that either the harmful effects of surgical trauma on Bruch's membrane or pre-existing sub-RPE vessels or the attraction of macrophages, which break down Bruch's membrane and stimulate neovascular membrane formation, play an important role. A large prospective trial is mandatory to estimate the exact risk of a disciform reaction after cataract extraction and to discover any predictable risk factors or causes that can be avoided.

ACKNOWLEDGMENTS

Concluding remarks

Their is no doubt that the presence of a BLD correlates with aging of the human macula. A causal relationship with other aging changes in the macula, such as the thickening and calcification of Bruch's membrane, the presence of hard or soft drusen, degenerative changes. in the RPE and atrophy of the choriocapillaris and choroid is much more difficult to estimate, because these abnormalities all have a marked relationship with age. After all, atrophy of the choriocapillaris seems to be an important factor in ARMD.

A BLD does not consist of an accumulation of inorganic elements such as the calcifications in Bruch's membrane, but is partly composed of an excessive amount of basement membrane material, derived from an epithelium, which can make its own basement membrane. However, like the basement membrane of the RPE, the composition of a BLD differs from that of other basement membranes, such as vascular basement membranes. What are generally considered to be the main components of basement membranes, seem to be just minor components of the RPE basement membrane and BLD. The question whether long-spacing collagen consists of another arrangement of basement membrane material and therefore cannot be recognized by anti-basement membrane antibodies, remains unanswered. Further investigations with other approaches are needed to reveal the identity of the remaining components. Furthermore the question remains whether the excess of basement membrane material is due to a higher production rate, a slower turnover rate or the presence of abnormal proteins which cannot be recognized by the normal phagocytic system. The low immunoreactivity of BLD with antibodies against collagen type IV, laminin and HSPG is in favor of the latter suggestion.

It is now know that BLD and similar deposits, which are mainly composed of long-spacing collagen, are not unique to the macula, but can also be found in other parts of the eye and in other tissues. However, the location of BLD in the macula at the edge of the outer blood-retinal barrier and close to the watershed zone of the inner and outer parts of the retina has important consequences for the pathogenesis of ARMD.

The question of whether the presence of BLD causes or enhances further

degeneration of the macula or is just one of the results of an already ongoing degeneration, remains unanswered. The same holds for the problem of what to do when BLD is already present in the macula and how to prevent the formation of BLD. Attempts should be made to visualize the BLD clinically, because it probably predicts advanced degeneration of the macula with future loss of central vision better than the frequently observed small hard drusen.

According to the results of chapter 9, an (auto)immune disease as a causal factor of ARMD is not likely.

The increased prevalence of ARMD in pseudophakic eyes must be taken seriously. The development of disciform macular degeneration may be caused by controllable factors and could thus be prevented prior to cataract extraction and implantation of an intraocular lens. A large prospective clinical study is needed here.

A major handicap of this kind of research is the lack of an appropriate animal experimental model or a cell culture model in which the formation or production of BLD can be induced and controlled. Until now researchers have had to depend on the nearly uncontrollable offer of post-mortem human eyes, which are often of insufficient quality or inadequately preserved for modern laboratory techniques. Surgically enucleated eyes are often not suitable for research on age-related abnormalities, because the eyes are always enucleated for abnormalities other than aging and the age of these patients is often not high enough. Therefore, considerable effort should be directed towards inducing ARMD in an animal species in order to be able to understand fully the process of the development of ARMD and of all the internal and external factors that influence this process.

SUMMARY

This thesis deals with the problem of age-related macular degeneration (ARMD), focused on the histopathological changes in the human macula on the interface of the retina and choroid.

Chapter 1: ARMD is nowadays the leading cause of blindness in the western world in people above the age of 65 years. With the proportional increase of the number of elderly in the population, the social problem of ARMD will also increase. Patients with ARMD suffer from a diminished or total loss of central vision, usually bilateral and are thus severely disabled. Clinical signs are the presence of drusen, pigment disturbances of the RPE, geographic atrophy or subretinal neovascularization with leakage of serous fluid or hemorrhage and the formation of a fibrovascular scar. Possibilities for therapy are limited: drug treatment is based on prevention or limitation of further deterioration, but results are ambiguous. Laser photocoagulation, to prevent (further) damage of the fovea, is limited to certain cases, but can delay progress of the disease for several years. Surgical procedures are in an initial phase yet, but so far the functional results are disappointing.

In Chapter 2 the normal anatomy and histology of the human macula is described for a better understanding of this thesis.

In Chapter 3 the histological aging changes in the human macula are dealt with. Much attention is paid to the different stages of ARMD and to current terminology, which can be often confusing and misleading.

Chapter 4: The aim of this research was to get a better understanding of the histopathogenesis of ARMD. Special attention was paid to the investigation of the prevalence, distribution, ultrastructure, elemental composition and immunohistochemistry of Basal Laminar Deposit (BLD) in the macula, which is considered to be a precursor or early stages of age-related macular degeneration. The histological aging changes in the human macula were classified and quantified and these changes were analyzed statistically in order to learn more about the onset, development and causal factors of ARMD. Morphometric analysis and element analysis of other structures in the macula were performed to reveal possible causal factors for the formation of BLD and the development of ARMD. In addition, the ultrastructure of sub-RPE deposits in the peripheral retina was

compared to BLD in the macula of the same eyes. The influence of cataract extraction and implantation of an artificial intraocular lens, with or without a UV-filter, on aging and degeneration of the macula was investigated and compared with an age-matched control group.

Chapter 5: The age distribution and frequency of occurrence, as well as correlations among histologic macular changes, including the formation of a BLD, drusen and thickening and calcification of Bruch's membrane, were studied by light microscopy. A series of 182 unpaired post-mortem human maculae from patients between 8 and 100 years of age, were studied. In addition, 45 maculae of contralateral eyes and the peripheral retina of 50 eyes were studied. BLD was found in 39% of the maculae starting at age 40. In 37% of the maculae, hard drusen were found starting at age 34. Soft drusen were found in 10% beginning at age 54. In 92%, Bruch's membrane was thickened starting at age 19, and calcifications in this membrane were found in 59% starting at age 33. All changes correlated strongly with age (P<0.0001). No sex differences were found. Fellow eyes showed similar aging changes (P<0.001). The presence of BLD in the macula correlated with BLD-like sub-RPE deposits in the peripheral retina (corr.coeff.0.39; P<0.003), whereas drusen in the macula correlated with drusen in the peripheral retina (corr.coeff.0.42; P=0.001). Geographic atrophy was found in 6.6% of the eyes from subjects older than 70 years and subretinal neovascularization in 3.8%, especially in the maculae whith large amounts of BLD. Although aging changes were frequently seen, only a small percentage of the maculae showed advanced stages of ARMD. Definite causal connections between certain aging changes and the development of ARMD could not be made.

Chapter 6: The ultrastructural nature and distribution of BLD were studied in 42 human maculae. Three types of BLD were identified: early type BLD, late type BLD and flocculent BLD. With light microscopy the early and late types of BLD could be distinguished from flocculent BLD. By electron microscopy the early and late type differed in the ratio of long-spacing collagen and homogeneous granular material. BLD was found from age 19 on, not only between the RPE cells and their basement membrane, but more often or sometimes exclusively on the choriocapillaris side of Bruch's membrane. No direct relationship was found with other aging changes, such as calcifications in Bruch's membrane, accumulation of lipofuscin granules in the RPE cells, or drusen in the macular area. Material similar to BLD can be found in the trabecular system, the cornea, and also in many other

organs and tissues, often close to the basement membrane of various types of epithelium. On a structural and morphometrical basis, we think that BLD is similar to fibrous long-spacing collagen and excessive amounts of basement membrane material and thus does not seem to be a purely ocular abnormality.

Chapter 7: To learn more about the chemical composition of BLD and the role of zinc in ARMD, we investigated the elements in BLD, as well as in surrounding structures in 38 postmortem human maculae by electron probe X-ray microanalysis (EPMA). BLD and capillary vessel walls of the choriocapillaris appeared to contain no typical elements. Calcium, phosphorus, sulfur, zinc and chlorine were detected in the lipofuscin granules in the RPE. Pigment granules of the RPE and choroidal melanocytes contained predominantly sulfur and copper and, to a lesser degree zinc, calcium and iron. Local calcifications in Bruch's membrane were composed of large amounts of calcium and phosphorus and smaller amounts of zinc, iron and chlorine. Metal mirror fixation of the maculae, followed by freeze-drying and vapor fixation, showed additional amounts of sodium and potassium. X-ray microanalysis on freeze-dried and vapor fixed tissue was proved to be comparable to analysis of aldehyde-fixed and acetone-dehydrated tissue. From these experiments, no conclusions could be drawn about the origin of BLD. No relationship was found between the detection of zinc in the melanin of the RPE or in calcifications of Bruch's membrane and the presence of BLD or drusen in the macula.

Chapter 8: The location of a BLD, between the RPE plasma membrane and its basement membrane and in the OCZ of Bruch's membrane, and the ultrastructure of a BLD suggest that it is composed of excessive amounts of basement membrane material. The main components of basement membranes are type IV collagen, heparan sulfate proteoglycans (HSPG) and laminin. Labelled antibodies against these components can therefore be used for the identification and localization of basement membrane material by means of immuno-histochemical techniques. In this study the presence of type IV collagen, laminin and HSPG was determined in aged human maculae by immunohistochemistry and immunoelectron microscopy. Tests for the presence of type VI collagen and fibronectin, theoretically possible components of BLD, were also performed. We obtained 76 eyes from 68 human subjects at autopsy or after surgical enucleations for anteriorly located choroidal melanomas. The finely granular component of BLD stained positive with antibodies against type IV collagen, HSPG and laminin. The

long-spacing collagen component of BLD did not. Neither component of BLD was stained with antibodies against type VI collagen and fibronectin. We conclude that a BLD consists partly of excess basement membrane material.

Chapter 9: In subretinal neovascularization capillaries originating from the choriocapillaris must cross Bruch's membrane to reach the sub-RPE space. Thus gaps in Bruch's membrane have to be formed prior to subretinal neovascularization. Histologic examination of eyes with subretinal neovascularization or disciform scars has shown macrophages adjacent to thin areas and ruptures in Bruch's membrane. This has been interpreted as phagocytosis of Bruch's membrane. The purpose of this study was to investigate whether immune complex deposits can be detected in maculae with early stages of ARMD and to explain the macrophage reaction prior to the disciform reaction. We examined a series of 20 human maculae by direct immunofluorescence light microscopy to detect the presence of immune complexes with antibodies directed against immunoglobulins, fibrinogen and complement factors. Transmission electron microscopy of several maculae was performed to identify the macrophages. Macrophages were observed in close relation to the readily recognizable long-spacing collagen, which suggested that long-spacing collagen was selectively internalized by these cells. Definite immune complex deposits were not found in BLD or drusen. Linear deposits of fibrinogen and complement were frequently found in the OCZ of Bruch's membrane. However, because of the absence of immunoglobulins, it seems unlikely that these aspecific deposits might cause chemoattraction of macrophages and play a role in the initial phase of the development of subretinal neovascularization and disciform macular degeneration.

Chapter 10: In some eyes with a BLD in the macula, light microscopic sections of the peripheral retina revealed almost similar deposits between the RPE and BrM. Because the exact pathogenesis of ARMD and the exact origin of the BLD are unknown, we studied the ultrastructure of these peripheral sub-RPE deposits. Parts of the equatorial and peripheral regions of the retina of 10 human eyes, with BLD-like deposits between the RPE and BrM, were examined by electron microscopy. In 8 of these 10 eyes the ultrastructure of these deposits was amorphous and finely granular. Five of the 8 deposits also contained small amounts of long-spacing collagen. Ultrastructurally, the deposits were similar to an early type BLD in the macula. In the remaining 2 of these 10 eyes, the deposits appeared not to be BLD but to consist of flat, elongated drusen. We concluded

that a BLD can develop not only in the macula but also in the peripheral region of the retina.

Chapter 11: The exact quantification of the thickening of Bruch's membrane and changes in the blood vessels of the choriocapillaris and the thickness of the choroid with aging and the correlation of these changes with the development of ARMD are still unclear. We performed a light microscopic computer-aided quantitative analysis of the thickness of BrM, the density of the choriocapillaris meshwork, the capillary diameter and the choroidal width in 95 histologically normal human maculae of subjects aged 6 to 100 years and in 25 maculae with BLD, geographic atrophy or disciform scarring. In normal maculae the thickness of BrM increased by 135% (from 2.0 to 4.7 μm) over 10 decades, the density of the choriocapillaris meshwork decreased by 45% (from 0.75 to 0.41), the capillary diameter decreased by 34% (from 9.8 to 6.5 μm) and the choroidal width decreased by 57% (from 194 to 84 μm). In maculae with BLD, geographic atrophy or disciform scarring, the choriocapillary density was reduced to 63%, 54% and 43%, respectively, of normal (after age correction) and the choriocapillary diameter was 81%, 73% and 75% of normal, respectively. The choroidal width was not significantly changed. The thickness of BrM was significantly decreased only in disciform scarring (81% of normal). We concluded that, after age correction, a significant atrophy of the choriocapillaris was found for maculae with ARMD and a significant decrease in thickness of Bruch's membrane was found for maculae with a disciform scar.

Chapter 12: After cataract extraction with implantation of an artificial intraocular lens without an UV-light filter the increased transmission of UV-light is believed to speed up the development of age-related macular degeneration by producing free radicals in the retina. We hypothesized that mechanical trauma during cataract surgery could also increase the prevalence of disciform macular degeneration.

The maculae of 82 randomly selected post-mortem human pseudophakic eyes and 16 fellow phakic eyes were examined by light microscopy. The presence of a basal laminar deposit, hard and soft drusen, thickening and calcification of Bruch's membrane, geographic atrophy, subretinal neovascularization and disciform scars was assessed in a standardized way. An age-matched series of 126 post-mortem phakic eyes was used as control group. Age at the time of death ranged from 62 to 100 years for both the pseudophakic eyes (mean 81,3 years)

and the control group (mean 78,5 years). The time between lens implantation and death ranged from 3 to 168 months (mean 52 months).

There was no significant difference between the two age-matched groups, except for a higher prevalence of hard drusen (Exact trend test, $P = 0.038$) and disciform scars for the pseudophakic eyes (Fisher's exact test, $P = 0.007$). There was no significant correlation between either age-related changes in the macula or disciform degeneration and the length of time between cataract surgery and death. No significant difference was found between pseudophakic eyes with or without UV-filter. No significant differences were found between pseudophakic eyes with brown or blue irises or after intra or extracapsular cataract extraction.

Among patients who have received an artificial intraocular lens the prevalence of disciform macular degeneration is increased. Our findings do not confirm that this is caused by an increase in UV-light. The possibility that the surgical trauma is the initiating factor, leading to the development of breaks in Bruch's membrane and subsequent subretinal neovascularization has to be examined in a larger prospective study.

SAMENVATTING

In dit proefschrift wordt het probleem van de Seniele (=ouderdoms) Macula Degeneratie (SMD) besproken aan de hand van het onderzoek dat voor deze promotie is verricht. Daarbij hebben we vooral gekeken naar de histopathologische veranderingen in de humane macula, op het grensvlak van retina en choroidea.

Hoofdstuk 1: SMD is de belangrijkste oorzaak voor sociale blindheid in de westerse wereld bij mensen ouder dan 65 jaar. Met de toenemende vergrijzing zal dit sociale probleem alleen maar groter worden. Patiënten met SMD hebben een verminderde gezichtsscherpte of zelfs een totaal verlies van het centrale gezichtsveld. Meestal is deze aandoening bilateraal en zijn deze mensen als gevolg daarvan ernstig gehandicapt.

De kenmerken bij funduscopie zijn: de aanwezigheid van multipele Drusen, verstoringen van het retinale pigmentepitheel, geografische atrofie of subretinale neovascularisatie met sereuze lekkage of bloedingen met daarop volgend de vorming van een fibrovasculair litteken.

De mogelijkheden voor therapie zijn heden ten dage nog beperkt: medicamenteuze behandeling is gebaseerd op preventie van SMD of het stoppen van het reeds aanwezige proces. De resultaten die hiermee geboekt worden zijn echter zeer twijfelachtig. Laser fotocoagulatie om (verdere) schade aan de fovea te voorkomen, is beperkt tot speciale gevallen, maar kan het ziekteproces zeker enkele jaren vertragen. Chirurgische procedures zijn momenteel in opkomst en zijn veelbelovend, maar tot dusver zijn de funktionele resultaten nog teleurstellend.

In hoofdstuk 2 wordt de normale anatomie en histologie van de humane macula beschreven, voor een beter begrip van de rest van het proefschrift.

In hoofdstuk 3 worden de histologische leeftijdsveranderingen in de humane macula beschreven. Veel aandacht wordt hierbij besteed aan de verschillende stadia van SMD en aan de huidige terminologie, die vaak verwarrend en misleidend is.

Hoofdstuk 4: Het doel van dit onderzoek is om een beter inzicht te krijgen in de pathogenese van SMD, waarbij de aandacht vooral uitging naar de prevalentie, distributie, ultrastructuur, element-samenstelling en immunohistochemie van Basal Laminar Deposit (BLD), een voorstadium van SMD waar nog weinig van bekend is. De histologische veranderingen in macula's van alle leeftijden werden

geklassificeerd, gekwantificeerd en vervolgens statistisch geanalyseerd om een beter inzicht te krijgen in het begin, het verloop en eventuele causale factoren en correlaties in het ontstaan van SMD. Er werd tevens morfometrie en element-analyse aan de omringende structuren van het BLD verricht om aanwijzingen te krijgen in de richting van mogelijke causale faktoren voor het ontstaan van BLD. Aanvullend onderzoek werd verricht naar sub-RPE deposities in de perifere retina van de ogen waarin ook BLD in de macula was gevonden. De invloed van cataract extractie en de implantatie van een intraoculaire kunstlens, met of zonder UV-filter, op de veroudering en degeneratie van de macula werd onderzocht aan de hand van een grote serie pseudofake ogen en vergeleken met een leeftijds-vergelijkbare kontrole groep.

Hoofdstuk 5: Van een serie van 182 ongepaarde normale humane post-mortem ogen, afkomstig van alle leeftijden tussen 8 en 100 jaar, werden de macula's lichtmicroscopisch onderzocht. De histologische verouderings-verschijnselen zoals het voorkomen van BLD, Drusen, verdikking en verkalking van de membraan van Bruch werden semi-kwantitatief geklassificeerd en statistisch geanalyseerd. Tevens werden de macula's van 45 contralaterale ogen en de perifere retina van 50 ogen bestudeerd. BLD werd gevonden in 39% van de macula's vanaf de leeftijd van 40 jaar. In 37% van de macula's werden harde Drusen gevonden vanaf 34 jaar. Zachte Drusen werden in 10% van de macula's gezien beginnend vanaf 54 jaar. In 92% van de gevallen was de membraan van Bruch verdikt vanaf 19 jaar en verkalkingen in deze membraan werden gezien in 59% van de gevallen vanaf 33 jaar. Al deze veranderingen waren sterk gecorreleerd met de leeftijd (P<0,0001). Er werden geen geslachtsverschillen gevonden. Gelijke veranderingen werden in de contralaterale ogen gevonden (P<0,001). De aanwezigheid van BLD in de macula was gecorreleerd met de aanwezigheid van BLD-achtige sub-RPE deposities in de perifere retina (corr.coeff. 0,39, P<0,003). Eveneens waren Drusen in de macula gecorreleerd met Drusen in de perifere retina (corr.coeff. 0,42, P=0,001). Geografische atrofie werd gevonden in 6,6% van de ogen ouder dan 70 jaar, terwijl subretinale neovascularisatie gezien werd in 3,8% van deze macula's en dan met name in macula's met grote hoeveelheden BLD. Ofschoon deze verouderingsveranderingen frequent werden gevonden, zagen we slechts in een klein percentage van de ogen ver gevorderde stadia van ouderdoms macula degeneratie. Duidelijke causale verbanden tussen bepaalde verouderingsveranderingen en het ontstaan van

ouderdoms macula degeneratie konden niet gelegd worden.

Hoofdstuk 6: In een serie van 42 macula's hebben we de ultrastructuur en de leeftijdsverdeling van BLD bestudeerd. Drie typen BLD werden gezien: het vroege type, het late type en flocculent (vlokkig) BLD. Lichtmicroscopisch zijn de vroege en late vorm te onderscheiden van het flocculente BLD. Met elektronen microscopie verschilden de vroege en late vorm met name in de verhouding van het long-spacing collagen ten opzichte van het homogene granulaire materiaal. BLD werd gevonden vanaf de leeftijd van 19 jaar. Het werd niet alleen gezien tussen het RPE en de bijbehorende basaal membraan, maar vaker nog of soms zelfs uitsluitend in de membraan van Bruch aan de zijde van de choriocapillaris. Er werd geen directe relatie gevonden met het voorkomen van andere verouderings-verschijnselen, zoals verkalkingen in de membraan van Bruch, stapeling van lipofuchsine granulae in het RPE of het voorkomen van Drusen in de macula's. Op BLD gelijkend materiaal wordt ook gevonden in het trabekel systeem van het oog, in de cornea en in vele andere organen en weefsels. Het wordt vaak gezien in de nabijheid van basaal membranen van diverse soorten epitheel. Op basis van morfologische en morfometrische gegevens denken we dat BLD gelijk is aan long-spacing collagen en overmatige hoeveelheden basaal membraan materiaal. Daarom blijkt het niet een pure oogafwijking te zijn.

Hoofdstuk 7: Om meer te weten te komen over de chemische samenstelling van het BLD en om de rol van zink te bepalen bij het ontstaan van ouderdoms macula degeneratie hebben we met behulp van röntgenmicroanalyse de elementen bepaald in BLD en in de omringende structuren, in de macula's van 38 humane post-mortem ogen. BLD en de capillairwand van de choriocapillaris bevatten geen specifieke elementen. Calcium, fosfor, zwavel, zink en chloor werden gevonden in de lipofuchsine granulae van het RPE. De melanine korrels van het RPE en melanocyten van de choroidea bevatten voornamelijk zwavel en koper, en in mindere mate zink, calcium en ijzer. Lokale verkalkingen in de membraan van Bruch zijn voornamelijk samengesteld uit grote hoeveelheden calcium en fosfor en kleinere hoeveelheden zink, ijzer en chloor. Na zeer snelle cryofixatie tot -182 °C, gevolgd door vriesdrogen en dampfixatie werden tevens natrium en kalium aangetoond. We hebben aangetoond dat voor de overige elementen de resultaten van röntgenmicroanalyse na cryofixatie, vriesdrogen en dampfixatie vergelijkbare resultaten geeft als na aldehyde fixatie en aceton dehydratie van het weefsel. Uit dit onderzoek konden echter geen konklusies worden getrokken voor wat betreft

de oorsprong van het BLD. Er werd geen relatie gevonden tussen de aanwezigheid van zink in het melanine van het RPE of in verkalkingen van de membraan van Bruch en de aanwezigheid van BLD of Drusen in de macula's.

Hoofdstuk 8: De plaats van het BLD tussen het RPE en de basaal membraan en in de buitenste collagene zone van de membraan van Bruch dichtbij de basaal membraan van de choriocapillaris en de ultrastructuur van het BLD suggereren dat het bestaat uit abnormale hoeveelheden basaal membraan materiaal. De hoofdkomponenten van basaal membranen zijn collageen type IV, laminine en heparan sulfaat proteoglycanen (HSPG). Gelabelde antilichamen tegen deze komponenten kunnen daarom gebruikt worden bij de identificatie en lokalisatie van basaal membraan materiaal met behulp van immunohistochemische technieken. In dit hoofdstuk hebben we de aanwezigheid getest van collageen type IV, laminine en HSPG in oude humane macula's met behulp van immunohistochemie en immuno-electronenmicroscopie. Testen voor de aanwezigheid van collageen type VI en fibronectine, theoretisch mogelijke bestanddelen van BLD, werden ook uitgevoerd. Een serie van 76 ogen van 68 mensen werd gebruikt, afkomstig van obducties of chirurgische enucleaties wegens een buiten de macula gelokaliseerd melanoom. De fijn-granulaire komponent van het BLD kleurde positief met antilichamen tegen collageen type IV, laminine en HSPG. Het long-spacing collagen kleurde niet aan. Geen van de komponenten van BLD kleurde aan met antilichamen tegen collageen VI en fibronectine. We konkludeerden dat het BLD tenminste gedeeltelijk bestaat uit basaal membraan materiaal.

Hoofdstuk 9: Bij subretinale neovascularisatie moeten de capillairen van de choriocapillaris de membraan van Bruch passeren om de sub-RPE ruimte te bereiken. Daarom moeten er dus eerst gaten in de membraan van Bruch zijn ontstaan. Bij histologische bestudering van macula's met subretinale neovascularisaties of een disciform litteken zien we macrofagen dichtbij dunne plekken of breuken in de membraan van Bruch. Dit is geïnterpreteerd als fagocytose van materiaal van de membraan van Bruch. Het doel van dit gedeelte van het onderzoek is om na te gaan of immuunkomplex deposities kunnen worden aangetoond in macula's met vroege stadia van ouderdoms macula degeneratie, welke aanleiding zouden kunnen geven voor deze macrofaag reaktie. Met behulp van immunofluorescentie microscopie is een serie van 20 humane macula's getest op de aanwezigheid van immuunkomplexen met behulp van antilichamen tegen immunoglobulinen, complement factoren en fibrinogeen. Transmissie elektronen

microscopie werd gedaan op verscheidene macula's om macrofagen te identificeren. Macrofagen werden waargenomen in nauwe relatie tot long-spacing collagen in de buitenste collagene zone van de membraan van Bruch, waarbij de suggestie werd gewekt dat dit materiaal selectief werd gefagocyteerd. Immuunkomplex deposities werden niet gevonden in BLD of Drusen. In de buitenste collagene zone van de membraan van Bruch werden frequent lineaire deposities gezien van complement en fibrinogeen. Wegens het ontbreken van immunoglobulinen is het onwaarschijnlijk dat deze deposities van aspecifieke stoffen aanleiding geven tot chemoattractie van macrofagen en daarmee een rol zouden spelen in de initiële fase van het ontstaan van subretinale neovascularisaties en disciforme macula degeneratie.

Hoofdstuk 10: In een aantal ogen met BLD in de macula werden bij lichtmicroscopie van de perifere retina gelijksoortige afzettingen gevonden tussen het RPE en de membraan van Bruch. Van een serie van 10 humane ogen met dergelijke deposities werden delen van de equatoriale en perifere retina bestudeerd met elektronen microscopie. In 8 van deze 10 ogen was de ultrastructuur van dit materiaal amorf en fijn granulair. Vijf van deze acht deposities bevatten tevens geringe hoeveelheden long-spacing collagen. De ultrastructuur van deze deposities was gelijk aan het vroege type BLD in de macula. In de resterende twee ogen bleken de deposities niet te bestaan uit BLD, maar uit afgeplatte en langgerekte Drusen. Deze resultaten bevestigen dat BLD niet alleen in de macula wordt gevonden maar ook in perifere delen van de retina.

Hoofdstuk 11: In de literatuur zijn geen exacte gegevens bekend omtrent de kwantificering van de verdikking van de membraan van Bruch, van veranderingen in de choriocapillaris en de dikte van de choroidea met het toenemen van de leeftijd en de correlatie van deze veranderingen met het ontstaan van ouderdoms macula degeneratie. Met behulp van een computer gestuurd beeldanalyse systeem hebben we de dichtheid van het choriocapillaris netwerk, de capillair diameter en de dikte van de membraan van Bruch en de choroidea gekwantificeerd in een serie van 95 histologisch normale humane macula's, verdeeld over alle leeftijden van 6 tot 100 jaar, en in een serie van 25 pathologische macula's met BLD, geografische atrofie of disciforme macula degeneratie. In normale macula's verminderde de dichtheid van het capillair netwerk van de choriocapillaris met 45% (van 0,75 tot 0,41) in het verloop van 10 decaden. De capillair diameter nam af met 34% (van 9,8 tot 6,5 μm), de dikte van de membraan van Bruch nam toe met 135% (van

2,0 tot 4,7 μm) en de dikte van de choroidea nam af met 57% (van 194 tot 84 μm). In macula's met BLD, geografische atrofie of disciforme degeneratie was, na leeftijdskorrektie, de dichtheid van de choriocapillaris respectievelijk 63%, 54% en 43% van normaal en was de capillaire diameter respectievelijk 81%, 73% en 75% van normaal. De dikte van de choroidea was niet significant veranderd. De dikte van de membraan van Bruch was alleen in macula's met een disciform litteken significant verminderd (81% van normaal). We kunnen dus konkluderen dat er een significante atrofie van de choriocapillaris werd gevonden in ogen met vroege en late stadia van ouderdoms macula degeneratie en er een significante afname van de dikte van de membraan van Bruch werd gezien in macula's met een disciform litteken.

Hoofdstuk 12: Aangenomen wordt dat na cataract extractie met implantatie van een intraoculaire kunstlens zonder UV-filter, de ontwikkeling van ouderdoms macula degeneratie versneld kan worden doordat de toegenomen hoeveelheid UV-licht voor een toename van de hoeveelheid vrije radicalen in de retina zorgt. Er werd verondersteld dat het mechanische trauma van de cataract chirurgie mogelijk ook een toename zou kunnen geven van het ontstaan van ouderdoms macula degeneratie. De macula's van 82 willekeurig geselecteerde pseudofake humane post-mortem ogen en 16 fake contralaterale ogen werden lichtmicroscopisch bestudeerd op de aanwezigheid van BLD, harde en zachte Drusen, verdikking en verkalking van de membraan van Bruch, geografische atrofie, subretinale neovascularisatie en een disciforme litteken. Een leeftijdsgekontroleerde serie van 126 fake post-mortem ogen werd gebruikt als kontrole groep. De leeftijd ten tijde van overlijden varieerde van 62 tot 100 jaar voor zowel de pseudofake groep (gemidd. leeftijd 81,3 jaar) als de kontrole groep (gemidd. leeftijd 78,5 jaar). De tijdsduur verlopen tussen implantatie van de lens en enucleatie varieerde van 3 tot 168 maanden (gemidd. 52 maanden).

Er was geen verschil tussen beide groepen, behalve een hogere prevalentie van harde Drusen (Exact trend test, P=0,038) en van disciforme littekens (Fisher's exact test, P=0,007) in pseudofake ogen. Er was geen significante correlatie tussen zowel het voorkomen van veroudering veranderingen in de macula als de aanwezigheid van een disciform litteken en de tijdsduur, verstreken tussen cataract extractie en implantatie van de lens en enucleatie. Er werd geen significant verschil gevonden tussen pseudofake ogen met of zonder UV-filter. Bij patiënten met een intraoculaire kunstlens wordt dus een hogere prevalentie van disciforme macula

degeneratie gevonden. De resultaten van dit onderzoek laten zien dat dit waarschijnlijk niet wordt veroorzaakt door een toename van de hoeveelheid UV-licht. De mogelijkheid dat het chirurgisch trauma de initiërende factor is, welke leidt tot het ontstaan van breuken in de membraan van Bruch met daaropvolgend de vorming van een disciform litteken zou in een grote, prospectief opgezette klinische studie moeten worden onderzocht.

REFERENCES

1.Abrahamson DR. Recent studies on the structure and pathology of basement membranes. J Pathology 1986;149:257-78

1a.Auroux M, Nawar NNY, Rizkalla N. Testicular aging: vascularization and gametogenesis modifications in the Wistar rat. Arch Androl 1985;14(2-3):115-121.

2.Banfield WG, Lee CK, Lee CW. Myocardial collagen of the fibrous long-spacing type. Arch Pathol 1973;95:262-6

3.Banks CN, Hutton WK. Blindness in New South Wales: an estimate of the prevalence and some contributing causes. Aust J Ophthalmol 1982;9:285-8

4.Barondes M, Pauleikhoff D, Chisholm IC, Minassian D, Bird AC. Bilaterality of drusen. Brit J Ophthalmol 1990;74:180-2

5.Barsky SH, Hannah JB. Extracellular hyaline bodies are basement membrane accumulations. Am J Clin Pathol 1987;87:455-60

6.Baudouin Ch, Fredj-Reygrobellet D, Peyman GA, Lapalus Ph, Gordon B, Bazan NG, Gastaud P. Etude immunohistologique des membranes neovasculaires sous-retiniennes au cours des degenerescences maculaires lieés a l'age. Ophthalmologie 1991;5:61-4

7.Bazan HEP, Bazan NG, Feeney-Burns L, Berman ER. Lipids in human lipofuscin-enriched subcellular fractions of two age populations. Invest Ophthalmol Vis Sci 1990;31:1433-43

8.Berman ER, Schwell H, Feeney L. The retinal pigment epithelium: Chemical composition and structure. Invest Ophthalmol Vis Sci 1974;13:675-87

9.Bird AC. Pathogenesis of retinal pigment epithelial detachment in the elderly; the relevance of Bruch's membrane change. Eye 1991;5:1-12

10.Bird AC, Marshall J. Retinal pigment epithelial detachments in the elderly. Trans Ophthalmol Soc UK 1986;105:674-82

11.Blumenkranz MS, Russell SR, Robey MG, Kott-Blumenkranz R, Penneys N. Risk factors in age-related maculopathy complicated by choroidal neovascularization. Ophthalmology 1986;96;552-8

12.Borges J, Zong-Yi Li, Tso MOM. Effects of repeated photic exposures on the monkey macula. Arch Ophthalmol 1990;108;727-33

13.Bosman FT, Cleutjens J, Beek C, Havenith M. Basement membrane heterogenity. Histochemical J 1989;21:629-33

14.Boulton M, Docchio F, Dayhaw-Barker P, Ramponi R, Cubeddu R. Age-related changes in the morphology, absorption and fluoresence of melanosomes and lipofuscin granules of the retinal pigment epithelium. Vision Res 1990;30;1291-1303

15.Bressler NM, Bressler SB, Fine SL. Age-related macular degeneration. Surv Ophthalmol 1988;32:375-413

16.Bressler NM, Bressler SB, Gragoudas ES. Clinical characteristics of choroidal neovascular membranes. Arch Ophthalmol 1987;105:209-13

17.Bressler NM, Bressler SB, West SK, Fine SL, Tayler HR. The

grading prevalence of macular degeneration in Chesapeake
Bay watermen. Arch Ophthalmol 1989;107:847-52

18. Bruijn WC de, Cleton-Soeteman MI. Application of Chelex
standard beads in integrated morphometrical and X-ray
microanalysis. Scanning Microsc 1985;II:115-29

19. Bruns RR, Press W, Engval E. Type VI collagen in
extracellular, 100-nm periodic filaments and
fibrils:identification by immunoelectron microscopy.
J Cell Biol 1986;103;393-404

20. Bruns RR. Beaded filaments and long-spacing fibrils:
relation to type VI collagen. J Ultrastruc Res
1984;89:136-45

21. Burns RP, Feeney-Burns L. Clinico-morphologic correlations
of drusen of Bruch's membrane. Trans Am Ophthalmol Soc
1980;78:206-22

22. Cameron J, Skubitz APN, Furchi LT. Type IV collagen and
corneal epithelial adhesion and migration. Invest
Ophthalmol Vis Sci 1991;32:2766-73

23. Campochiaro PA, Glaser BM. Endothelial cells release a
chemo attractant for retinal pigment epithelial cells in
vitro. Arch Ophthalmol 1985;103:1876-80

24. Campochiaro PA, Jerdan JA, Glaser BM. The extracellular
matrix of human retinal pigment epithelial cells in vivo
and its synthesis in vitro. Invest Ophthalmol Vis Sci
1986;27:1615-21

25. Capon MRC, Marshall J, Krafft JI, Alexander RA, Hiscott PS,
Bird AC. Sorsby's fundus dystrophy. Ophthalmology
1989;96:1769-77

26. Carlemalm E, Garavito RM, Villiger W. Resin development for
electron microscopy and an analysis of embedding at low
temperature. J Microsc 1982;126:123-43

27. Chapman JA, Armitage PM. An analysis of fibrous long
spacing forms of collagen. Connective Tissue Res
1972;1:31-7

27aChen JC, Fitzke FW, Pauleikhoff D, Bird AC. Poor choroidal
perfusion is a cause of visual impairment in age-related
macular degeneration. Invest Ophthalmol Vis Sci 1989;30
(Suppl):153.

28. CNIB: Canadian National Institute for the Blind - National
Society for the prevention of blindness: Causes of
blindness - Statistics for new cases registered with CNIB
in 1970-1976. New York.

29. Coffey AJH, Brownstein S. The prevalence of macular drusen
in postmortem eyes. Am J Ophthalmol 1986;102:164-71.

30. Conn HJ. Staining procedures used by the biological stain
commission. 2nd rev. ed. Baltimore: Williams &
Wilkins,1960

31. Coscas G, Soubrane G, Ramahefasolo C, Fardeau C. Perifoveal
laser treatment for subfoveal choroidal new vessels in
age-related macular degeneration. Arch Ophthalmol
1991;109:1258-65

32. Cravioto H, Lockwood R. Long-spacing collagen in human
acoustic nerve tumors. In vivo and in vitro observations.
J Ultrastruct Res 1968;24:70-85

33. Das A, Frank RN, Zhang NL, Turczyn TJ. Ultrastructural
localization of extracellular matrix components in human

retinal vessels and Bruch's membrane. Arch Ophthalmol 1990;108;421-9

33aDas A, Puklin JE, Frank RN, Zhang NL. Ultrastructural immunocytochemistry of subretinal neovascular membranes in age-related macular degeneration. Ophthalmology 1992;99:1368-76

34.Davies MJ, Slater TF. The use of electron-spin-resonance techniques to detect free-radical formation and tissue damage. Proc Nutr Soc 1988;47;397-405

35.Davis WL. An electron microscopic, histochemical and analytical X-ray microanalytical study of calcification in Bruch's membrane from human eyes. J Histochem Cytochem 1981;29:601-8

36.Delaney WV, Oates RP. Senile macular degeneration: a preliminary study. Ann Ophthalmol 1982;14:21-4

37.Dorey CK, Wu G, Ebenstein D, Garsd A, Weiter JJ. Cell loss in the aging retina. Invest Ophthalmol Vis Sci 1989;30:1691-9

38.Duvall J, McKechnie NM, Lee WR, Rothery S, Marshall J. Extensive subretinal pigment epithelial deposit in two brothers suffering from dominant retinitis pigmentosa. Graefe's Arch Clin Exp Ophth 1986;224:299-309

39.Edelmann L. Freeze-substitution and the preservation of diffusible ions. J Microscopy 1991;161:217-28

40.Ellinger A, Pavelka M. Post-embedding localization of glycoconjugates by means of lectins on thin sections of tissues embedded in LR White. Histochem J 1985;17:1321-36

41.Elman MJ, Fine SL, Murphy RP, Patz A, Auer C. The natural history of serous retinal pigment epithelium detachment in patients with age-related macular degeneration. Ophthalmology 1986;93:224-30

42.Fantone JC, Ward PA. Role of oxygen-derived free radicals and metabolites in leukocyte-dependent inflammatory reactions. Am Assoc Pathol 1982;107:397-418

43.Farkas TG, Sylvester V, Archer D, Altona M. The histochemistry of Drusen. Am J Ophthalmol 1971;71;1206-15

44.Faure JP, Bloch-Michel E, Le Hoang P, Vadot E, Immunopathologie de l'oeil. Société Francaise d'Ophthalmologie et Masson. Paris, 1988 pp.291-327

45.Feeney-Burns L, Ellersieck MR. Age-related changes in the ultrastructure of Bruch's membrane. Am J Ophthalmol 1985;100:686-97

46.Feeney-Burns L, Berman ER, Rothman H. Lipofuscin of human retinal pigment epithelium. Am J Ophthalmol 1980;90:783-91

47.Feeney-Burns L, Burns RN, Gao Chun-Lan. Age-related macular changes in humans over 90 years old. Am J Ophthalmol 1990;109:265-78

48.Feeney-Burns L, Gao Chun-Lan, Tidwel M. Lysosomal enzyme cytochemistry of human RPE, Bruch's membrane and drusen. Invest Ophthalmol Vis Sci 1987;28:1138-47

49.Feeney-Burns L, Neuringer M, Gao Chun-Lan. Macular pathology in monkeys fed semipurified diets. Prog Clin Biol Res 1989;314:604-22

50.Ferris FL. Senile macular degeneration: review of epidemiologic features. Am J Epidemiol 1983;118:132-51

51. Fidzianska A, Glinka Z, Walski M. An ultrastructural study of the vascular and muscular basement membranein Duchenne-type dystrophy. Clin Neuropathol 1987;6:257-61
52. Fine BS, Yanoff M. Ocular histology. New York, NY: Harper & Row Publishers Inc; 1979 pp. 46-9, 219-26, 261-5
53. Fine BS. Lipoidal degeneration of the retinal pigment epithelium. Am J Ophthalmol 1981;91:469-73
54. Fine SL, Hawkins BS, Maguire MG. Krypton laser photocoagulation for neovascular lesions of age-related macular degeneration. Arch Ophthalmol 1991;109:300
55. Fishman ML, Oberg MA, Hess HH, Engel WK. Ultrastructural demonstration of calcium in retina, retinal pigment epithelium and choroid. Exp Eye Res 1977;24:341-53
56. Foreman J. Federal agency to develop cataract management guidelines by january 1991. Arch Ophthalmol 1990;108:1391
57. Frank RN, Green WR, Pollack IP. Senile macular degeneration clinicopathologic correlations of a case in the predisciform stage. Am J Ophthalmol 1973:75:587-94
58. Friedman E, Smith TR, Kuwabara T. Senile choroidal vascular patterns and drusen. Arch Ophthalmol 1963;69:220-30
59. Friedman E. The laminated cytoplasmic inclusions in the sensory epithelium of the human macula. J Ultrastruct Res 1965;12:92-103
60. Friedman E, Tso MOM. The retinal pigment epithelium. II Histologic changes associated with age. Arch Ophthalmol 1968;79:315-20
60a Friedman E, Smith TR. Pathogenesis: senile changes of the choriocapillaris of the posterior pole. Transact Am Acad Opththal Oto-Laryngol 1965;69:652-661.
61. Friedman I, Cawthorne T, Bird ES. Broad-banded striated bodies in the sensory epithelium of the human macula and in neurinoma. Nature 1965;207:171-4
61a Friedman E, Ivry M, Ebert E, Glynn R, Gragoudas E, Seddon J. Increased scleral rigidity and age-related macular degeneration. Ophthalmology 1989;96:104-108.
62. Fryczkowski AW, Sherman MD, Allinson RM, Payne CM. Chorioretinal anastomoses in age-related macular degeneration. Ann Ophthalmol 1989;21:370-8
63. Fung WE. Interferon alpha 2a for treatment of age-related macular degeneration. Am J Ophthalmol 1991;112:349-50
63a Garner A. Pathology of macular degeneration in the elderly. Trans Ophthalmol Soc UK 1975;95:54-61
64. Garron LK, Feeney ML, Hogan MJ, McEwen WK. Electron microscopic studies of the human eye. Am J Ophthalmol 1958;27-35
65. Gass JDM. Drusen and disciform macular detachment and degeneration. Arch Ophthalmol 1973;90:206-17
66. Gass JDM, Clarkson JG. Angoid streaks and disciform macular detachment in Paget's disease (osteitis deformans). Am J Ophthalmol 1973:75:576-85
67. Ghadially FN. Ultrastructural pathology of the cell and matrix. Stoneham, MA: Butterworths Publishers Inc.; 1988 3rd ed. pp. 589-99, 608- 13, 787-821, 1054-67, 1215-59
68. Gjessing HGA. Gibt es einen antagonismus zwischen cataracta senilis und Haabscher seniler makula veränderungen? Acta Ophthalmologica 1953;31:401-21

69. Glaser BM, Campochiaro PA, Davis JL, Sato Misao. Retinalpigment epithelial cells release inhibitor of neovascularization. Arch Ophthalmol 1985;103:1870-5

70. Glauert AM. Fixation, dehydration and embedding of biological specimen. North-Holland Publishing Co; Amsterdam: 1981. Chapter 2-6

71. Goldberg J, Flowerdew G, Smith E, et al. Factors associated with age-related macular degeneration. An analysis of data from the first national Health And Nutrition Examination Survey. Am J Epidemiol 1988;128:700-10

72. Gottsch JD, Pou S, Bynoe LA, Rosen GM. Hematogenous photosensitization. A mechanism for the development of age-related macular degeneration. Invest Ophthalmol Vis Sci 1990;31:1674-82

73. Greaves AH, Sarks JP, Sarks SH. Adult vitelliform macular degeneration: a clinical spectrum. Aust and New Zealand J Ophthal 1990;18:171-8

74. Green WR, Key SN. Senile macular degeneration: a histopathologic study. Trans Am Ophthalmol Soc 1977;75:180-254

75. Green WR, McDonnel PJ, Yeo JH. Pathologic features of senile macular degeneration. Ophthalmology 1985;92:615-27

76. Gregor Z, Bird AC, Chisholm IH. Senile disciform macular degeneration in the second eye. Brit J Ophthalmol 1977;61:141-7

77. Gregor Z, Joffe L. Senile macular changes in the black african. Brit J Ophthalmol 1978;62:547-50

78. Grindle CFJ, Marshall J. Ageing changes in Bruch's membrane and their functional implications. Trans Ophthalmol Soc UK 1978;98:172-5

79. Grossniklaus HE, Frank E, Green WR. Subretinal neovascularization in a pseudophakic eye treated with krypton laser photocoagulation. Arch Ophthalmol 1988;106:78-81

80. Halliwell B. How to characterize a biological antioxidant. Free Rad Res Comms 1990;9:1-32

81. Hamburg A. Aphakia versus pseudophakia: a clinical pathological study. Int Ophthalmology 1985;7:223-30

82. Havenith MG, van Zandvoort EH, Cleutjens JP, Bosman FT. Basement membrane deposition in benign and malignant naevo-melanocytic lesions: an immunohistochemical study with antibodies to type IV collagen and laminin. Histopathology 1989;15:137-46

83. Havenith MG. Tumor cell-extracellular matrix interactions: studies with antibodies to basement membrane components. Thesis. Maastricht, the Netherlands; 1988.

84. Hawkins WR, Newsome DA. Zinc supplementation for macular degeneration. Arch Ophthalmol 1991;109:1345

85. Hampton GR, Nelsen PT. Age-related macular degeneration: principles and practice. Raven Press, New York 1992 chapter 2

86. Heriot WJ, Henkind P, Bellhorn RW, Burns MS. Choroidal neovascularization can digest Bruch's membrane. A prior break is not essential. Ophthalmology 1984;91:1603-8

87. Hewitt AT, Nakazawa K, Newsome DA. Analysis of newly synthesized Bruch's membrane proteoglycans. Invest

162

Ophthalmol Vis Sci 1989;30:478-86

88. Hirano K, Kobayashi M, Kobayashi K, Hoshino T, Awaya S. Experimental formation of 100 nm periodic fibrils in the mouse corneal stroma and trabecular meshwork. Invest Ophthalmol Vis Sci 1989;30;869-74

89. Hogan MJ. Role of the retinal pigment epithelium in macular disease. Trans Am Acad Ophthalmol Otol 1972;76:64-80

90. Hogan MJ, Alvarado JA, Weddell JE. Histology of the human eye. Saunders Company, Philadelphia, 1971. pp.154-82, 344-72

91. Holmberg AK. Schlemm's canal and the trabecular meshwork. An electron microscopic study of the normal structure in man and monkey. Docum Ophthal 1965;19:339-66

92. Hyman LG, Lilienfeld AM, Ferris FL, Fine SL. Senile macular degeneration: a case control study. Am J Epidemiol 1983;118:213-27

93. Inhoffen W, Nuessgens Z. Rheological studies on patients with posterior subretinal neovascularization and exudative age-related macular degeneration. Graefe's Arch Clin Exp Ophthalmol 1990;228:316-20

94. Ishibashi T, Patterson R, Ohnishi Y, Inomata H, Ryan SJ. Formation of drusen in the human eye. Am J Ophthalmol 1986;101:342-53

95. Ishibashi T, Sorgente N, Patterson R, Ryan SJ. Aging changes in Bruch's membrane of monkeys: An electron microscopic study. Opthalmologica 1986;192:179-90

96. Iwamoto T, Witmer R, Landolt E. Light and electron microscopy in absolute glaucoma with pigment dispersion phenomena and contusion angle deformity. Am J Ophthalmol 1971;72:420-34

97. Iwasaki M, Inomata H. Lipofuscin granules in human photoreceptor cells. Invest Ophtalmol Vis Sci 1988;29:671-9

98. Jalkh AE, Nasrallah FP, Marinelli I, Van de Velde F. Inactive subretinal neovascularization in age-related macular degeneration. Ophthalmology 1990;97:1614-9

99. Jensen AD. Cataract PPOs. Arch Ophthalmol 1990;108:501-2

100. Jonasson F, Thordarson K. Prevalence of ocular disease and blindness in a rural area in the eastern region of Iceland during 1980 through 1984. Acta Ophthalmologica 1987;65(suppl):40-3

101. De Jong PTVM, Vrensen GFJM, Willekens BLJC, Mooy CM. Free running neodymium-YAG laser coagulation of the human fovea. Retina 1989;9:312-8

102. Kahn HA, Leibowitz HM, Ganley JP, et al. The Framingham Eye Study II. Association of ophthalmic pathology with single variables previously measured in the Framingham Heart Study. Am J Epidemiol 1977;106:33-41

103. Kajikawa K Nakawishi I, Yamamura T. The effect of collagenase on the formation of fibrous long spacing collagen aggregates. Lab Inv Res 1980;43:410-17

104. Karam LR, Simic MG. Detecting irradiated foods; use of hydroxyl radical biomarkers. Anal chem 1988;60:1117a-1119a

105. Karcioglu ZA. Zinc in the eye. Surv Ophthalmol 1982;27:114-22

106.Kenyon KR, Maumenee AE, Ryan SJ, Withmore PV, Green WR. Diffuse drusen and associated complications. Am J Ophthalmol 1985;100:119-28

107.Killingsworth MC. Age-related components of Bruch's membrane in the human eye. Graefe's Arch Clin Exp Ophthalmol 1987;225:406-12

108.Killingsworth MC, Sarks JP, Sarks SH. Macrophages related to Bruch's membrane in age-related macular degeneration. Eye 1990;4:613-21

109.Killingsworth MC. Bruch's membrane in the human eye: changes in normal ageing and age-related macular degeneration. Thesis; 1989, New South Wales, Australia.

110.Kirchof B, Kirchof E, Ryan SJ, Dixon JFP, Barton BE, Sorgente N. Macrophage modulation of retinal pigment epithelial cell migration and proliferation. Graefe's Arch Clin Exp Ophthalmol 1989;227:60-6

111.Klein BE, Klein R. Cataracts and macular degeneration in older americans. Arch Ophthalmol 1982;100:571-3

112.Klien BA. Angoid streaks. A clinical and histopathologic study. Am J Ophthalmol 1947;30;955-67

113.Kohno T, Sorgente N, Ishibashi T, Goodnight R, Ryan SJ. Immunofluorescent studies of fibronectin and laminin in the human eye. Invest Ophthalmol Vis Sci 1987;28:506-14

114.Korte GE, Burns MS, Bellhorn RW. Epithelium-capillary interactions in the eye: the retinal pigment epithelium and the choriocapillaris. Int Rev Cytology 1989;114:221-48

114aKorte GE, Bellhorn RW, Burns MS. Remodelling of the retinal pigment epithelium in response to intraepithelial capillaries: evidence that capillaries influence the polarity of epithelium. Cell Tissue Res 1986;245:135-142.

115.Korte GE, Reppucci V, Henkind P. RPE destruction causes choriocapillary atrophy. Invest Ophthalmol Vis Sci 1984;25:1135-45

116.Kraff MC, Sanders DR, Jampol LM, Lieberman HL. Effect of an ultraviolet-filtering intraocular lens on cystoid macular edema. Ophthalmology 1985;92:366-9

116aKrey HF. Segmental vascular patterns of the chorio-capillaris. Am J Ophthalmol 1975;80:198-202.

117.Lavery MA, Green WR, Jabs EW, Luckenbach MW, Cox JL. Ocular histopathology and ultrastructure of Sanfillipo's syndrome, type III-B. Arch Opthamol 1983;101:1263-74

118.Lavin MJ, Eldem B, Gregor ZJ. Symmetry of disciform scars in bilateral age-related macular degeneration. Brit J Ophthalmol 1991;75:133-6

119.Lee AK. Basement membrane and endothelial antigens: their role in evaluation of tumor invasion and metastasis. Advances in Immunohistochemistry 1988;16:363-75

120.Leibowitz H, Krueger DE, Maunder LR, et al. The Framingham Eye Study Monograph; an ophthalmological and epidemiological study of cataract, glaucoma, diabetic retinopathy, macular degeneration, and visual acuity in a general population of 2631 adults, 1973-1977. Surv Ophthalmol 1980;24:335-610

121.Leopold I.H. Zinc deficiency and visual impairment. Am J Ophthalmol 1978;85:871-5

122. Lerche W. Elektronenmikroskopische Beobachtungen ueber altersbedingte veraenderungen an der Bruchschen Membran des Menschen. Verhandlungen der Anatomischen Gesellschaft 1964;60;123-32
123. Lerman S. Ocular phototoxicity. N Engl J Med 1988;319:1475-7
124. Lerman S. Radiant energy and the eye. McMillan Publishing Co., New York. 1980. pp.115-83
125. Lewis H, Straatsma BR, Foos RY. Chorioretinal juncture. Multiple extramacular drusen. Ophthalmology 1986;93:1098-1112
126. Liles MR, Newsome DA, Oliver PD. Antioxidant enzymes in the aging human retinal pigment epithelium. Arch Ophthalmol 1991;109:1285-8
127. Linner JG, Livesey SA, Harrison DS, Steiner AL. A new technique for removal of amorphous phase tissue water ice crystal damage: A preparative method for ultrastructural analysis and immunoelectron mirosopy. J Histochem Cytochem 1986;34:1123-35
128. Linsenmayer TF, Bruns RR, Mentzer A. Type VI collagen: immunohistochemical identification as a filamentous component of the extracellular matrix of the developping avian corneal stroma. Developmental Biology 1986;118:425-31
129. Liu IY, White L, La Croix AZ. The association of age-related macular degeneration and lens opacities in the aged. Am J Public Health 1989;79:765-9
130. Livesey SA, Buescher ES, Krannig GL, Harrisson DS, Linner JG, Chiovetti R. Human neutrophil granule heterogeneity: immunolocalization studies using cryofixed, dried and embedded specimens. Scanning Microsc Suppl. 1989;3:231-40
131. Löffler KU, Lee WR. Basal linear deposit in the human macula. Graefe's Arch Clin Exp Ophthalmol 1986;224:493-501
132. Löffler KU, McMenamin PG. Evaluation of subretinal macrophage-like cells in the human fetal eye. Invest Ophthalmol Vis Sci 1990;31:1628-36
133. Luse SA, Zopf d, Cox JW. An electron microscopic study of in vitro and in vivo long-spacing collagen. Anat Record 1963;145:254
134. Luxenberg MN. Age-related macular degeneration and ghost cell glaucoma. Arch Ophthalmol 1991;109:1304-5
135. Macular photocoagulation study group. Argon laser photocoagulation for neovascular maculopathy. Five-year results from randomized clinical trials. Arch Ophthamol 1991;109:1109-14
136. Macular photocoagulation study group. Laser photocoagulation of subfoveal recurrent neovascular lesions in age-related macular degeneration. Results of a randomized clinical trial. Arch Ophthalmol 1991;109:1232-41
137. Macular photocoagulation study group. Subfoveal neovascular lesions in age-related macular degeneration. Arch Ophthalmol 1991;109:1242-57
137a Maguire P, Vine AK. Geographic atrophy of the retinal pigment epithelium. Am J Ophthalmol 1986;102:621-625.
138. Mainster MA, Ham WT, Delori FC. Potential retinal hazards.

Instrument and environmental light sources. Ophthalmology 1983;90:927-32

139. Maltzman BA, Mulvihill MN, Greenbaum A. Senile macular degeneration and risk fators: a case-control study. Ann Ophthalmol 1979;1197-1201

139a Mancini MA, Frank RN, Keirn RJ, Kennedy A, Khoury JK. Does the retinal pigment epithelium polarize the chorio-capillaris? Invest Ophthalmol Vis Sci 1986;27:336-345.

140. Marshall GE, Konstas AG, Lee WR. Ultrastructural distribution of collegen types I-VI in aging human retinal vessels. Brit J Ophthalmol 1990;74:228-32

140a Marshall GE, Konstas AGP, Abraham S, Lee WR. Extracellular matrix in aged human ciliary body: an immunoelectron microscope study. Invest Ophthalmol Vis Sci 1992;33:2546-60

140a Marshall GE, Konstas AGP, Reid GG, Lee WR. Type IV collagen and laminin in Bruch's membrane and basal laminar deposit in the human macula. Br J Ophthalmol 1992;76:607-14

141. Marshall GE, Konstas AG, Lee WR. Immunogold fine structural localization of extracellular matrix components in aged human cornea; I Types I-IV collagen and laminin. Graefe's Arch Clin Exp Ophthalmol 1991;229:157-63

142. Marshall GE, Konstas AG, Lee WR. Immunogold fine structural localization of extracellular matrix components in aged human cornea; II collagen types V and VI. Graefe's Arch Clin Exp Ophthalmol 1991;229:164-71

143. McMahon MS, Weiss JS, Riedel KG, Albert DM. Histopathological findings in necropsy eyes with intraocular lenses. Brit J Ophthalmol 1985;69:452-8

144. McMenamin PG, Lee WR, Aitken DAN. Age-related changes in the human outflow apparatus. Ophthalmology 1986;93:194-209

145. Meredith TA, Braley RE, Aaberg TM. Natural history of serous detachments of the retinal pigment epithelium. Am J Ophthalmol 1979;88:643-51

146. Merin S, Blair NP, Tso MOM. Vitreous fluorophotometry in patients with senile macular degeneration. Invest Ophthalmol Vis Sci 1987;28;756-9

147. Meyer KT, Heckenlively JR, Spitznas M, Foos RY. Dominant retinitis pigmentosa. A clinicopathologic correlation. Ophthalmology 1982;89:1414-24

148. Michels M, Sternberg P. Operating microscope-induced retinal phototoxicity: pathophysiology, clinical manifestations and prevention. Surv Ophthalmol 1990;34:237-52

149. Migheli A, Attanasio A. Two methods for flat embedding sections in LR White cut from paraffin blocks. Biotechnic and Histochemistry 1991;4:89-92

150. Mohos SC, Wagner BM. Damage to collagen in corneal immune injury. Arch Path 1969;88:3-20

151. Nakaizumi Y. The ultrastructure of Bruch's membrane I. Human, monkey, rabbit, guinea pig, and rat eyes. Arch Ophthalmol 1964;72:380-7

152. Nakaizumi Y. The ultrastructure of Bruch's membrane III.

The macular area of the human eye. Arch Ophthalmol 1964;72:395-401

153. Nasrallah F, Jalkh AE, Trempe CL, McMeel JW, Schepens CL. Subretinal hemorrhage in atrophic age-related macular degeneration. Am J Ophthalmol 1989;107:38-41

154. Naumann GOH, Apple DJ. Pathology of the eye. Springer-Verlag. New York 1986 pp.628-31

155. Newman GR. Use and abuse of LR White. Histochem J 1987;19:118-20

156. Newsome DA, Swartz M, Leone NC, Elston RC, Miller E. Oral zinc in macular degeneration. Arch Ophthalmol 1988;106:192-8

157. Newsome DA, Rothman R. Zinc uptake in vitro by human retinal pigment epithelium. Invest Ophthalmol Vis Sci 1987;28:1795-9

158. Newsome DA, Hewitt AT, Huh W, Robey PG, Hassell JR. Detection of specific extracellular matrix molecules in drusen, Bruch's membrane, and ciliary body. Am J Ophthalmol 1987;104;373-81

159. Newsome DA, Swartz M, Leone NC, Hewitt AT, Wolford F, Miller ED. Macular degeneration and elevated serum ceruloplasmin. Invest Ophthalmol Vis Sci 1986;27:1675-80

160. Nishimura T, Goodnight R, Prendergast RA, Ryan SJ. Activated marophages in experimental subretinal neovascularization. Ophthalmologica 1990;200:39-44

161. Nishimura T, Zhi-Ren Zhu, Ryan SJ. Effects of sodium-Iodate on experimental subretinal neovascularization in the primate. Ophthalmologica 1990;200:28-38

162. Oka S, Ogino K, Houbara T, Yoshimura S, Okazaki Y, Takemoto T, Kato N, Iida Y, Uda T. An immunohistochemical study of copper, zinc-containing superoxide dismutase detected by a monoclonal antibody in gastric mucosa and gastric cancer. Histopathology 1990;17:231-6

162a Olver J, Pauleikhoff D, Bird A. Morphometric analysis of age changes in the choriocapillaris. Invest Ophtalmol Vis Sci 1991;31(Suppl):47

163. Oosterhuis JA. Laser treatment of age-related maculopathy (AMD) with subretinal neovascularization (SRN). Fortschr Ophthamol 1990;87:52-61

164. Panessa-Warren BJ. Basic biological X-ray microanalysis. Scanning electron microscopy 1983;1:113-23

165. Panessa BJ, Zadunaisky JA. Pigment granules: a calcium reservoir in the vertebrate eye. Exp Eye Res 1981;31:593-604

166. Pauleikhoff D, Barondes MJ, Minassian D, Chisholm IH, Bird AC. Drusen as risk factors in age-related macular disease. Am J Ophthalmol 1990;109:38-43

166a Pauleikhoff D, Marshall J, Bird AC. Histochemical and morphological correlation of aging changes in Bruch's membrane. Invest Ophthalmol Vis Sci 1989;30 (Suppl):153.

167. Pauleikhoff D, Chen JC, Chisholm IH, Bird AC. Choroidal perfusion abnormality with age-related Bruch's membrane change. Am J Ophthalmol 1990;109:211-7

168. Pauleikhoff D, Harper CA, Marshall J, Bird AC. Aging changes in Bruch's membrane. Ophthalmology 1990;97;171-8

169. Penfold PL, Killingsworth MC, Sarks SH. Senile macular degeneration: The involvement of giant cells in atrophy of the retinal pigment epithelium. Invest Ophthalmol Vis Sci 1986;27:364-71

170. Penfold P, Killingsworth M, Sarks SH. An ultrastructural study of the role of leucocytes and fibroblasts in the breakdown of Bruch's membrane. Aust J Ophthalmol 1984;12:23-31

171. Penfold P, Provis JM, Madigan MC, van Driel, Bilson. Angiogenesis in normal human retinal development: the involvolvement of astrocytes and macrophages. Graefe's Arch Clin Exp Ophthalmol 1990;228:255-63

172. Penfold PL, Provis JM, Furby JH, Gatenby PA, Bilson FA. Autoantibodies to retinal astrocytes associated with age-related macular degeneration. Graefe's Clin Exp Ophthalmol 1990;228:270-4

173. Penfold PL, Provis JM, Bilson FA. Age-related macular degeneration: ultrastructural studies of the relationship of leucocytes to angiogenesis. Graefe's Arch Clin Exp Opthalmol 1987;225:70-6

174. Peyman GA, Blinder KJ, Paris CL, Alturki W, Nelson NC, Desai U. A technique for retinal pigment epithelium transplantation for age-related macular degeneration secondary to extensive foveal scarring. Ophthal Surg 1991;22:102-8

175. Pflugfelder ME, Forster RK. Intravitreal Vancomycin. Retinal toxicity, clearance, and interaction with gentamycin. Arch Ophthalmol 1987;105:831-7

176. Philp NJ, Nachmias VT. Polarized distribution of Integrin and Fibronectine in retinal pigment epithelium. Invest Ophthalmol Vis Sci 1987;28:1275-80

177. Pizarello LD. The dimensions of the problem of eye disease among the eldery. Ophthalmology 1987;94:1191-5

178. Pollack A, Heriot WJ, Henkind P. Cellular processes causing defects in Bruch's membrane following krypton laser photocoagulation. Ophthalmology 1986;93:1113-9

179. Pollack A, Korte GE, Weitzner AL, Henkind P. Ultrastructure of Bruch's membrane after krypton laser photocoagulation. I Breakdown of Bruch's membrane. Arch Ophthalmol 1986;104:1372-6

180. Pollack A, Korte GE, Weitzner AL, Henkind. Ultrastructure of Bruch's membrane after krypton laser photocoagulation II. Repair of Bruch's membrane and the role of marophages. Arch Ophthalmol 1986;104:1377-82

181. Potts AM, Pin Chit Au. The affinity of melanin for inorganic ions. Exp eye res 1976;22:487-91

182. Rao NA, Romero JL, Fernandez MAS, Sevanian A, Marak GE. Role of free radicals in uveitis. Surv Ophthalmol 1987;32:209-13

183. Rao NA, Thaete LG, Delmage JM, Sevanian A. Superoxide dismutase in ocular structures. Invest Ophthalmol Vis Sci 1985;26:1778-81

184. Recasens JF, Green K. Effects of endotoxin and anti-inflammatory agents on superoxide dismutase in the rabbits. Ophthalmic Res 1990;22:12-8

185. Remé CE. Autophagy in visual cells and pigment epithelium.

Invest ophthalmol Vis Sci 1977;16:807-14

186. Rodrigues MM, Katz SI, Foidart JM, Spaeth GL. Collagen, factor VIII, antigen, and immunoglobulins in the aqueous drainage channels. Ophthalmology 1980;87:337-45

187. Rodriguez FJ, Foos RY, Lewis H. Age-related macular degeneration and ghost cell glaucoma. Arch Ophthalmol 1991;109:1304-5

188. Roomans GM. Introduction in X-ray microanalysis in biology. J of electron microscopy technique 1988;9:3-17

189. Roth SI, Stock EL, Jutabha R. Endothelial viral inclusions in Fuch's corneal dystrophy. Hum Pathol 1987;18:338-41

190. Rothman RJ, Newsome DA. Zinc uptake by human retinal pigment epithelium. Invest Ophthalmol Vis Sci 1986;27:262

191. Roy M, Kuehl E. Age-related macular degeneration: from neurovascularization to atrophic. Ann Ophthalmol 1989;21:429-31

192. Sarks JP, Sarks SH, Killingsworth MC. Evolution of geographic atrophy of the retinal pigment epithelium. Eye 1988;2:552-77

193. Sarks SH. Drusen and their relationship to senile macular degeneration. Austr J Ophthalmol 1980;8;117-30

194. Sarks SH. Drusen patterns predisposing to geographis atrophy of the retinal pigment epithelium. Austr J of Ophthalmol 1982;10:91-7

195. Sarks SH. The fellow eye in senile disciform degeneration. Trans Aust Coll Ophthamol 1970;2:77-82

196. Sarks SH. New vessel formation beneath the retinal pigment epithelium in senile eyes. Brit J Ophthal 1973;57;951-65

197. Sarks SH. The aging eye. Med J Aust. 1975;2:602-4

198. Sarks SH. Senile choriodal sclerosis. Brit J Ophthalmol 1973;57:98-109

199. Sarks SH. Ageing and degeneration in the macular region: a clinico-pathological study. Brit J Ophthalmol 1976;60:324-41

200. Sarks SH, van Driel D, Maxwell L, Killingsworth MC. Softening of drusen and subretinal neovascularization. Trans Ophthal Soc UK 1980;100:414-22

201. Schachat AP. Management of subfoveal choroidal neovascularization. Arch Ophthalmol 1991;109:1217-8

202. Schaft TL van der, de Bruijn WC, Mooy CM, Ketelaars GAM, de Jong PTVM. Is basal laminar deposit unique for age-related macular degeneration?
Arch Ophthalmol 1991;109:420-5

203. Schaft, TL van der, Mooy CM, de Bruijn WC, Oron FG, Mulder PGH, de Jong PTVM. Histologic features of the early stages of age-related macular degeneration. Ophthalmology 1992;99:278-86

204. Schaft, TL van der, de Bruijn WC, Mooy CM, Ketelaars GAM, de Jong PTVM. Element analysis of the early stages of age-related macular degeneration. Arch Ophthalmol 1992;110:389-94

205. Schatz H, McDonald HR. Atrophic macular degeneration. Rate of spread of geographic atrophy and visual loss. Ophthalmology 1989;96:1541-51

206. Shallal A, McKechnie NM, Al-Mahdawi S. Immunochemistry of the outer retina. Eye 1988;2(suppl):180-201

207. Shan-Rong Shi, Key ME, Kalra KL. Antigen retrieval in formalin-fixed, paraffin-embedded tissues: an enhancement method for immunohistochemical staining based on microwave oven heating of tissue sections. J Histochem Cytochem 1991;39:741-8

208. Silverston BA, Bergon D, Grushka E, Kristol L, Hirsch I, Algur N. Copper and zinc levels after external damage by laser photocoagulation to the retinal pigment epithelium. Metab Pediatr Syst Ophthalmol 1985;8:61-8

209. Silverstone BZ, Landau L, Berson D, Sternbuch J. Zinc and Copper metabolism in patients with senile macular degeneration. Ann Ophthalmol 1985;17:419-22

210. Slater M. Adherence of LR White sections to glas slides for silver enhancement immunogold labeling. Stain Technology 1989;64:297-299

211. Small ML, Green WR, Alpar JJ, Drewry RE. Senile macular degeneration. A clinicopathologic correlation of two cases with neovascularization beneath the retinal pigment epithelium. Arch Ophthalmol 1976;94:601-7

212. Smiddy WE, Glaser BM, Green WR, Connor TB, Roberts AB Lucas R, Sporn MB. Transforming growth factor beta. A biologic chorioretinal glue. Arch Ophthalmol 1989;107:577-80

213. Sobin SS, Bernick S, Ballard KW. Histochemical characterization of the aging microvasculature in the human and other mammalian and non-mammalian vertebrates by the periodic acid-Schiff reaction. Mechanisms of ageing and development 1992;63:183-92

214. Soubrane G, Coscas G, Francais C, Koenig F. Occult subretinal new vessels in age related macular degeneration. Ophthalmol 1990;97:649-57

215. Spalton DJ, Hitchings RA, Hunter PA. Atlas of clinical ophthalmology. London, England: Gower Medical Publishing; 1984

216. Spencer WH, editor. Ophthalmic Pathology; An atlas and textbook. 3rd edition. Saunders, Philadelphia. 1985. pp.924-89

217. Sperduto RD, Ferris FL, Kuriny N. Do we have an nutritional treatment for age related cataract or macular degeneration? Arch Ophthalmol 1990;108:1403-5

218. Stark WJ, Maumenee AE, Fagadau W, Datiles M, Baker CC, Worthen D, Klein P, Auer C. Cystoid macular edema in pseudophakia. Surv Ophthalmol 1984;28(suppl):442-51

219. Stark WJ, Worthen DM, Holladay JT et all. The FDA report on intraocular lenses. Ophthalmology 1983;90:311-7

220. Stock EL, Roth SI, Morimoto D. Desquamating endotheliopathy. Arch Ophthalmol 1987;105:1378-81

221. Strahlman ER, Fine SL, Hillis A. The second eye of patients with senile macular degeneration. Arch Ophthalmol 1983;101:1191-3

222. Stramm LE, Haskins ME, Aguirre GD. Retinal pigment epithelial glycosaminoglycan metabolism: intracellular versus extracellular pathways. Invest Ophthalmol Vis Sci 1989;30:2118-31

223. Sucs FE, Klaus V. Aspects épidémiologiques de la dégénérence maculaire liée à l'âge. Ophthalmology

1992;6:3-7
224. Sun CN, White HJ. An electron-microscopic study of a schwannoma with special reference to banded structures and peculiar membranous multiple-chambered spheroids. J Pathol 1974;114:13-6
225. Sunness JS, Massof RW, Johnson MA, Bressler NM, Bressler SB, Fine SL. Diminished foveal sensitivity may predict the development of advanced age-related macular degeneration. Ophthalmology 1989;96:375-81
226. Szöllösi D. Periodisch structurierte Körper (PSK) in the perivitelline space of rat and mouse embryos. J Ultrastruc Res 1975;53:222-6
227. Tabatabay CA, D'Amico DJ, Hanninen LA, Kenyon KR. Experimental drusen formation induced by intravitreal aminoglycoside injection. Arch Ophthalmol 1987;105:82630
228. Takeuchi T, Takeya M, Imanishi H. Ultrastructural changes in peripheral nerves of the fingers of three vibration-exposed persons with Raynaud's phenomenon. Scan J Work Environ Health 1988;14:31-5
228a Takizawa T, Hatakeyama S. Age-associated changes in the microvasculature of human adult testis. Acta Path Jap 1978;28:541-554 (english)
229. Taylor HR, Munoz B, West S, Bressler NM, Bressler SB, Rosenthal FS. Visible light and risk of age-related macular degeneration. Trans Am Ophthalmol Soc 1990;88:163-78
230. Thaete LG, Crouch RK, Schulte BA, Spicer SS. The immunolocalisation of copper-zinc superoxide dismutase in canine tissues. J Histochem Cytochem 1983;13;1399-1406
231. Timms BG. Postembedding immunogold labeling for electron microscopy using "LR White" resin. Am J Anat 1986;175(2-3):267-75
232. Timpl R, Wiedemann H, Van Delden V, Furthmayr H, Kuehn K. A network model for the organization of type IV collagen molecules in basement mebranes. Eur J Biochem 1981;120:203-11
233. Tripathi BJ. Fine structure of mesodermal tissues of the human eye. Trans Ophthal Soc UK 1974;94:663-97
233a Torczynski E, Tso MOM. The architecture of the choriocapillaris at the posterior pole. Am J Ophthalmol;81:428-40.
234. Tso MOM. Pathogenetic factors of aging macular degeneration. Ophthalmology 1985;92:628-35
235. Tso MOM. Experiments on visual cells by nature and man:in search of treatment for photoreceptor degeneration. Invest Ophthalmol Vis Sci 1989;30:2430-54
236. Tso MOM, Friedman E. THe retinal pigment epithelium. I Comparative histology. Arch Ophthalmol 1967;78;641-9
237. Tso MOM, Friedman E. The retinal pigment epithelium III: growth and development. Arch ophthalmol 1968;80;214-6
238. Ulshafer RJ, Allen CB, Nicolaissen B, Rubin ML. Scanning electron microscopy of human drusen. Invest Ophthalmol Vis Sci 1987;28:683-9
239. Ulshafer RJ, Allen CB, Rubin ML. Distributions of elements in the human RPE. Arch Ophthalmol 1990;108:113-7
240. Van der Hoeve J. Senile Maculadegeneration und senile Linsentrübung. Von Graefe's Archiv für Ophthalmologie

1918;98:1-6

241. Vander JF, Morgan CM, Schatz H. Growth rate of subretinal neovascularization in age-related macular degeneration. Ophthalmology 1989;96:1422-9

242. Vander JF, Federman JL, Greven C, Slusher MM, Gabel VP. Surgical removal of massive subretinal hemorrhage associated with age-related macular degeneration. Ophthalmology 1991;98:23-7

243. Vidaurri-Leal J, Hohman R, Glaser BM. Effect of vitreous on morphologic characteristics of retinal pigment epithelial cells. Arch Ophthalmol 1984;102:1220-3

244. Vinding T. Pigmentation of the eye and hair in relation to age-related macular degeneration. Acta Ophthalmologica 1990;68:53-8

245. Vinding T. Visual impairment of age related macular degeneration. Acta Ophthalmologica 90;68;162-67

246. Vinding T. Age-related macular degeneration. Macular changes, prevalence and sex ratio. Acta Ophthalmologica 1989;67:609-16

247. Von der Mark H, Aumailley M, Wick G, Fleischmajer, Timpl R. Immunochemistry, genuine size and tissue localization of collagen VI. Eur J Biochem 1984;142;493-503

248. Weiter JJ. Macular degneration. Is there a nutritional component? Arch Ophthalmol 1988;106:183-4

248a Weiter J, Fine BS. A histologic study of regional choroidal dystrophy. Am J Ophthalmol 1977;83:741-50.

249. Weiter JJ, Delori FC, Wing GL, Fitch KA. Relationship of senile macular degeneration to ocular pigmentation. Am J Ophthalmol 1985;99:185-7

250. Weiter JJ, Delori FC, Wing GL, Fitch KA. Retinal pigment epithelial lipofuscin and melanin and choroidal melanin in human eyes. Invest Ophthalmol Vis Sci 1986;27;145-52

251. Wells KK, Folberg R, Goeken JA, Kemp JD. Temporal artery biopsies. Correlation of light microscopy and immunofluorescence microscopy. Ophthalmology 1989;96:1058-64

252. Werner JS, Steele VG, Pfoff DS. Loss of human photoreceptor sensitivity associated with chronic exposure to ultraviolet radiation. Ophthalmology 1989;96:1552-8

253. Williamson J, Caird FI. I Epidemiology of ocular disorders in old age. In: The eye and its disorders in the elderly. Wright. Bristol, 1986

254. Wolff HH, Maciejewski W, Scherer R, Braun-Falco C. Immunoelectronmicroscopic examination of early lesions in histamine induced immune complex vasculitis in man. Brit J Dermatol 1978;99:13-22

255. Wroblewski J, Wroblewski R. Why low temperature embedding for X-ray microanalytical investigations? A comparison of recently used preparation methods. J Microsc 1986;142:351-62

256. Wyszynski RE, Bruner WE, Cano DB, Morgan KM, Davis CB, Sternberg P. A donor-age-dependent change in the activity of alpha-mannosidase in human cultured RPE cells. Invest Ophthalmol Vis Sci 1989;30:2341-47

258. Yanoff M, Fine BS. Ocular pathology. 3rd ed. Philadelphia,

PA: JB Lippingcott;1989:301-5

258aYan Y. Age-related microvascular changes in skin. Chung-Kuo-I-Hsueh-Yuan-Hsueh-Pao) 1990;12(1):9-12 (eng.abstract)

259. Young RW. The renewal of rod and cone outer segments in the rhesus monkey. J Cell Biol 1971;49:303-18

260. Young RW. Pathophysiology of age-related macular degeneration. Review. Surv Ophthalmol 1987;31:291-306

261. Young RW. Solar radiation and age-related macular degeneration. Surv Ophthalmol 1988;32:252-69

262. Yurchenco PD, Furthmayr H. Self-assembly of basement membrane collagen. Biochemistry 1984;23:1839-50

263. Zabel RW, MacDonald IM Mintsioulis G, Addison DJ. Scheie's syndrome. An ultrastrutural analysis of the cornea. Ophthalmology 1989;96:1631-8

264. Zhi-Ren Zhu, Goodnight R, Ishibashi T, Sorgente N, Ogden TE, Ryan SJ. Breakdown of Bruch's membrane after subretinal injection of vitreous. Opthalmology 1988;95:925-9

265. Zrenner E. Lichtinduzierte Schäden am Auge. Fortschr Ophthalmol 1990;87(suppl):41-51

List of publications

1) "Is basal laminar deposit unique for age-related macular degeneration?"
   Van der Schaft TL, de Bruijn WC, Mooy CM, Ketelaars GAM,
   de Jong PTVM.
   Archives of Ophthalmology 1991;109:420-425

2) "Histologic features of the early stages of age-related macular degeneration.
   A statistical analysis."
   Van der Schaft TL, Mooy CM, de Bruijn WC, Oron FG, Mulder PGH,
   de Jong PTVM.
   Ophthalmology 1992;99:278-286

3) "Element analysis of the early stages of age-related macular degeneration."
   Van der Schaft TL, de Bruijn WC, Mooy CM, Ketelaars GAM, de Jong PTVM.
   Archives of Ophthalmology 1992;110:389-394

4) "Immunohistochemical light and electron microscopy of basal laminar
   deposit."
   Van der Schaft TL, Mooy CM, de Bruijn WC, Bosman FT, de Jong PTVM.
   (submitted)

5) "Early stages of age-related macular degeneration: An immunofluorescence
   and electron microscopy study."
   Van der Schaft TL, Mooy CM, de Bruijn WC, de Jong PTVM.
   (submitted)

6) "Basal laminar deposit in the aging peripheral human retina."
   Van der Schaft TL, de Bruijn WC, Mooy CM, de Jong PTVM.
   (accepted for publication: Graefe's Arch Clin Exp Ophthalmol)

7) "Morphometric analysis of Bruch's membrane, the choriocapillaris and choroid in normal aging and age-related macular degeneration."
Ramrattan RS, Van der Schaft TL, Mooy CM, de Bruijn WC, Mulder PGH, de Jong PTVM.
(submitted)

8) "Increased prevalence of disciform macular degeneration after cataract extraction with implantation of an artificial intraocular lens."
Van der Schaft TL, Mooy CM, de Bruijn WC, Mulder PGH, Pameyer J, de Jong PTVM.
(submitted)

9) "Results of penetrating keratoplasty for pseudophakic bullous keratopathy with the exchange of an intraocular lens."
Van der Schaft TL, van Rij G, Renardel de Lavalette JGC, Beekhuis WH.
British Journal of Ophthalmology 1989;73:704-8

Dankwoord

Het schrijven van een dankwoord is een moeilijke zaak, omdat men gedurende een promotieonderzoek door zeer vele mensen begeleid, geholpen, gesteund, geadviseerd en bekritiseerd wordt. Het noemen van namen en personen houdt bijna als vanzelfsprekend in dat men anderen vergeet, hetgeen misschien nog wel zwaarder weegt dan het wel vermelden van mensen.

Daarom zou ik iedereen, die op enigerlei wijze een bijdrage heeft geleverd aan mijn onderzoek, aan de totstandkoming van dit proefschrift of aan de gezellige sfeer tijdens deze 4 jaar, heel hartelijk willen danken.

Toch zou ik nog in het bijzonder mijn promotor, Paulus de Jong willen danken voor zijn inzet, vasthoudendheid, snelheid en kommentaar, Neeltje Mooy, voor haar lessen in de ophthalmo-pathologie, solidariteit, goede ideeën, gastvrijheid en morele steun, en Wim de Bruijn voor zijn begeleiding met de electronenmicroscopie en zijn uitgebreide achtergrondkennis hierover en zijn filosofische beschouwingen over het onderzoek.

De afdeling Pathologie wil ik bedanken voor de bijzondere gastvrijheid waarmee ze mij deze 4 jaar hebben omringd en voor het bieden van de mogelijkheid dit onderzoek op deze afdeling uit te voeren.

Zonder de voortdurende en welwillende hulp van de corneabank van het Interuniversitair Oogheelkundig Instituut (IOI) te Amsterdam en Eurotransplant Leiden was dit onderzoek niet mogelijk geweest. Daarvoor mijn hartelijke dank.

De leden van de promotiecommissie wil ik bedanken voor hun bereidheid zich te verdiepen in dit omvangrijke proefschrift.

En tenslotte wil ik Nicolette, mijn vrouw, bedanken voor haar steun, geduld, het meedenken en natuurlijk het kostwinnerschap.

Curriculum Vitae

Theo van der Schaft werd geboren op 12 november 1958 te Rotterdam. Na zijn eindexamen Atheneum-B in 1977 aan het Emmauscollege Rotterdam heeft hij in afwachting van een plaats voor de studie geneeskunde, Scheikundige Technologie gestudeerd aan de TH-Delft en zijn militaire dienstplicht vervuld. Vanaf 1980 studeerde hij geneeskunde aan de Erasmus Universiteit Rotterdam en slaagde in 1987 cum laude voor zijn arts-examen. Vervolgens werkte hij gedurende anderhalf jaar als AGNIO (assistent geneeskunde niet in opleiding) chirurgie in het Bergwegziekenhuis Rotterdam. Van januari 1989 t/m december 1992 heeft hij als AIO (assistent in opleiding tot wetenschappelijk onderzoeker) zijn promotie onderzoek verricht bij het instituut Oogheelkunde van de Erasmus Universiteit Rotterdam, op de afdeling Pathologische Anatomie. Vanaf 1 januari 1993 is hij als AGIO (assistent geneeskunde in opleiding) oogheelkunde verbonden aan het Oogziekenhuis Rotterdam.